

## INFORMATION TO USERS

This manuscript has been reproduced from the microfilm master. UMI films the text directly from the original or copy submitted. Thus, some thesis and dissertation copies are in typewriter face, while others may be from any type of computer printer.

The quality of this reproduction is dependent upon the quality of the copy submitted. Broken or indistinct print, colored or poor quality illustrations and photographs, print bleedthrough, substandard margins, and improper alignment can adversely affect reproduction.

In the unlikely event that the author did not send UMI a complete manuscript and there are missing pages, these will be noted. Also, if unauthorized copyright material had to be removed, a note will indicate the deletion.

Oversize materials (e.g., maps, drawings, charts) are reproduced by sectioning the original, beginning at the upper left-hand corner and continuing from left to right in equal sections with small overlaps. Each original is also photographed in one exposure and is included in reduced form at the back of the book.

Photographs included in the original manuscript have been reproduced xerographically in this copy. Higher quality 6" x 9" black and white photographic prints are available for any photographs or illustrations appearing in this copy for an additional charge. Contact UMI directly to order.

# UMI

A Bell & Howell Information Company  
300 North Zeeb Road, Ann Arbor, MI 48106-1346 USA  
313/761-4700 800/521-0600



**Order Number 9521276**

**New mobile cellular systems**

**Hadad, Zion, Ph.D.**

**City University of New York, 1995**

**Copyright ©1995 by Hadad, Zion. All rights reserved.**

**U·M·I**  
300 N. Zeeb Rd.  
Ann Arbor, MI 48106



**NEW MOBILE CELLULAR SYSTEMS**

**by**

**ZION HADAD**

A dissertation submitted to the Graduate Faculty in Engineering in partial  
fulfillment of the requirement for the degree of Doctor of Philosophy,

**The City University of New York**

**1995**

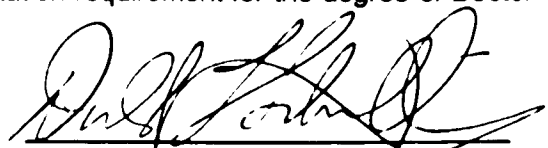
© 1995

ZION HADAD

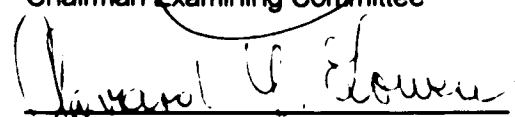
All Rights Reserved

This manuscript has been read and accepted for the Graduate Faculty in Engineering in satisfaction of the dissertation requirement for the degree of Doctor of Philosophy.

10/21/94  
DATE

  
Professor Donald L. Schilling  
Chairman Examining Committee

10/31/94  
DATE

  
Dean Gerard Lowery  
Executive Officer

\_\_\_\_\_  
Professor J. Barba

\_\_\_\_\_  
Professor S. Maric

\_\_\_\_\_  
Professor N. Schinberg

\_\_\_\_\_  
Dr. S. Davidovici

\_\_\_\_\_  
Supervisory Committee

**THE CITY UNIVERSITY OF NEW YORK**

**Abstract****NEW MOBILE CELLULAR SYSTEMS**

by

**Zion Hadad****Advisor: Professor Donald L. Schilling**

In this research two types of Spread Spectrum Code Division Multiple Access (CDMA) systems are proposed and considered. Direct Sequence Broadband Code Division Multiple Access (B-CDMA) in an Overlay application and a Frequency Hopping Code Division Multiple Access (FH-CDMA) technique are presented.

The Overlay B-CDMA (O-B-CDMA) signal can overlay the existing cellular telephone spectrum (825 to 894 MHz) thereby providing additional capacity to the network. This method allows high quality voice and high speed data services to coexist with the existing cellular services: Advanced Mobile Phone System (AMPS) and Time Division Multiple Access (TDMA). The low level of mutual interference experienced between the existing cellular telephone system and the B-CDMA overlay system is shown. This approach has been proven successful by actual field testing in Des Moines, Iowa. A minimal system was used for the field test, The

system, consisted of a single base station, equipped with a receive notch filter, four remote units working simultaneously, each at a data rate of 64 Kbps, overlaying 40 AMPS users and surrounded by other AMPS cells . The tested system did not include any type of diversity (spatial, RAKE, or hand-off of any kind, etc.).

This research also includes an analysis of a FH-CDMA system that performs in either a clear band of frequencies or as an overlay. The proposed FH system includes a six sectored base station, maximal ratio diversity combining at the base, switching diversity at the base toward the remote is assumed, and a six ring topology for efficient area coverage. The system also uses Reed-Solomon Forward Error Correcting Code with erasure decoding.

This research also includes a new approach for the rejection of narrow band interference. This has been simulated, implemented, and successfully tested.

## **ACKNOWLEDGMENTS**

I would like to take this opportunity to thank everyone that supported this work with special thanks going to Professor Donald L. Schilling. It was wonderful of him to let me work and learn from him. Don, every moment of being with you was an experience for me and I will never forget what you have done for me. I also want to thank Dr. Tuvia Apelewicz for creating this opportunity. Also, I want to say thank you to Dr. Joseph Garodnick for the wonderful time we had working together and a special thanks to Annette Schilling for her advice and help offered for any problem that would come up.

Special thanks to Dean G. Lowen of the City University for letting me transfer in from UCSD California in the spring of 1992. Thank you for taking such good care of me as a student.

A Special thanks to all the InterDigital employees. The management for allowed me to be the leader of the OVERLAY project and the other employees for not only helped me but allowed me to be a part of the team that made history by developing the first prototype of the Cellular Overlay System and the subsequent successful demonstration in Des-Moines IOWA. Thank you Avi Silverberg, Shu Chu, Dr. Yan Zang, Bob Regis, John Bird, Eric Dietmann, Caesar Carrero, Mary Gray, Dr. Saeed Ghassemzadeh. I also want to say thank you to the research group of InterDigital:

Donald Greico, Dr. Gary Lomp, Dr. Emanuel Kanterakis, Dr. Kowalski John and Dr. Kourosh Parsa. Special thanks to the telephone group consisting of Mr. Victor Zelmanovich and Mr. Remus Albu.

Special thanks to Tadiran, Israel for sending me to USA.

Special thanks also to CUNY for the effort and care afforded me as an international student.

Very special thanks to my three children Liad, Ran and Nadav for being patient and understanding the importance of their father obtaining his degree. I hope that I will be able to makeup to them all the time that was spent working towards this degree.

Special thanks to my family which supported me through this difficult time. Thank you Father and Mother for being such wonderful parents.

Finally, to my lovely wife Brooria, to which this book is dedicated. She deserves this recognition and my gratitude, having been put through just as much or more than myself. Brooria, I love you for being a special friend and wonderful wife.

**Table Of content**

<b>1. INTRODUCTION</b>	<b>1</b>
<b>1.1 Statement of the problem</b>	<b>3</b>
<b>1.2 Anticipated Benefits.</b>	<b>4</b>
<b>1.3 Previous Work</b>	<b>4</b>
<b>2. BACKGROUND AND TECHNICAL APPROACH.</b>	<b>5</b>
<b>2.1 Introduction</b>	<b>5</b>
<b>2.2 Characteristics of Spread Spectrum</b>	<b>5</b>
<b>2.3 Principles of Operation</b>	<b>6</b>
<b>3. OVERLAY DIRECT SEQUENCE CODE DIVISION MULTIPLE</b>	
<b>ACCESS</b>	<b>8</b>
<b>3.1 Abstract</b>	<b>8</b>
<b>3.2 Introduction</b>	<b>8</b>

<b>3.3 B-CDMA OVERLAY</b>	<b>9</b>
3.3.1. Approximate B-CDMA Capacity Analysis	10
3.3.2. Fade Depth	16
3.3.3. The Notch Filter To Increase Capacity	21
3.3.4. Description of The Overlay Experiment	29
3.3.5. Calculation of The Number of Users In The Reverse Link	33
3.3.6. Reverse Link Simulation For APC Set Level	44
<b>4. OVERLAY FH-CDMA</b>	<b>48</b>
<b>4.1 Introduction</b>	<b>48</b>
<b>4.2 Approximate FH-CDMA Capacity Analysis</b>	<b>48</b>
<b>4.3 System Description</b>	<b>50</b>
4.3.1 Concentric Rings to Reduce Interference	51
4.3.2. Sectored Antennae Can Minimize Interference	54
4.3.3 Rings Sectored Antennas Can Minimized Interference.	55
4.3.4 Forward Power Control	56
4.3.5 Reverse Power Control	57
4.3.6 Rings and Sectored Antennae Can Increase Capacity C By A Factor of 6	58
4.3.7 Choosing the Hop Duration	61
4.3.8 Diversity	63

	x
4.3.9 Hand-off	63
4.3.10 Overlay	64
4.3.11 Modulation Technique	65
4.3.12 Synchronous Orthogonal FH/CDMA	65
4.3.13 Synchronization	68
4.3.14 Coding	69
<b>5. CONCLUSION</b>	<b>71</b>
<b>FIGURES</b>	<b>74</b>
<b>TABLES</b>	<b>148</b>
<b>REFERENCES</b>	<b>154</b>

**LIST OF TABLES**

Table 2.2.1	Digital Telephony - Common Air Interface.	149
Table 3.3.1	Spillover Results for B-CDMA Adjacent Cell Interference.	150
Table 3.3.4.1	Experimentally Determined System Characteristics	35
Table 3.3.6.1	Number of BCDMA users as a Function of APC levels, AMPS and CDMA, threshold for AMPS being in a notch = - 92	151
Table 3.3.6.2	Number of BCDMA users as a Function of APC levels, AMPS and CDMA, threshold for AMPS being in a notch = - 97	152
Table 3.3.6.3	Number of BCDMA users as a Function of APC levels, AMPS and CDMA, threshold for AMPS being in a notch = -102	153

**LIST OF FIGURES**

Figure 1:	Tentative Frequency Plain.	75
Figure 1.1a:	Showing the congestion in a shared frequency band.	76
Figure 1.1b:	Showing the congestion in a AMPS cell.	77
Figure 2.3a:	Simplified Spread Spectrum Direct Sequence System.	78
Figure 2.3b:	FH Spread Spectrum System.	79
Figure 3.3a:	CDMA uses 10 Mchips/s in a 10MHz BW to overlay each user.	80
Figure 3.3b:	Base stations do not jam.	81
Figure 3.3c:	Mobiles do not jam.	82
Figure 3.3.2.1:	Fade depth in City college.	83
Figure 3.3.2.2:	Fade depth in Port Washington.	83
Figure 3.3.2.3:	Fade depth in Manhattan..	83
Figure 3.3.2.4:	Delay Spread in Port Washington.	84
Figure 3.3.2.5:	Delay Spread in Port Washington.	84
Figure 3.3.2.6:	Excess Delay Spread in Manhattan.	85
Figure 3.3.2.7a:	Faded signal.	86
Figure 3.3.2.7b:	APC control Signal.	86
Figure 3.3.2.7c:	Despread Output power for fixed step algorithm.	86
Figure 3.3.2.8a:	Faded signal	87
Figure 3.3.2.8b:	APC control Signal.	87

Figure 3.3.2.8c: Despread Output power for adaptive step algorithm.	87
Figure 3.3.3.1: Cellular Overlay Base.	88
Figure 3.3.3.2a: Complex notch filter amplitude response.	89
Figure 3.3.3.2b: Complex notch filter Phase response.	89
Figure 3.3.3.3a: Output QPSK Constellation of Complex Notch Filter.	90
Figure 3.3.3.3b: Output QPSK Constellation of Magnitude Notch Filter-50 Notches.	90
Figure 3.3.3.3c: Output QPSK Constellation of Magnitude Notch Filter-No Notches.	90
Figure 3.3.3.4: Basic Block Diagram of Spread Spectrum Transceiver With Notch Filters Transmitter and in Receiver	91
Figure 3.3.3.5: Transmit 32 kbps data , LPF at 20 kHz.	92
Figure 3.3.3.6: 8 Mchips/s PN sequence.	93
Figure 3.3.3.7: Spectrum of a notched filtered PN sequence.	94
Figure 3.3.3.8: Zoomed received spectrum.	95
Figure 3.3.3.9: Received output 32kbps data after despreading and LPF	96
Figure 3.3.3.10a: Transmit notched O-B-CDMA signal at the output of PA 200 Watts (one dB compression).	97
Figure 3.3.3.10b: Zoomed Transmit notched O-B-CDMA signal at the output of PA 200 Watts (one dB compression).	98
Figure 3.3.4.0: Base stations Coverage of US-CELLULAR at Des Moines IOWA.	99

Figure 3.3.4.1:	Subscriber unit.	100
Figure 3.3.4.2:	The BCDMA & AMPS Antennae	101
Figure 3.3.4.3:	The Clive B-CDMA Overlay System.	102
Figure 3.3.4.4:	AMPS POWER Load at Clive base station at day time.	103
Figure 3.3.4.5:	AMPS POWER Load At Clive Base Station.	104
Figure 3.3.5.1a:	Channel Output From Notch Filter With AMPS (lower curve ).	105
Figure 3.3.5.1b	channel output from notch filter with AMPS and CDMA (left curve ), No signal (right)	106
Figure 3.3.5.2a	One CDMA with AMPS received at the Remote unit.	107
Figure 3.3.5.2b	Spillover from Ankeny Base Station and down town Des Moines received at the remote unit.	108
Figure 3.3.5.2c	Received signal 5 miles from the BS..	108
Figure 4.1	Frequencies Locked out.	109
Figure 4.3.a	FH-CDMA block diagram.	110
Figure 4.3.b	Orthogonal & non orthogonal Hopping.	111
Figure 4.3.c	FH-CDMA using concentric Frequency Bands.	112
Figure 4.3.d	FH-CDMA using sectors Frequency Bands.	113
Figure 4.3.e	FH-CDMA using concentric and sectors. Frequency Bands.	114
Figure 4.3.1.1	SNR calculation for rings.	115
Figure 4.3.1.2	Outage and Block error rate for regular cell, $\sigma = 0$ .	116

Figure 4.3.1.3	Outage and Block error rate for regular cell, $\sigma = 8$ .	117
Figure 4.3.1.4	Outage and Block error rate for rings cell without APC correction, $\sigma = 8$ .	118-119
Figure 4.3.2.1	SNR calculation for sectored cell.	120
Figure 4.3.2.2	Outage and Block error rate for regular sectored cell, $\sigma = 0$ .	121-122
Figure 4.3.2.3	Outage and Block error rate for regular sectored cell, $\sigma = 8$ .	123-124
Figure 4.3.4:	Calculation of the S/I Produced at Mobile Due to an Interfering Base.	125
Figure 4.3.6.1	Showing The Radios of a Rings to achieve a constant user density.	126
Figure 4.3.6.2	Outage and Block error rate for rings cell with APC correction, $\sigma = 0$ .	127-127
Figure 4.3.6.3	Outage and Block error rate for rings cell with APC correction $\sigma = 8$ .	129-130
Figure 4.3.6.4	Outage and Block error rate for rings & sector cell with APC correction, $\sigma = 0$ .	131-132
Figure 4.3.6.5	Outage and Block error rate for rings & sector cell with APC correction, $\sigma = 8$ .	133-134

Figure 4.3.6.6	Average outage and Block error rate for rings & sector cell with APC correction, $\sigma = 0$ .	135
Figure 4.3.6.7	Average outage and Block error rate for rings & sector cell with APC correction, $\sigma = 8$ .	136
Figure 4.3.6.8a	The SNR at the remote at different locations in the cell, with one cell interfere.	137
Figure 4.3.6.8b	The SNR at the remote at different locations in the cell, with six cell interfere.	138
Figure 4.3.7.1	Frequency selective fading.	139
Figure 4.3.7.2	Proposed FH-CDMA Frame Structure.	140
Figure 4.3.8	Showing How Frequencies Are Selected In FH-CDMA To Achieve Space Diversity.	141
Figure 4.3.11	Power Spectral Densities of the Modulation.	142
Figure 4.3.12	Reed Solomon code for selecting FH-CDMA sequences.	143
Figure 4.3.12d	Crosscorrelation of FH-CDMA sequences using Reed Solomon Code.	144
Figure 4.3.13	FH Receiver.	145
Figure 6.1	B-CDMA traffic as function of AMPS traffic .	146
Figure 6.2	mobile Technologies efficiency comparison.	147

## 1. INTRODUCTION

Over the last decade, and in particular over the last several years, the demand has grown rapidly for mobile Telecommunications systems capable of communicating toll quality voice and data rates up to 144 Kbps. Such systems are referred to as Personal Communication Systems (PCS) and Future Public Land Mobile Telephone Systems (FPLMTS). Currently the RF spectrum is extremely congested. If additional communication service is needed, more spectrum must be found or more efficient techniques be used. Recently (September 1993 ) the FCC allocated spectrum for PCS in the 1.85-1.97 Ghz and 2.13-2.20 Ghz frequency bands within the United States (see Figure 1). The problem- of spectral congestion is not only a domestic problem but a world-wide one. The International Telecommunications Union's CCIR has numerous study groups looking into spectrum reallocation to meet a myriad of needs.

The reallocation of spectra is a very delicate political matter. It entails taking spectra already allocated to one group and setting it aside for another group. Where does the existing group move? Who pays for the move? Remember that for a group of users to change its frequency band of operation requires that the entire RF receiving and transmitting systems be changed.

While the reallocation of spectra is clearly one way to improve the efficiency of spectrum utilization, and the taking of some "sparsely" used government bands and transferring them to commercial use is another, "spread spectrum" is still another. Spread Spectrum (SS) allows new users to share the spectrum with existing users, thereby postponing and, in some cases, eliminating the need for reallocation of spectrum with its obvious cost and political considerations. In the case of newly opened "virgin" spectrum, the total capacity of the assigned spectrum may be larger using a spread spectrum cellular system than is possible by other cellular methods such as Frequency Division Multiple Access (FDMA) or Time Division Multiple Access (TDMA), for the following reasons:

- a. The capacity in a FDMA or TDMA system is determined by the largest interference that exists in the surrounding cells, whereas the capacity of a SS system is determined by the average of all of the interference falling in the baseband.
- b. SS systems inherently employ frequency diversity which averages the multipath effects.
- c. Voice Activity Detection (VAD) can be used to decrease the average interference and thereby increase the capacity.

Thus, using the Spread Spectrum - Code Division Multiple Access (SS-CDMA) system proposed here results in significantly increased spectral efficiency.

To illustrate this, two SS techniques are proposed; Direct Sequence (DS) with application of Overlay Broadband Code Division Multiple Access (O-B-CDMA) and Frequency Hop (FH) spread spectrum with an application of Frequency Hopping - Code Division Multiple Access (FH-CDMA). In the O-B-CDMA, a new method for rejecting narrow band interference has been developed capable of sharing the spectrum with multiple, fixed frequency microwave users.

### **1.1 Statement of The Problem**

Figure 1.1a and 1.1b illustrates the problem. Note that the spectrum shown is sparsely used, and the channels being used are distributed throughout the frequency band. As a result, the number of additional, standard microwave transmission systems that can operate in the band are limited. Using CDMA, the number of additional users can be made significantly greater than by using standard FM microwave. Here using FH-CDMA, frequencies occupied by the Standard Microwave Users (SMU) or by the standard cellular system (AMPS) could be "locked-out" and hence not hopped on. Hence the SMU or AMPS are not interfered with by the FH-CDMA users nor does the SMU/AMPS interfere with the FH-CDMA users. The DS/CDMA system actually shares the same spectrum with the SMU/AMPS and hence, some interference with the SMU is encountered. To reduce the interference the DS/CDMA system notches the DS spectrum in the frequencies that are been used by the SMU/AMPS.

## **1.2 Anticipated Benefits.**

The implications of a successful outcome are enormous! A spread spectrum cellular telephone system could operate in the same band as the standard FDMA cellular telephone system without altering the existing system, yet provide a significant capacity increase. A stand-alone SS/CDMA system, could provide a significant increase in capacity. Finally a SS/CDMA cellular telephone system that can operate in a congested microwave band without interfering with existing fixed frequency users is a major contribution.

## **1.3 Previous Work**

Table 1.3 presents a comparison between the new wireless systems under development which didn't employ SS. Qualcomm [4] was the first to begin an investigation into replacing the existing cellular system by a DS/CDMA system. SCS Mobilecom [6] was the first to investigate the feasibility of using DS/CDMA cellular telephony as a co-primary user which is called OVERLAY. This work is the first for overlay on the AMPS system that may include 57 frequencies per cell. ERICSSON, the developers of the GSM system are looking into a FH-CDMA-TDMA system, AT&T is developing a prototype FH-CDMA, and the research and development center of Motorola are proposing a FH-CDMA-TDMA system for the PCS band, None of these manufacturers are currently considering extending their systems to OVERLAY.

## **2. BACKGROUND AND TECHNICAL APPROACH.**

### **2.1 Introduction**

Spread spectrum has a long and interesting history. It has been, and still is, used extensively in military communications systems, both to permit communications which are not detectable by enemy jamming systems (this property of spread spectrum is called "low probability of interception", or LPI), and to resist jamming by an enemy desiring to disrupt communications.

### **2.2 Characteristics of Spread Spectrum**

Spread spectrum (DS,FH) is typically designed to be "transparent" to other users, i.e., spread spectrum signals are designed to provide negligible interference to the communication of other, existing, users and indeed, it is difficult to determine if a spread spectrum signal is actually present. We call characteristics of this type low Probability of Interception (LPI) and Low Probability of Detection (LPD), and they are requirements for successful military communication. It is these LPI and LPD features of spread spectrum that will allow transmission between users of a spread spectrum network without the existing users experiencing significant interference.

Spread spectrum is also "jam" or interference resistant. In a military communication system, once an enemy detects a communication in progress, it transmits noise or other signals to interfere with or jam the communications. A spread spectrum

receiver spreads the spectrum of the interfering signal and hence reduces the interference so that it does not noticeably degrade system performance. It is this feature of interference reduction that also makes spread spectrum useful for commercial communications, i.e., the spread spectrum wave forms can be overlaid on top of existing narrow band signals. Spread spectrum is also multipath resistant as will be explained later.

### **2.3 Principles of Operation**

There are primarily two main spread spectrum techniques, direct sequence spread spectrum (DS/SS) (see Figure 2.3a) which is an amplitude modulation technique and, frequency hopping spread spectrum (FH/SS), which is a frequency modulation technique (see Figure 2.3b). The goal of each of these techniques is to take the power that is to be transmitted and spread it over a very wide bandwidth so that the power per unit bandwidth (Watts/Hertz) is minimized. When this is accomplished, the transmitted spread spectrum power received by an existing user, having a relatively narrow bandwidth, is only a small fraction of the actual transmitted power.

In addition, in the direct sequence spread spectrum CDMA system one can insert a notch filter in the transmitter and in the receiver, to remove power to be transmitted from or in the bandwidth of a neighboring SMU/AMPS. In the FH-CDMA system proposed here, we will "lock out" frequencies being used by a neighboring SMU/AMPS.

The feature of Direct Sequence spread spectrum that results in interference reduction is that the spread spectrum receiver actually spreads the received energy of any interference over the same wide bandwidth as the signal while compressing the bandwidth of the desired received signal to its original bandwidth. For example in [6], if the original bandwidth of the desired signal is only 32 KHz the power of an interfering signal 48MHz wide is reduced by

$$N=48 \times 10^6/32 \times 10^3 =750.$$

Note that for any FH/DS spread spectrum system to operate properly, it is necessary for the receiver to acquire the correct frequency/chip position of the incoming waveform, and it must continually track that frequency/chip position to insure that loss-of-lock will not occur. The two processes of acquisition and tracking form the synchronization subsystem of a spread spectrum receiver. The former operation is typically accomplished by a search of as many hop/chip positions as necessary until one is found which results in a large correlation between the chip sequence of the incoming signal and the hop/chip sequence of the locally generated spreading sequence at the receiver. The latter operation is often performed with an "early-late gate". The importance of the combined synchronization process cannot be overstated, for if synchronization is not both achieved and maintained, the desired signal cannot be despread.

### **3. Overlay Direct Sequence Code Division Multiple Access**

#### **3.1 Abstract**

A Broadband Code Division Multiple Access (B-CDMA) technique is presented that will overlay the existing cellular telephone spectrum (825 to 894MHz). The overlay will provide additional capacity to the network while allowing high quality voice and high speed data services to be coexistent with the existing cellular services (AMPS and TDMA). The advantages of using B-CDMA in a fading environment are analyzed. The low level of mutual interference between the existing cellular telephone system and the B-CDMA overlay system is shown. During June, July 1994 the O-B-CDMA system has been integrated demonstrated in Des Moines IOWA.

#### **3.2 Introduction**

The cellular providers are limited in the service that can presently be provided. AMPS service has a capacity limitation of approximately 57 users per base station, no privacy, a high frequency of outages due to susceptibility to fading, and little capability to transmit data. TDMA and the proposed Narrow band-CDMA services, each results in a capacity increase and provides privacy, but the voice quality remains poor, data rates are low.

Broadband-CDMA (B-CDMA) provides higher capacity than the above mentioned technologies due to its resistance to fading, wired-line voice quality, and data rate on demand up to ISDN rates, thereby permitting multimedia communications. Further, B-CDMA can overlay and share the spectrum with the existing AMPS or TDMA cellular users.

### 3.3 B-CDMA OVERLAY

The O-B-CDMA system connects to the AMPS cellular system directly by coupling to the sectored antennas shown in Figure 3.3a. Assume, for example, that there are 3, sectored, antennas. The bandwidth spacing used by the AMPS system is 30 KHz/channel and each channel is spaced 630 kHz apart, rather than 210 kHz apart, as is in the case when using an omnidirectional antenna in the base. Thus, as shown in the Figure, frequency 1 is in sector one, frequency 2 is in sector two and frequency 3 is in sector three, etc.

In order for Broadband CDMA to operate properly, four conditions must be simultaneously met. When these four conditions are met, coexistence is insured. For example, in Figure 3.3b we see that Condition 1 is that the CDMA base station should not jam the AMPS mobile. In this Figure the AMPS mobile is shown placed at the edge of 3 cells where it is interfered with by three CDMA base stations. This is the worst case position.

The second condition, which can also be illustrated using Figure 3.3b, is that the AMPS base stations should not jam the CDMA mobile. The worst-case condition is when the CDMA mobile is placed between the three base stations so that three AMPS base stations are jamming it directly.

Figure 3.3c shows the remaining two conditions: Condition 3 is that the CDMA mobiles do not jam the AMPS base stations and condition 4 is that the AMPS mobiles do not jam the CDMA base station.

Conditions 1 and 4 are largely satisfied by using *notch filters* in the CDMA base transmitter and receiver. While Conditions 2 and 3 can also be satisfied by using notch filters in the CDMA mobile units, it is instructive to initially assume that the mobile units do not employ a notch filter.

### 3.3.1. Approximate B-CDMA Capacity Analysis

Condition 2 is to prove that the AMPS base station does not jam the CDMA mobile.

In Figure 3.3.b we see that the three AMPS base stations are jamming a CDMA mobile at the junction of three cells. The interference to the CDMA mobile caused by the AMPS system is  $I = 3n_A P_C^F / G_C$  where  $P_C^F$  is the power received at the CDMA mobile from the AMPS base, on a per user basis. The processing gain is  $G_C = W/f_b$  for a CDMA bandwidth  $W$  and data rate  $f_b$ .  $n_A$  is the number of AMPS users/sector. The maximum number of AMPS users per sector in a 10 MHz band, using 3

sectors, is  $n_A=16$ . The worst case interference to the CDMA mobile by the CDMA base stations occurs when the mobile is jammed by three base stations. In this case the interference is

$$I = 3\alpha n_c P_C^F / G_c \quad (3.3.1.1)$$

where  $\alpha \approx 1/2$  because one-half of the time a user is not talking and during this time the user is not transmitting. Hence, on the average, twice as many users can operate on the same channel. This is called "voice activity detection". The received CDMA power, per user, is  $P$  and therefore the signal to interference ratio is

$$\left( \frac{S}{I} \right)_{C,M}^F = \frac{P_C^F G_c}{3\alpha n_c P_C^F + 3n_A P_A^F} \quad (3.3.1.2)$$

In order to compare this system performance to the performance that we get in a narrowband CDMA system we set  $f_b = 8\text{kbps}$  and we find  $G_c = 10\text{MHz}/8\text{kbps} = 1250$ . Let the signal-to-interference ratio be set to equal 4dB. Solving Eq. (3.3.1.2) yields

$$n_c + (P_A^F / P_C^F) n_A = 167 \quad (3.3.1.3)$$

To satisfy Condition 3, that the CDMA mobiles do not jam the AMPS base, we use Figure 3.3c. The interference to the AMPS base caused by the CDMA users,  $I_{Ac}$   $= 2\alpha n_c P_c^R / G_A$ , where the factor of 2 is assumed to account for the effect of spillover power from CDMA mobiles in surrounding cells. Actually, the "spillover" depends on the hand-off region, the standard deviation ( $\sigma$ ) of the lognormal distribution for shadowing, the number of antenna sectors employed, the propagation exponent, the distribution function for the density of subscribers (here assuming a uniform density) and etc. It can also be shown that spillover decreases with increasing chip rate.

The power that the AMPS base receives from an AMPS mobile is  $P_A^R$ . The signal to interference ratio is therefore,

$$\left(\frac{S}{I}\right)_{A,R}^R = \frac{P_A^R}{I_{AA}^R + \frac{2\alpha n_c P_c^R}{G_A}} \quad (3.3.1.4)$$

where  $G_A = 10\text{MHz}/15\text{kHz} = 667$ . (15kHz is the IF bandwidth of the AMPS system.)

The interference  $I_{AA}^R$  is the interference to an AMPS signal received at the base, from distant AMPS signals operating at the same frequency. Due to frequency reuse this interference is small.

If we assume that the signal-to-interference ratio at the AMPS base is 17dB, Eq. (1.4) reduces to

$$\alpha_{nc} = 4.4 (P_A^R / P_C^R) \quad (3.3.1.5)$$

### 3.3.1.1 Simulation

During the last year some simulations has been performed at InterDigital. One of the Simulations performed of a B-CDMA cellular system overlaying an AMPS cellular system. The base stations of both of these systems were assumed to be co-located and cell sizes were assumed identical. Each B-CDMA user is assumed to be operating at 8kb/s and spread over a 10MHz bandwidth. Voice communications with voice activity detection is employed and is assumed to result in increasing the numbers of users by a factor of 2, i.e.,  $a = 1/2$ . Adaptive power control (APC) is used and a 1dB error is considered in these simulations. The Monte Carlo simulations assumed that the AMPS and B-CDMA mobiles were uniformly distributed in regular hexagonal cells with a radius of 6 miles, with 1, 3 or 6 sectors in each cell. The propagation loss model assumed  $R^2$  loss before and  $R^4$  loss after a breakpoint given by  $d_0 = 4 h_t h_r / \lambda$  where  $h_t = 5$  feet. is the mobile transmit antenna height,  $h_r = 300$  feet. is the base receive antenna height and the wavelength  $\lambda = 1$  feet. Thus,  $d_0 = 6000$  feet. The base antenna pattern was parabolic, with a 4dB loss at  $\pm 60$  degrees. for the 3-sector case and  $\pm 30$  degrees for the 6-sector case, and had a limiting front-to-back ratio of 20dB. A log-normal

shadow loss with an 8 dB standard deviation was used. Power control and hand-off was also included.

In this simulation 40 notch filters were used in the base transmitter and 40 notch filters were placed in the base receiver. Each notch filter was positioned in frequency to the largest AMPS users as seen at the base station. In addition, each notch filter was 40dB deep and had a bandwidth of 60kHz. It was found that notch filters in the remote units do not significantly improve performance and so such notches are not used. Furthermore, it was shown that the removal of the notches from either the base transmitter or the base receiver, severely limits the B-CDMA capacity. Hence the results shown below all employ base station notch filters both in the transmitter and receiver.

### **Spillover**

The results presented below are for 1, 3 & 6 sectors per antenna. Each sector in each cell is considered to have equal loading. This result affects the internal user loading, which is the capacity. For example, there has been continual discussion in the literature as to the magnitude of the effect of the users in adjacent cells on the number of users in the desired cell. Table 3.3.1, presents simulation "spillover" results as a function of the number of sectors, and the hangover threshold. For example, in a  $S=3$  sector system, with a hangover threshold  $h=3\text{dB}$ , a user  $U$  in a cell  $A$ , who has traveled to cell  $A$  from an adjacent cell  $B$ , will remain synchronized

to cell B until the power received by this user from base station A exceeds the power received from base station B by  $h = 3\text{dB}$ . Thus, user U is considered to be in cell B although user U is physically located in cell A until a hysteresis power of  $3\text{dB}$  is achieved. As a result, APC requires user U to increase his power in order to reach base station B, thereby increasing the jamming of base station A by user U. Consider now that the handover threshold (or hysteresis) is increased to  $h=6\text{dB}$ . In this case users in cell B jam cell A even more.

These conceptual results are verified in Table 3.3.1 which shows that, for  $S=3$  sectors, the spillover factor  $k$  increases from 0.25 to 0.41 to 0.66 as the handover threshold increases from  $h=0\text{dB}$  to  $3\text{dB}$  to  $6\text{dB}$ . This means that if there are  $n$ , B-CDMA users in each sector of each cell, the interference appears to have been caused by  $(1 + k)n$  users. In Eq. (3.3.1.4), it was assumed that  $k = 1$ . Table 3.3.1 also shows that for the same handover threshold, the spillover factor/or interference increases as the number of sectors increase. This is due to the fact that users in adjacent sectors are detected by the antenna as a result of its finite antenna gain characteristic. Thus users in adjacent sectors may provide interference to the users in a desired cell. In this simulation we employ  $h=6\text{dB}$ .

In addition, since fading decreases with increased bandwidth, less power must be transmitted as the bandwidth increases. Hence spillover decreases with increased bandwidth.

### 3.3.2. Fade Depth

The received signal generally consists of delayed versions of the transmitted signal. These are the multipath signals. Those delayed versions of the signal that arrive within a chip duration and subtract, cause the received signal to "fade". Those multipath signals arriving outside the chip duration result in an increase in the interference level, since these components look like additional CDMA signals; however, they do not produce fading. Furthermore, the power contained in each of these greatly delayed signals is significantly reduced by the "processing gain" of the B-CDMA system. The processing gain is the ratio of the bandwidth of the spread spectrum signal, divided by the information bit rate, which is  $G_c = f_s/f_b = 1250 = 31\text{dB}$ .

The fade depth is inversely proportional to the bandwidth of the B-CDMA signal, i.e., the wider the signal bandwidth, the smaller the chip duration and the fewer the multipath components that fall within a chip duration. Hence, the probability of a frequency-flat fade decreases as the bandwidth increases.

Figures 3.3.2.1 through 3.3.2.3 present the fade probability and fade depth as a function of signal bandwidth. Experimental results were obtained for the bandwidths 48, 30, 22, 11, 2MHz and CW. These experiments were performed in

an office, in the suburbs and in downtown New York City. Note the increase in the fade depth, as a function of signal bandwidth. Note particularly that the fade depth varies only slightly for bandwidths exceeding 11MHz but increases sharply for bandwidths of 5MHz or less. this results are giving us the power of the signal which include the sum of all the multipath, But this measurement does not tell us about the behavior of the signal after despreading which may be one multipath ray or some other multipath that comes within the chip time. most importantly, we doesn't know the amplitude level and phase behavior of that despread signal relative to the other multipath rays that are outside the despread chip time, If we are working with receiver of one "finger" (despreader), The question is, is this finger the best one to use? If this is not the best how much amplitude are we losing? This question led us to build a channel sounder to measure the delay spread to determine if we need RAKE for B-CDMA, and if need a RAKE what type of RAKE?.

### **3.3.2.1 RAKE**

A "RAKE" receiver is a tapped delay line receiver attempts to collect the signal energy from all the received signal paths that fall within the span of the delay line and carry the same information. Its action is somewhat analogous to an ordinary garden rake and, consequently, the name "RAKE receiver". In our case the RAKE receives each multipath signal, delays each by an appropriate amount and then combines them following some algorithm. Thus, a RAKE receiver is a space diversity receiver that uses the fact that multipath signals are arriving from different

directions with different delays and amplitude. This signals are collected in a "time diversity receiver". In our channel sounder experiment, a RAKE receiver was used to display each of the received multipath signals. Figures 3.3.2.4 and 3.3.2.5 show the results obtained when using a scanner receiver to search different time delays for multipath. These experiments were all performed in suburban environments in which the transmitter and receiver were not within line-of-sight of one another. Figures 3.3.2.4 and 3.3.2.5 show the close-in multipath. Note that each pulse is 20ns in duration and that the extent of the multipath is typically less than 120ns. Note also that the power in the multipath signal is about 6dB below the largest returned signal. Figure 3.3.2.6 shows additional experimental results, obtained in Manhattan, using an extended RAKE which views the signal for 4ms. In this experiment a transmitter was placed on the top of a building located on 23rd Street and 6th Ave., in New York City. The receiver was on the ground between 26th and 27th Streets and 6th Ave., out of sight of the antenna. Note that the primary returns were 6 to 10dB, or more, greater than any of the observed multipaths. The last experiment was at Central Park here we again were took measurements of delay spread Initially we were locked to the Line Of Sight (LOS) ray which was the biggest, When we went out of Line Of Sight we kept locking on the same ray that become smaller relative to the other multipath (all the rays were out of LOS at that point), for this type of behavior we need a RAKE unless one can make a coverage area that has, all the time LOS with any base (switching diversity by hand-off from base to base).

Summarizing, we find that wider band B-CDMA systems suffer less fading since the chip duration enables us to break the time interval of multipath spread to subgroups of a time of arrival, each subgroup has duration of a chip time, each subgroup is despread separately: all the despread subgroup is then combined coherently after multiplying with the optimal complex weight. We find that if the chip duration is less than the multipath spread of the channel. then the need for a time diversity system such as a RAKE is small, therefore at 10MHz there is little need for a RAKE receiver. (Of course, a RAKE receiver could be used to further enhance the performance of a B-CDMA system by increasing the processing gain).

### **3.3.2.2 Mobility And Adaptive Power Control**

A spread spectrum base station receives all of the incoming signals simultaneously. Thus, if any signal is received at a higher level than the others, that signal's receiver will have a higher signal-to-noise ratio and therefore a lower bit error rate. The Broadband-CDMA base station insures that each mobile transmits at the correct power level by telling the remote, every 500ms, whether to increase or to decrease its power. This technique is called Adaptive Power Control (APC).

#### **Simulation**

Simulations has been performed by InterDigital. Figure 3.3.2.7a shows a typical fading signal which is received at the base along with 10 other independently fading signals and thermal noise having the same power as one of the signals.

Note that the fade duration is about 5ms which corresponds to vehicular speed exceeding 60mph. Figure 3.3.2.7b and 3.3.2.7c illustrates the results obtained when using a particular APC algorithm. In this case, whenever the received signal changes power, the base station informs the remote and the remote varies its power by  $\pm 1$ dB. Figure 3.3.2.7b shows the APC control signal at the remote. Figure 3.3.2.7c shows the received power at the base station. Note that the APC failed to accurately track the deep fades and as a result 9dB fades resulted. This reduced power level resulted in a  $BER=1.4 \times 10^{-2}$ .

Figure 3.3.2.8a shows the same fade; however, now a different APC algorithm is employed. In this case the control voltage results in the remote unit changing its power by a factor of 1.5 in the same direction, or by a factor of 0.5 in the opposite direction. In this particular implementation the minimum step size was 0.25dB and the maximum step size was 4dB. The resulting control voltage is shown in Figure. 3.3.2.8b and the resulting received power from the remote unit is shown in Figure. 3.3.2.8c. Note that the error is usually limited to +2dB with occasional decreases in power by 5 to 6dB resulting in a  $BER \approx 8 \times 10^{-4}$ , a significant improvement compared to the previous algorithm. The use of interleaving and FEC usually can correct any errors resulting from the rarely observed power dips.

Initially this APC algorithm didn't work correctly at the Overlay field test application because the AMPS users power combined with the CDMA users

practical correction to this algorithm was erasure of a bed control signals that are arriving to the remote unit.

### **3.3.3. The Notch Filter To Increase Capacity**

The notch filter is used to allow an increased number of CDMA users to operate without interfering with the existing AMPS users and also to prevent the AMPS users from interfering with the CDMA users. To accomplish this purpose, the notch filter can be placed in the base and in the remote subscriber; in the transmitter and in the receiver of each. Simulation results show that it is most important to place the notch filters in the CDMA base station.

#### **3.3.3.1. Theory**

The algorithms [11] for narrow-band interference suppression may be classified into two general categories. The nonparametric techniques employ the FFT algorithm for performing a spectral analysis that specify the transversal filter. With this algorithm no prior knowledge regarding the interference is assumed. The second category is based on linear prediction and is termed parametric. The interference is modeled as by passing white noise through an all pole filter.

#### **3.3.3.2. Filter Based On Nonparametric Method**

The basis for the nonparametric method is that the spectrum of the PN sequence is relatively flat while the spectrum of the narrow-band interference is highly

peaked. The first step is to estimate the power spectral density of the received signal once we have the estimate of the power spectral density we can have the transversal filter by doing the IDFT of  $H(k)$  where  $H(k)$  is defined by

$$h(n) = \sum_{k=0}^{N-1} H(k) e^{-j \frac{2\pi}{N} nk}, n = 0, 1, \dots, N - 1 \quad (3.3.3.1)$$

where  $H(k)$  is defined by

$$H(k) = \frac{1}{\sqrt{P\left(\frac{k}{N} F_s\right)}} e^{-j \frac{2\pi}{N} \left(\frac{N-1}{2}\right) k} \quad (3.3.3.2)$$

where  $P(f), 0 \leq f \leq F_s$ , denotes the estimate of the power spectral density and  $F_s$  denotes the sampling rate.

The filter needs to be linear phase This is achieved because  $H(k) = H^*(N - k)$  since  $P(f) = P(F_s - f)$ . Hence,  $h(n)$  is symmetric  $h(n) = h(N - 1 - n)$ . In fact, the filter whitens the spectrum of the incoming signal.

### 3.3.3.3. Filter Based on Linear Prediction

Instead of using the received signal to estimate the spectrum directly the estimate of the narrow-band interference is based on modeling the interference as white noise passed through an all-pole filter. The filter is all-zero filter having zero positions that coincide with the estimated pole positions,

An estimate of the sampled interference  $l(k)$  is formed from the sampled received signal  $r(k)$ , we can predict  $l(k)$  from  $r(k-1), r(k-2), \dots, r(k-m)$ . that is,

$$\hat{i}(k) = \sum_{l=1}^m a_l r(k-l) \quad (3.3.3.3)$$

where  $\{a_l\}$  are coefficients of the linear predictor which are predicted by minimizing the mean square error between  $r(k)$  and  $l(k)$ , which is defined as

$$E(m) = E[r(k) - \hat{i}(k)]^2 = E\left[r(k) - \sum_{l=1}^m a_l r(k-l)\right]^2 \quad (3.3.3.4)$$

Minimization of  $E(m)$  with respect to the predictor coefficients  $\{a_l\}$  is accomplished by using the orthogonality principle in Mean Square Estimation (MSE) this leads to the set of linear equations

$$\sum_{l=1}^m a_l \rho(k-l) = \rho(k), \dots k = 1, 2, \dots, m \quad (3.3.3.5)$$

where

$$\rho(k) = E[r(m)r(k+m)] \quad (3.3.3.6)$$

is the autocorrelation function of the received signal  $r(k)$ . The equations in 3.3.3.5 are called Yule-Walker and can be written in matrix form as

$$R_m a_m = b_m \quad (3.3.3.7)$$

where  $R_m$  is the  $m \times m$  autocorrelation matrix,  $a_m$  is the vector of filter coefficients, and  $b_m$  is a vector of autocorrelation coefficients  $\rho(k)$ ,  $1 \leq k \leq m$ . The matrix  $R_m$  is a Toeplitz matrix which is efficiently inverted by use of the Levinson-Durbin algorithm. By using the predicted coefficients in Eq. 3.3.3.3 we find  $\hat{i}(k)$  the estimate of the interference, and subtract it from  $r(k)$ ,  $[r(k)=s(k)+i(k)+n(k)]$ . The difference  $r(k) - \hat{i}(k)$  is processed further in other to get the data.

Eq. 3.3.3.5 requires knowledge of the autocorrelation function  $\rho(k)$ . There are some methods to predict the autocorrelation function one method is using a block of  $N$  samples of  $\{r(k)\}$  and then direct estimation of  $\rho(k)$  by using

$$\hat{\rho}(k) = \sum_{n=0}^{N-k} r(n)r(n+k), \dots k = 0, 1, \dots, m. \quad (3.3.3.8)$$

Now substitute in 3.3.3.5 and use the Levinson-Durbin algorithm .

#### 3.3.3.4. Performance Simulation. and Implementation

In our implementation we had to notch out up to 100 AMPS signals with minimum spacing of 30khz. The BW of the CDMA signal is 8 MHz (the chip rate is 8 Mcps ). A block diagram of the receiver with notch shown in Figure 3.3.3.1 the spread DS signal is received and filtered & passed through a LNA, filter, Mixer, IF BPF at 70

MHz and BW of 8 MHz, AGC amplifier/attenuator, QPSK demodulator that has two output signals, the in phase (I) and the quadrature (Q), these two signals passed through two matched filters and then converted to digital by using 12 bits A/D with sampling rate of 15.35 MHz, In the baseband notch filter the signal converted to the frequency domain by using a pipe line complex FFT of 1024 points, the 1024 complex output of the FFT is then multiplied by a MASK that is produced by the notch filter controller, the output of the complex multiplier then converted through the IFFT to the time domain. An overlap and add algorithm was used and out of 1024 point we used just 512 points. The notched signal then converted back to analog through a D/A and recover filter. The output of the notched filter is then apply to the despanders and to the QPSK demodulator that implemented digitally as well.

The notch filter was design to work in a fixed mode and in an adaptive mode. In the fixed mode we are notching the fixed AMPS frequencies of the desired base and some frequencies from the neighbor cell if he is in our sectored antenna beam, In the adaptive mode the received signal is sampled at the rate of 1024 times 15 KHz, FFT of 1024 samples performed, and an algorithm that looks for the frequencies need to be notched. The list of frequencies to be notched is transferred to an algorithm that estimate the autocorrelation function, and the filter coefficient. The algorithm simulates the NB AMPS signals as a sum of a narrow-band (30kHz) gaussian noise (colored noise ). The Levinson-Durbin algorithm performed on the estimated autocorrelation function. Then the coefficients for the transversal filter is

calculated (this is the impulse response of the filter). The implementation of the filter was based on the convolution theorem and the overlap and add method, which is performing a FFT transform on the signal and on the filter impulse response, then multiply them and perform an IFFT, while taking care to the "tails" of the FFT.

To achieve a notch depth of 50 dB and a processing gain of 21 dB, we used an AVD of 12 bits and the other calculation in the notch was with higher dynamic range. A MASK (the filter coefficients at the frequency domain) that calculated the notch controller with 29 notched frequencies is shown in Figure 3.3.3.2a and 3.3.3.2b. In Figure 3.3.3.2a the magnitude response of the filter, and one can see that the linear prediction did not yield the required notch depth, Furthermore by looking to the phase response of the filter in Figure 3.3.3.2b we can see that the filter is not linear phase as required.

The output SNR at the receiver is maximized when the receiver consists of a filter, say  $H(f)$  followed by a filter matched to  $H(f)S(f)$ . Thus, a matched filter with frequency response characteristic  $H^*(f)S^*(f)$  will maximize the output SNR. If  $H(f)$  represents the filter with impulse response  $h(t)$ , then  $H^*(f)$  represent a filter with impulse response  $h(-t)$ . Thus, the cascade of these two filters is a filter having an even impulse response. Since we implement the 512 tap FIR filter by using a FFT, it is very easy for us to implement two such cascade filter in the MASK (frequency domain). The complex MASK that was used initially was replaced by a MASK that is

just the magnitude (real) of the complex MASK  $[H(k)H^*(k), k=1,2,\dots,N]$ . Figures 3.3.3.3 show the constellation of a QPSK signal that is shown at the desreader output. Figure 3.3.3.3a show the QPSK constellation after complex MASK with 40 notches one can measure that the SNR is low as 6 dB, In Figure. 3.3.3.3b we used the magnitude MASK with 40 notches and the SNR improved to roughly 19 dB. In Figure. 3.3.3.3c we used a magnitude MASK with one notch at zero (center frequency) and some emphasis on the higher frequencies for matching with the channel, one can see that the SNR improved close to the theoretic processing gain which is 20.5 dB.

#### **3.3.3.5. New Notch Algorithm**

One can see that the notch filter processor using FFT and IFFT is a very powerful and expensive processor. after we proved that the concept of the overlay is a working system we then needed to find a good, inexpensive, and small size, solution. The new solution to the problem is to use a PN that is already notched in the transmitter and in the receiver.

Figure 3.3.3.4 shows the basic block diagram of the spread spectrum transceiver using notch filters. Refer first to the transmitter section. The periodic PN sequence is first notched and then mixed with the data. The data has been interleaved, FEC encoded and low pass filtered. The data-PN product is then up converted, amplified and transmitted. If Figure 3.3.3.12 represents the base station, the data-

PN product for each of the CDMA users is first combined before being inputted to the transmitter block.

In the receiver, the local PN sequence is first notched and then used to despread the received spread spectrum signal. The two notch filters usually identical, and the notch in the base transmitter for user 1 could be matched to the notch in the mobile of user 1 for optimum performance.

The frequencies to be notched can be ascertained in the base by the FFT and also by side information conveyed by the AMPS base station. The frequencies notched in the mobile are sent to the mobile by the base station and could be determined using the FFT shown in Figure 3.3.3.4.

The simulation results presented below emulate a BCDMA overlay on the 10MHz AMPS cellular band. Figure 3.3.3.5 shows a sample function of the 32kb/s data to be transmitted. This data is low pass filtered to 20kHz. The data before and after filtering is shown. Figure 3.3.3.6 shows a sample function of the 8Mchips/s PN sequence used in the B-CDMA overlay. This sequence is band limited to 5MHz to generate an RF bandwidth of 10MHz. The notches were 60kHz wide and, for the purpose of providing an "artistic" picture, were uniformly distributed over 10MHz. The baseband time sequence of the PN signal is therefore band limited to 5MHz. Figure 3.3.3.7 shows the spectrum of the notch filtered PN sequence.

The notches are approximately rectangular since they are generated by the removal of those specific PN frequencies. Figure 3.3.3.8 shows a "zoomed" portion of the received spread spectrum signal with the 40 notches, 40 AMPS interferers (shown here for simplicity as CW interferers) and 101 CDMA users. Figure 3.3.3.9 shows the unfiltered transmitted data as well as the received output data after filtering using a 20kHz filter. Note that some errors in the data exist, however, these are readily corrected by the FEC.

The channel has been implemented and performed with a  $10^{-1}$  BER at  $J/S = 70$  dB, This includes a 50 dB NB interference rejection. (The quantisation error of 8 bits has been used to represent the notched PN code). Figure 3.3.3.10a,b shows the transmit spectrum out of the power amplifier, The notch depth is limited by the compression point of the 200 Watt PA.

#### **3.3.4. Description Of The Overlay Experiment**

The field tests were taken at base station Clive in the Des Moines (latter on we made another field test at base station Ankeny), a cellular system operated by US Cellular. Figure 3.3.4 shows the location of the base stations used in the Des Moines area. Note that there is a considerable variation in power levels due to dips and rises in the terrain.

### **The Overlay Description**

The OVERLAY project has basically two building blocks: The Base and Remote units. Figure 3.3.3.1 show the base block diagram, The base is built from an RF unit, modem boards, notch filter, telephone interface and echo chancellor unit. The remote unit is build from RF unit, modem unit, phone interface and data interface for the video system.

The modem is described in Figure 3.3.4.1. The design is based on a one finger despreader (no RAKE ) with the next specification :

1. Processing gain of 20 dB (0.5 dB implementation lose)
2. Acquisition performance :
  - a) Attack time 6 sec at the remote, 50 ms at the base with scan relative.
  - b) The attack probability is 90% at a J/S=15 dB in 6 second
  - c)The probability of FA is 0.001%.
3. Tracking performance: lost lock at 20.5 dB
4. Power Control Algorithm :, based on close loop algorithm.
5. Modulation technique : QPSK, 76 kbps
6. No hand-off was incorporated yet.

The notch filter was designed to provide 50 dB deep notches However, due to non linear phase problems 30 dB notch depths were obtained.

The power amplifier was designed for a 200 Watt compression point but we actually got just 140 W due to matching problems.

No Hand off - The system at this point is a one cell system and it dose not include hand-off. In the case of a regular single cell, CDMA does not have any real problem, It does not have any Co Channel Interference (CCI). In the case of Overlay we have uncontrolled CCI from the AMPS system. This CCI come from surrounding, covering and overlapping AMPS cells. We found in our first visit to Des Moines, in August 1993, that in some points the difference in power levels received at the mobile from one base to the other base can be more than 30 dB, The solution to the shadowing problem at the edge of a cell is to employ include hand-off diversity between two or three base stations at the mobile as part of a RAKE receiver.

The AMPS antenna used at Clive was an Omnidirectional antenna with a full-load capacity of 40 users. Arriving at the antenna are interference. We got some protection against multipath fading with the price of degradation in our system. B-CDMA antenna was co-located with the AMPS antenna but was sectored to a beamwidth of 105 degrees. As a result the B-CDMA antenna provided 4 dB more gain than the omnidirectional antenna. This is illustrated in Figure 3.3.4.2. The AMPS power transmitted from the base was measured at 20W/users. Thus, when 40 users are present, 800W are transmitted. The CDMA power transmitted from the base was able to be varied from a total power of 5W to a total power of 140W.

These results are illustrated in Figure 3.3.4.3. Note that the product of the cable loss and antenna gain is 11dB for the sectored B-CDMA antenna and 7dB for the co-located omnidirectional AMPS antenna.

The total power received at the Clive base due to the AMPS users is shown in Figure 3.3.4.4. Each point shown in the received power averaged over 1 minute. Figure 3.3.4.5 shows the total power received, averaged during each hour, during a typical 24 hour period. Using Figure 3.3.4.5 we find that the worst case power received at the AMPS base station is -60dBm.

The amount of power seen by the B-CDMA antenna is approximately 5dB below -60dBm since the B-CDMA antenna has a 105° sector and therefore "sees" only 30% of the received power. However, the B-CDMA antenna has an increased antenna gain of 4dB. Hence, the received AMPS power at the B-CDMA receiver is -61dBm.

The power received at the B-CDMA receiver due to the B-CDMA power/mobile was adjusted to be -93dBm and maintained relatively constant by the adaptive power control system described in Section 3.3.2.2. If there are  $N_B$  B-CDMA users in a cell, where  $N_B$  is large, variations in received power from each user, due to imperfect power control, would still result in an average received power of approximately -93dBm.

The power received at the AMPS receiver due to the B-CDMA users is -97dBm since the AMPS antenna has 4dB less gain than the B-CDMA antenna.

#### **3.3.4.1. B-CDMA Spectrum**

The B-CDMA signal used in this test was spread to a bandwidth of 8MHz and data was transmitted at the rate of 64kb/s. Thus, each 64kb/s user corresponds to 8, 8kb/s users. Furthermore, as the data rate decreases, the signal power needed for any user to transmit each bit of data also decreases in order to keep the energy constant. Thus, each 8kb/s signal can be transmitted with 9dB less power than each 64kb/s signal.

#### **3.3.4.2. Signal-To-Noise Ratio**

The S/N ratio assumed needed for good AMPS operation was 17dB. The S/N ratio needed for good B-CDMA reception ( $P_e=10^{-5}$  after FEC decoding) was S/N=4dB.

The results presented in this section and in Section 3.3.5 are summarized in Table 3.3.4.1.

#### **3.3.5. Calculation Of The Number Of Users In The Reverse Link**

In this section, the experimental results obtained are used to calculate the number of B-CDMA remote users. Figure 3.3.5.1 shows the output I channel of the notch filter. The upper curve is the output without connecting the antenna to the system,

The lower one is with the antenna connected but without any CDMA signals in the air. The noise floor of the receiver is at a level of  $K_B \cdot T \cdot 10\text{kHz} \cdot N.F = -174 + 40 + 7 = -127\text{dBm dBm}/10\text{kHz}$ . The CW that are shown after the notch filter are peaking level of  $-100\text{ dBm}$ , If one integrates this spill over AMPS signals in this curve one can get about  $-90\text{ dBm}$  integrated noise which equivalent to two CDMA users, that are arriving at level of  $-93\text{ dBm}$  each.

### 3.3.5.1. At The AMPS Base

The power received at the AMPS base due to a B-CDMA user is  $-97\text{dBm}$ . This power is reduced since the B-CDMA signal has a bandwidth of  $8\text{MHz}$  and the AMPS bandpass filter is  $15\text{kHz}$ . Thus, the attenuation is

$$\text{Attenuation} = \frac{8M}{15K} = 533 = 27\text{dB}$$

The B-CDMA power received, per B-CDMA user, affecting each AMPS user is then (see Table 3.3.4.1)  $-97 - 27 = -124\text{dBm}$ . Referring to Table 3.3.4.1, the minimum power received at an AMPS base station due to a remote AMPS user occurs during hand-off and is greater than  $-92\text{dBm}$ . Thus, the number of B-CDMA users in a cell is  $N_B$ , where  $N_B$  is found from the equation:

$$S/N = 17 = (124 - N_B) - 92 \quad (3.3.5.1)$$

Hence

$$N_s = \begin{cases} 15dB = 31 \text{ BCDMA users operating at } 64 \text{ kb/s} \\ \text{OR} \\ 18dB = 62 \text{ BCDMA users operating at } 32 \text{ kb/s} \end{cases} \quad (3.3.5.2)$$

### 3.3.5.2. AT THE B-CDMA BASE: REVERSE LINK

Using the largest (worst case) averaged AMPS power of -60dBm (Table 3.3.4.1) and noting that the B-CDMA antenna only "sees" 105°(-5dB), so that the B-CDMA has 4dB higher gain, the maximum interfering AMPS power is

$$I_{AMPS} = -61dBm \quad (3.3.5.3)$$

The measured signal received by the B-CDMA base is -93dBm. The interference produced by

Table 3.3.4.1 Experimentally Determined System Characteristics

Characteristic	B-CDMA	AMPS
Antenna	105° sectored	Omnidirectional
$P_T$	adjustable 5W to	20W/user
Antenna Gain x Cable loss	140W	7dB
EIRP	11dB	20dBW/user
	18dBW to 32dBW	
	Total	

Power Received at base per B-CDMA subscriber	-93dBm	-97dBm
Total Power Received at base due to remote AMPS subscribers measured in 8MHz:  Minimum:  Maximum:	-79dBm  -61dBm	-78dBm  -60dBm
Power received at AMPS Base due to one AMPS remote subscriber, normal operating range:  hand-off interval:	N/A	-60dBm to -78dBm  -78dBm to -92dBm
Bandwidth	8 MHz	15 kHz/channel
Number of Channels (Simultaneous Users)	62, 32 kb/s	40 Maximum
Data Rate	64 kb/s	Analog voice

SNR	4dB (to achieve $P_e=10^{-5}$ ) after FEC decoding	17dB
RAKE	none	embedded in the nature of FM
DIVERSITY	none	two elements space diversity at the base
FEC	Rate $1/2$ , $K = 7$ , convolutional code with trellis decoding	None

each B-CDMA interferer level is on the average also -93dBm, and the interference, produced by the B-CDMA and AMPS users, is reduced by the processing gain, PG, where

$$PG = \frac{8MHz}{64kb/s} = 125(21dB) \quad (3.3.5.4)$$

This processing gain is, however, reduced by the notch filters in the receiver. This reduction was measured to be 3dB. The interference produced by each AMPS use is reduced by the notch filter by 30dB.

The signal-to-interference ratio is then

$$\frac{S}{I} = 4dB = \frac{P_B(PG)}{n_B P_B + P_{AMPS} \bullet A_{NF}} \quad (3.3.5.5)$$

where  $N_B$  is the number of B-CDMA users in a sector

$$P_B = -93dBm$$

$$PG = 21dB - 3dB = 18dB \text{ (due to reduction of received power due to Notched Filter)}$$

$$P_{AMPS} = -61dBm \text{ from Table 3.3.4.1}$$

$A_{NF} = 30\text{dB}$ ; attenuation produced by Notched Filter

Then

$$P_B(PG) = -93\text{dBm} + 18\text{dB} = -75\text{dBm} \quad (3.3.5.6)$$

$$P_{AMPS} \bullet A_{NF} = -61\text{dBm} - 30\text{dB} = -90\text{dBm} \quad (3.3.5.7)$$

Since the result in Eq (3.3.5.7) is much less than the result in Eq (3.3.5.6)

$$n_B P_B \sim -80 \text{ dBm} \quad (3.3.5.8)$$

and

$$N_B = 93 - 80 = 13\text{dB} \dots (\approx 20) \quad (3.3.5.9)$$

Thus, there are 20, 64kb/s B-CDMA subscribers in the sector. Hence there are 40, 32kb/s subscribers in the sector and in the cell. This result greatly exceeds the limitation placed by Eq (3.3.5.2). Note that the notched filter in the B-CDMA base receiver is critical for satisfactory overlay operations. The total number of B-CDMA users per cell determined by these results is:

$$N_s = \frac{50}{0.3} = 167 \text{ users\_at } 32 \text{ kbps} \quad (3.3.5.10)$$

This number neglects B-CDMA spill over and voice activity capability.

### 3.3.5.3. At The AMPS Remote Subscriber: Forward Link

As mentioned earlier, the AMPS base transmits 20W/user. The B-CDMA base transmits a total power  $P_{T,B}$  to  $n_B$  B-CDMA users in the 105° antenna sector. This power is increased by 4dB relative to the transmitted AMPS signal due to the difference in the antenna gains. Figure 3.3.5.2a show a received signal at the remote unit during a one CDMA user in the air. The CDMA base was transmit just one CDMA user and a pilot with half power level of a user (10 Watts), one can see that the AMPS SNR is about 27 dB/30 kHz means we can add more 15 CDMA users until we beginning to cause any degradation to the AMPS spec.

Figure 3.3.5.2b is showing similar performance to Figure 3.3.5.2a in distance of 4 miles from the base. Figure. 3.3.5.2c has been taken at a point that has line of site with two base stations during two CDMA users at the air. one can see the problem of spillover at a remote between two base stations and how much it is important to have any kind of diversity with the two received signals from two bases.

$$PG = \frac{8M}{15K} = 27dB \quad (3.3.5.11)$$

A S/N = 17dB is required by each AMPS user. The power  $P_{T,B}$  is reduced by the processing gain

Hence, with an AMPS power of 20W (13dBW)/user,  $S/N = aP_{\text{AMPS}}/P_{\text{T,B-CDMA}}/PG$   
 where

$$P_{\text{AMPS}} = 20\text{W (13dBW)}$$

$$PG = 27\text{dB}$$

and

$a = -4\text{dB}$  to normalize antenna gains

Therefore

$$17 = 13 - 4 - (P_{\text{T,B}} - 27) \quad (3.3.5.12a)$$

and

$$P_{\text{T,B}} = 19\text{dB watt users.} \quad (3.3.5.12b)$$

If 5W (7 dBW) is the minimum transmitted for each B-CDMA user, then without a notch filter in the B-CDMA base transmitter,

$$n_B = 12\text{dB} (=16) \quad (3.3.5.13)$$

Thus, 16, B-CDMA users can operate in the  $105^\circ$  sector at 64 kb/s.

Hence, (neglecting BCDMA spillover and voice activity capability) :

$$N_B = 106, 32 \text{ kb/s B-CDMA users can operate in a cell.} \quad (3.3.5.14)$$

If a transmit notch filter is used with, say a 10dB attenuation, the power, per B-CDMA user, need to be increased due the lose in the processing gain by 3dB (to 10W) and there are then

$$N_B = 19\text{dB} (\_79) \text{ B-CDMA, 64 kb/s users in the } 105^\circ \text{ sector} \quad (3.3.5.15)$$

This number clearly exceeds the B-CDMA user limit set in Eq. (3.3.5.2).

#### **3.3.5.4. At The B-CDMA Remote Subscriber: Forward Link**

Let the power transmitted by the B-CDMA antenna be  $P_{T,B-CDMA}$ . The power transmitted by the AMPS omnidirectional antenna is  $20 \times 40 = 800\text{W}$  (29dBW). The interference at the B-CDMA remote user then has two components;

where

$$P_I = P_{T,B} + a P_{AMPS} \quad (3.3.5.16)$$

and

$$P_{AMPS} = 29\text{dB} - 4\text{dB} = 25\text{dB} (\_ 316) \quad (3.3.5.17)$$

where

$a = -4\text{dB}$  is due to the difference in antenna gains.

Letting  $P_{T,B} = n_B \cdot 10\text{W}/\text{user}$  where there are  $n_B$  users in the sector covered by the CDMA antenna.

We see that

$$P_{T,B} = 10 + n_B \text{ in dBW} \quad (3.3.5.18)$$

Hence, the signal to interference ratio at a B-CDMA subscriber is:(neglecting spillover from other bases )

$$\frac{S}{I} = \frac{10PG}{10(n_B - 1) + 316} \quad (3.3.5.19)$$

Thus,

$$\frac{S}{I} = 4dB = 10dB + 21dB - 10 \log_{10} [10n_B + 316] \quad (3.3.5.20)$$

Therefore,

$$27dB = 501 = 10n_B + 316 \quad (3.3.5.21)$$

and

$$n_B = 18.5 \text{ users} / 105^\circ \text{ sector} \quad (3.3.5.22)$$

There are therefore

$$N_B = 61, 64 \text{ kb} / \text{s} \text{ or } 122, 32 \text{ kb} / \text{s} \quad (3.3.5.23)$$

B-CDMA users in the cell. This number exceeds the number of users found in Eq. (3.3.5.2). Therefore, as expected, the B-CDMA overlay capacity is determined by the reverse link at the AMPS base station.

### 3.3.6. Reverse Link Simulation For APC

During the OVERLAY experiment it appeared that the APC reference level at the base can be programmed for the AMPS system. In this simulation we trying to fined

the capacity of the CDMA as a function of the level that the AMPS and the CDMA signals set to be receive at the base.

The general formula for mobile radio propagation shown in Eq. 3.3.6.1 was used

$$P_r = (P_t - 40) - 61.7 - 38.4 \log \frac{r}{1 \text{ mi}} + 20 \log \frac{h_{\text{base}}}{100 \text{ ft}} + 10 \log \frac{h_{\text{mobile}}}{10 \text{ ft}} + (G_t - 6) + G_m \quad (3.3.6.1)$$

were  $G_t$  is the base antenna gain (CDMA:  $G_t = 15$  dB 60 degrees sectored antenna, AMPS:  $G_t = 9$  dB, omnidirectional),  $G_m$  is the mobile antenna gain = 3dB,  $h_{\text{base}}$  is antenna base height = 250 feet,  $h_m$ -antenna high remote is 5 feet,  $P_t$  remote = 3 Watts.

Other parameters for the simulation were lognormal shadowing  $\sigma=8$ dB, 48 AMPS users per base were assumed, Base CDMA notch depth assume 30 dB, cell radius  $R = 8$  miles.

The output of the simulation is shown in Tables 3.3.6.1, 3.3.6.2, 3.3.6.3 where we can see the number of CDMA users with SNR=3dB as a function of CDMA set level (change from -75dBm to -107.5 dBm ) and the AMPS set level ( change from -80 to -60 dBm ). The last row in the table show number of CDMA users while the worst case AMPS users SNR kept to be 17 dB minimum (neglecting rayligh fading ). the

crossing point between the two criteria gives the number of CDMA users available at that sector.

Tables 3.3.6.1, 3.3.6.2, 3.3.6.3 are runs of the simulation for three thresholds (TH) for the adaptive notch filter, The thresholds are determined if a notch filter will apply on a particular AMPS interferer. Table 3.3.6.1 show that for TH of -92 dBm the number of B-CDMA users is between 16 to 19 for BCDMA APC level of -87.5 dBm, It is shown that the number of notches that are applying for frequencies from the neighbor cell is between 20 to 23.

Table 3.3.6.2 show that for TH of -97 dBm the number of B-CDMA users is between 17 to 19 for B-CDMA APC level of -87.5 dBm. It is shown that the number of notches that are set for frequencies from the neighbor cell is between 25 to 31.

Table 3.3.6.3 shows that for TH of -102 dBm, the number of B-CDMA users is between 17.6 to 19.3 for B-CDMA APC level of -87.5 dBm, It is shown that the number of notches that are set at frequencies from the neighbor cell is between 30 to 39.

From the tables it appears that the APC algorithm for the CDMA must be accurate and a shift by 2.5 dB can cause some AMPS users at the edge of the cell to work with SNR of 14.5 dB If one wants to reduce the interference one needs to cut the

amount of the CDMA users by almost half. It looks, from the tables that the APC level of the AMPS is not critical unless The CDMA is required to work with levels that are less then -90dBm.

## **4. OVERLAY FH-CDMA**

### **4.1 Introduction**

A FH/CDMA system is proposed here for cellular telephony system. The frequency band used consists of two separate bands, one for transmission and the other for reception. For the OVERLAY application, existing users within each band may be "locked-out", as shown in Figure. 4.1, i.e., the frequencies chosen in the hop set are chosen to exclude those "locked-out" frequencies.

The resulting OVERLAY system is expected to significantly outperform conventional cellular systems by allowing far more users to use the same bandwidth than conventional cellular systems. In addition, the system can coexist with other fixed frequency microwave users.

In order for the OVERLAY-FH-CDMA to operate properly we need to feel the same four condition from 3.1. This mainly achieve by not using the same frequencies for the FH-CDMA system and the AMPS. The proposed FH system include a six sectored base station, maximal ratio diversity at the base, switching diversity at the base toward the remote is assumed, six rings of underlay/overlay for coverage area and Forward Error Correcting Code with erasure.

### **4.2 Approximate FH-CDMA Capacity Analysis**

The capacity of the FH-CDMA is given by:

$$N = \frac{W \cdot B}{R} \cdot \frac{1}{VA} \cdot FR \cdot FEC \cdot SEC \cdot FNLO \quad (4.2.1)$$

Where:

N-Simultaneous calls per cell.

W-spread spectrum bandwidth.

B- efficiency of modulation techniques.

FEC-the rate of the forward error correcting code.

R- rate of digitized voice.

VA-voice activity (voice duty cycle).

FR-Frequency reuse factor.

SEC-number of sectors in cell.

FNLO- frequencies not locked out factor.

For example if one uses W=10Mhz, VA=1/2, R=8Kbps, FR=1, FEC=1/2, QPSK modulation => B=1.3 =>channel spacing = R/(FEC\*B) = 12.5KHz, FNLO=1 and SEC=6 we will have max. 4800 calls per cell. In the OVERLAY case each FH CDMA sector will not use the AMPS frequencies of his cell and the frequencies that are used by the neighbor cell, that is within the sector coverage, this will eliminate 2/7 of our available frequencies at the 10 Mhz bandwidth so the factor FNLO will be 5/7, at this case N will reduce to 2740 per cell or 457 users per sector, This N can be increased by using adaptive algorithm to lockout AMPS frequencies that are interfered with the CDMA system.

### 4.3 System Description

The building blocks of the FH/CDMA system are shown in Figure 4.3a. Here the voice is first digitized. The hopping rate is 500 hops (SFH). Variable data rate of 8, 16, 32, 64, 144 kbps, can be offered for comparison We will show here 8 kbps. The Forward error correction (FEC) and erasure encoding is employed with rate 1/2 to 1/3, The modulation technique is QPSK with shaping using the square root of a raised-cosign filter (QPSK-SRC) The FH-CDMA system is orthogonal (see Figure 4.3b )& synchronous, i.e., all the remotes and the base unit changing frequencies at the same time, with 50 microsecond dead time between hops. The frequencies sequences are Reed Solomon (RS) code words, All the users within a sector/section are using the same sequences of frequencies but each one has a different cyclic shift i.e. no two users will have the same frequency at the same time. Users from different sector or cells are using different sequences such that no two users will collide more than once. The diversity that used is space diversity with up to four antennas with maximal ratio combined, The diversity at the remote unite is assumed to have up to four switching diversity controlled by the base. We divided the area surrounding the base to six sectors by using six sectored antenna at the base as shown in Figure 4.3c. We divided the cell to six concentric rings as shown in Figure 4.3.d each has different set of frequencies and different set level for Automatic Power Control (APC).Figure 4.3.e show rings and sectors combined.

For the OVERLAY FH-CDMA system we added a FFT processor to estimate the AMPS frequencies that are used by any cell that is within the sectored antenna (include our cell ) and to lockout this frequency from the FH list.

#### **4.3.1 Concentric Rings to Reduce Interference**

In an attempt to prevent intercellular interference, It is proposed to divide the cell into six concentric rings about the base stations, as shown in Figure 4.3.d. The bandwidth B was also divided into six groups and one group of frequencies was allocated to each ring each group of frequencies are spread in all over the band for achieving maximum frequency diversity. Thus, a user  $u_j$  in cell A, at a distance  $\rho^4$ , from the base station will be given a frequency  $f_{5,j}$ , falling within the frequencies of  $F_5$ , allocated to that ring. It is seen from Figure 4.3.d that the group of frequencies marked  $F_5$  in cell A is at a different radius from the base station than the group of frequencies  $F_5$  in cells B or C. The reason for this is to minimize the intercellular interference and thereby reduce the probability of error.

Note that a mobile user in cell A at frequency  $f_{5,j}$  in band  $F_5$  when transmitting to its base\_receives mobile-to-base interference from the six mobile users at frequency  $f_{5,j}$  in band  $F_5$  in the six surrounding cells. Interference caused by users in more distant cells can be neglected; the signal strength from mobiles in those cells to the base of cell A are severely attenuated since power decreases by at least the 4<sup>th</sup> power of the distance[3]. We assume a 4<sup>th</sup> power attenuation.

In order to explain why different system configurations were selected, it is useful to calculate the worst-case signal-to interference S/I ratio at the base of cell A. Consider that each group is allocated 10MHz/(6\*12.5) ≈ 133 frequencies. Then in group F4 there are about 133 mobile users, transmitting at frequencies  $f_{4,i}$ , to  $f_{4,133}$  using QPSK, and each user having a bandwidth of about 12.5kHz. It is possible that six interfering mobile users (each at the same frequency  $f_{4,i}$ ) one in each of the six surrounding cells, could be at a point closest to the base station of cell A, thereby creating maximum interference. Consider Figure 4.3.1.1 Since the interfering power received at the base station of cell A comes from mobiles  $u_B$  and  $u_C$ , and noting that the power decreases with the 4<sup>th</sup> power of the distance, we have in band F, :

$$\frac{S}{I} = \frac{P_A / S^4}{\left[ \frac{P_B}{8^4} + \frac{P_C}{9^4} \right]} \quad (4.3.1.1)$$

Assuming that  $P_A = P_B = P_C$  No automatic power control

$$\frac{S}{I} = 1.34 \quad (4.3.1.2)$$

In such a worst-case scenario, which, of course, has an extremely small probability of occurrence, the S/I ratio would be unacceptably small. In 4.3.4 we will show how power control is improving the S/I.

In Figure 4.3.1.2a,b,c,d,e,f a simulation results of a regular base station is shown, the simulation assumption about propagation and transmit power of the base is the same as the simulation at 3.3.6.0 and no shadowing. In Figure 4.3.1.2a we see the users distributed all over the cell (for convenient the cell appear as a circle instead of hexagon ), In Figure 4.3.1.2b we see the power that spill to a desired cell that seat at phase zero its look from the Figure that the neighbor users that are close to the desired base have about 13 dB higher interference, In Figure 4.3.1.2c we see the outage probability that is, the probability that the received signal at the desired base will be less then certain SNR, for SNR as parameter going from -10 dB to 40 dB it looks that under condition of no shadowing ( $\sigma=0$ ) and perfect power control the worst case SNR is zero dB, Figure 4.3.1.2d show the probability density function of the SNR.

Erasure Reed Solomon code is applied, where each symbol is transmitted in different frequency (hop ) and a block code is spread over 15 hops.

Figure 4.3.1.2.e,f show the block error rate of the received signal as a function of the SNR threshold for declaring symbol as erasure. for RS(15,5) and RS(15,7).

Figures 4.3.1.3a,b,c,d,e,f,g repeat Figure 4.3.1.2 but the standard deviation for the shadowing is  $\sigma=8$ .

Figures 4.3.1.4 a,b,c,d,e,f,g repeat Figure 4.3.1.3 for six concentric rings about the base stations, By looking at Figure 4.3.1.4.c we can see that the outer ring suffer from a bad outage as it shown in Eq. 4.3.1.2.

#### **4.3.2. Sectorized Antennae Can Minimize Interference**

By using directional antenna at the base we get improvement of the power received at the mobile unit. the mobile units received signal is the combined direct and reflected signals from scatters located in all directions around the Mobil and by that the RMS delay spread can be reduced dramatically which reduce the need of equalizer to combat against ISI (Inter symbol interference) caused by multipath fades. However the use of directional antenna at the mobile unit will add some gain. But it would limit reception to a certain angular sector. consequently, it is more or less to maintain level of reception over an omnidirectional coverage area.

The use of sectorized antenna minimized the Co-Channel Interference(CCI) (the power that spills over from one cell to the neighbor cell up link or down link).

In order to reduce the worst-case S/I condition described in Sec. 4.3.1, 6-sector antennae are selected, as shown in Figure 4.3c. In this case, each base station uses 6 antennas and each antenna transmits to users in its sector.

The worst-case mobile-to-base station interference occurs from a single user whose signal can be seen from the base station. This is illustrated in Figure 4.3.2.1

where we see user  $u_A$  communicating in band  $F_1$  at a frequency  $f_1$  to the base station at cell A. User  $u_B$  in cell B (below cell A in the Figure), is also transmitting in band  $F_1$  at the same frequency  $f_1$ . Since  $u_B$  is within the antenna beam width of the base station in cell A, user  $u_B$  will interfere with user  $u_A$ . However, it is readily seen that no other user in any of the other adjacent cells will interfere. Thus, assuming  $P_A = P_B$  the worst-case S/I produced by  $u_B$  is  $S/I = 16$  (=12dB). The average S/I is, of course, much higher.

Figures 4.3.2.2a,b,c,d,e,f,g shows the simulation results of base divided to 6 sectors with  $\sigma=0$ . In each sector there are now N users, in the cell we have 6N users. the outage (Figure 4.3.2.2c ) show some degradation compare to non sectored ring (with the price of six time the capacity )

Figures 4.3.2.3a,b,c,d,e,f,g shows the simulation results of base divided to 6 sectors with  $\sigma=8$ , The block error rate is almost unaccented.

### **4.3.3 Rings Sectored Antennas Can Minimized Interference.**

For achieving maximum capacity, The technique that is proposed here uses a "frequency group" consisting of rings with sectored antennas to minimize interference. In order to theoretically eliminate the intercell interference, the use of 6 rings with 6-segment antennae is considered. As seen from Figure 4.3.d each ring is sectored so as to insure no interference from users in adjacent cells.

For example, consider (4.3.d) the mobile user  $u_A$  shown in the outer ring in cell A in frequency band  $F_2$ . Interference to its sectored base station in cell A could only come from a mobile user  $u_B$  in inner ring at cell B in the band  $F_2$ . Since band  $F_2$  is divided into 6 sub bands, it is readily arranged that the frequencies used in  $F_2(A)$  do not correspond to the frequencies in  $F_2(B)$  within the same sector. Using this design, consisting of rings and sectors, there is no Interference between adjacent cells (ignoring multipath).

#### 4.3.4 Forward Power Control

Forward Power Control (FPC) is the adjustment of the power transmitted by the base to achieve a fixed receive power at the mobile. FPC can be employed to minimize the base-to-mobile interference. The purpose of FPC is to insure that the signal power transmitted by the base, received in any frequency ring, is the same. Thus, in Figure 4.3.d using FPC, more power would be transmitted to mobiles far from the base than to mobiles close to the base. Assuming a perfect FPC, the power received by a user  $u_1$ , a distance  $r_1$  from the base, would be the same as the power received by a user  $u_2$  a distance  $r_2$  from the base. If their transmitter powers are  $p_1$ , and  $p_2$  respectively, then

$$\frac{p_1}{p_2} = \left( \frac{r_1}{r_2} \right)^4 \quad (4.3.4.1)$$

Referring to Figure 4.3.4, base station A transmits, at frequency  $f_1$  a power  $p_A$  to user  $u_A$  a distance  $r_a$  from the base. Let base station B transmit, at frequency  $f_1$ , a

power  $p_B$  to user  $u_B$  a distance  $r_b$  from base station B. User  $u_B$  then receives a signal power  $S$  equal to

$$S = \frac{P_B}{(r_b)^4} \quad (4.3.4.2)$$

and an interfering power,  $I$ , where

$$I = \frac{P_A}{\rho^4} \quad (4.3.4.3)$$

If FPC were not used,  $P_A = P_B$  and

$$\frac{S}{I} = \left(\frac{\rho}{r_b}\right)^4 \quad (4.3.4.4)$$

If FPC is used,  $P_B = P_{ref_{mobB}} \cdot (r_b)^4$   $P_A = P_{ref_{mobA}} \cdot (r_a)^4$  so that

$$\frac{S}{I} = \left(\frac{\rho}{r_a}\right)^4 \frac{P_{ref_{mobB}}}{P_{ref_{mobA}}} \quad (4.3.4.5)$$

Thus, FPC does not consistently provide a S/I improvement. unless one will design the reference power and the frequencies carefully.

#### 4.3.5 Reverse Power Control

Reverse Power Control (RPC) requires that a mobile user is received at its base with the same power regardless of where in the cell the mobile is positioned.

- To determine if RPC can improve the S/I, refer to Figure 4.3.3

Assume that cells A and B have a radius  $r_0$ . Let  $u_A$  be placed a distance  $r_a$  from its base and  $u_B$  be placed a distance  $r_b$  from its base and on a line connecting both bases. Then the S/I is

$$\frac{S}{I} = \frac{P_B}{P_A} [2r_0 - r_b] \quad (4.3.5.1)$$

Without RPC,

$$\frac{S}{I} = \left( \frac{2r_0 - r_b}{r_b} \right)^4 \quad (4.3.5.2)$$

However, with RPC,  $P_B = P_{ref_{msgB}} (r_b/r_0)^4$   $P_A = P_{ref_{msgA}} (r_a/r_0)^4$

$$\frac{S}{I} = \frac{P_{ref_{msgB}}}{P_{ref_{msgA}}} \left( \frac{2r_0 - r_b}{r_a} \right)^4 \quad (4.3.5.3)$$

Since  $r_b$  can be larger or smaller than  $r_a$ , this type of RPC has no consistent advantage in this system, unless one will design the reference power and the frequencies carefully.

#### 4.3.6 Rings and Sectorized Antennae Can Increase Capacity C By A Factor of 6

##### 4.3.6.1 Reverse Link

The capacity of the system depicted in Figure 4.3.d can be increased by a factor of 6 if we:

- I. Let each sectorized-ring contain all of the frequencies allocated to that sectorized-ring. For example, each sectorized-ring  $F_2$  contains the same 133 frequencies.

II. Let the power transmitted by a user in a given ring be controlled by the base station and follow the rule shown below:

Ring	Band	Power Transmitted
outer	F2	$P_o$
	F3	$P_o$
	F1	$P_o$
	F4	$1.4P_o$
	F6	$3P_o$
	inner	F5

Using this set of transmitted powers, one can readily show that the worst-case S/I = 15dB and occurs for users in bands F1 and F4. The values for the transmitted power shown above have been selected to maximize the S/I ratio, neglecting adjacent sector interference and multipath.

If the spacing of the rings were selected to allow an equal user density, i.e., each sector-ring is of equal area as shown in Figure 4.3.6.1, the power transmitted in each ring is as follows:

Ring	Band*	Power Transmitted
Outer	F2	P.
	F3	P.
	F <sub>4</sub>	P.
	F4	1.12P <sub>0</sub> .
	F6	1.5P <sub>0</sub> .
inner	F5	2.4P <sub>0</sub> .

Then one can readily show that the worst-case S/I is 8.5dB. The values of the transmitted power shown above have again been selected to maximize the S/I ratio, neglecting adjacent sector interference and multipath.

Figure 4.3.6.2a,b,c,d,e,f,g, 4.3.6.3a,b,c,d,e,f,g are showing the improvement of apply different APC level to each ring for regular base (no sectors) where in Figure 4.3.6.2 the standard deviation  $\sigma=0$  and in Figure 4.3.6.3 the standard deviation  $\sigma=8$ .

Figure 4.3.6.4a,b,c,d,e,f,g, 4.3.6.5a,b,c,d,e,f,g are showing the improvement of apply different APC level to each ring for base that divided to rings and sectors where in Figure 4.3.6.4 the standard deviation  $\sigma=0$  and in Figure 4.3.6.5 the standard deviation  $\sigma=8$ .

Figure 4.3.6.6e,f,g, 4.3.6.7c,d,e,f,g are showing the average (all the rings ) improvement of apply different APC level to each ring for base that divided into rings and sectors, Where in Figure 4.3.6.6 the standard deviation  $\sigma=0$  and in Figure 4.3.6.7 the standard deviation  $\sigma=8$ .

#### 4.3.6.2 Forward Link

Figure 4.3.6.8 show the SNR of user that is located in a cell with rings (no sectors ) and APC correction, The user is located at different points and rings it is shown that the worst case location gives 7 dB SNR, The performance of the forward link are comparable to the performance of the reverse link.

#### 4.3.7 Choosing the Hop Duration

The above discussion neglected the effect on system performance of multipath fading. However, in Fig 4.3.7.1 one can see that a narrow band (12.5kHz) signal can fade by more than 14dB, When such fades occur, it is possible for the S/I to decrease dramatically and produce a significant number of errors.

Indeed, the primary purpose of frequency hopping is to move a signal at a frequency  $f_i$ , which is fading, to a new frequency  $f_j$  which may not be fading. However, to use the entire frequency band effectively, all frequencies must be used, even those which fade. Unfortunately, the fading frequencies vary with geography, cars, people, and office environment, so that there is no guarantee of a

to good" non-fading frequency. the solution for that is space diversity as it will show next. but sec 4.3.2-6 show that we need to protect our self from spillover (CCI).

One of the main criteria for the hop duration is the channel delay, the channel delay most to be less then 10 ms if we wont to avoid echo canceller in the system. On the other side long code word with interleaving will help to average the effect of a bad hop.

I propose a hopping rate which can accommodate bit rates from 8kb/s to 144kb/s, i.e., 8kb/s, 16kb/s, 32kb/s and 64kb/s, 144Kb/s. Higher data rates may require an equalizer as a result of multipath returns causing intersymbol interference. A proposed frame structure is shown in Figure 4.3.7.2 Since the frame is 0.5 ms in duration, the hop rate is 2khops/s. If Forward error correction using a rate -  $\frac{1}{2}$  to  $\frac{1}{3}$  will be use. Erasures are used since the presence of a deep fade during a hop is readily detected. the interleaving depth time will be ~ 8ms (16 hops), this 8ms delay does not require an echo-canceller for voice. In the simulation that perform in sec. 4.3.2-4.3.6 for RS (15,7) QPSK modulation with data rate of 8 kbps the channel rate is  $(15/7) * 8$  with nearly two symbols per hop the hop rate become  $(15/7) * 2 +$  (time between hope~50 micro sec. ). If we will add some signaling with the data we will have channel rate that is close to  $\frac{1}{3}$  (data rate of 24 kbps ).

#### **4.3.8 Diversity**

The performance of a FH system can be improved dramatically through the use of space diversity. With this procedure, two to four antennas at the base station receive the mobile's transmission and, using the optimal, maximal-ratio combining technique, obtain 2-4 order diversity. Furthermore, since it is known which antenna has received the stronger signal at each of the mobile's hop frequencies  $f_i$ , then during the next hop the base transmits to the mobile, at the same frequency  $f_i$ , using the antenna which received the larger power.

This procedure is illustrated in Figure 4.3.8 In this Figure, the transmit and receive bands are called the X and Y bands. The mobiles and the base station select frequencies from both bands. Note that the base transmits at the mobile's hop frequency one hop later. In this case, the multipath seen is "almost" reciprocal, particularly since a frame is only 0.5 msec.

Using the above procedure, the base has 2-4 maximal ratio combining and the mobile achieve 2-4 order switched space diversity, without any increased complexity in the mobile's handset.

#### **4.3.9 Hand-off**

The system design presented above depends on the ability of a mobile user to switch frequency bands when moving from sector-to sector and/or from ring-to ring. There is also a corollary requirement to provide an adequate number of

frequencies in the sector to accommodate different quantities of users. For example, in Figure 4.3d we can accommodate a maximum of 200 users per sector/ring. If 201 users appear in a sector and only, say, 150 users appear in an adjacent sector/ring, the sector size should be adjustable to meet the demand. This section addresses these concerns.

The frequency hopping mobile user changes frequency (hops) every 0.5ms. Thus, every second there are 2000 hops. When the base station records a power level decrease over a reasonably large number of hops, say 100 hops (50ms), it tells the mobile to switch to a new band of frequencies. In addition, as the mobile moves from sector-to-sector or from one cell to another, the mobile receives a slow hopping pilot signal sent from each sector. Thus, only 6 pilot signals are required to effect hand-off between sectors or cells. That is, the mobile receives the pilot signals from all nearby sectors. If a pilot signal strength exceeds that of its present pilot by a meaningful amount, then the mobile can request hand-off.

#### **4.3.10 Overlay**

In order to overlay on the fixed service microwave user, one of two approaches can be employed:

In the first approach, we recognize that the mobile users in a cell would affect, at most, one microwave user. The base station, knowing which band of frequencies is used by the microwave user, "locks-out" that band so that the number of users in

the band is significantly reduced. For example, if the allocated band is 15MHz and the microwave user has a bandwidth of 10MHz, then the number of users in the cell is only one-third of the maximum possible capacity. In the case of AMPS overlay the frequencies that are used by the desired and the covered neighbor AMPS base station will not use by the FH/CDMA system at the same base stations, so the capacity of the FH-CDMA will reduce to 5/7 of the available capacity.

#### **4.3.11 Modulation Technique**

Figure 4.3.11 show that by using Generalized Tamed FM with channel spacing of 6.25 KHz it is required  $E_b/N_0$  OF 11.9 dB at  $P_b=10^{-2}$  in AWGN with Adjacent Channel Interference Protection Ratio (ACIPR)of 13.22dB and by using Differentially-Coherent QPSK with square-root of raised-cosign filtering (DCQPSK-SRC) it is required  $E_b/N_0$  OF 7.25 dB at  $P_b=10^{-2}$  with Adjacent Channel Interference Protection Ratio (ACIPR)of 62.93dB. one can see that QPSK-SRC can give improvement of up to another 3dB, by using APC that relax the ACI requirement.

#### **4.3.12 Synchronous Orthogonal FH/CDMA**

It is recognized that as the number of users in a net increases, the possibility of two users hopping on to the same frequency band increases. Such an occurrence is called a collision and results in a significant increase in the probability of error.

If  $N$  bits occur during each frequency hop, a collision could result in a high probability of  $N/2$  bits being in error. Thus, the hop rate, which effectively governs the number of bits/hop, affects the maximum number of simultaneous CDMA users. Using the proposed synchronization technique presented here, collisions will be significantly reduced.

A FH CDMA system requires a time and frequency design approach. For example, as shown in Figure. 4.3b each user is given a set of frequencies  $f_1$ - $f_n$  on to which they can hop. Since a cell communicates simultaneously with  $K$  users it is proposed to transmit synchronously from the cell to these users. Thus there can be no collision in cell-to-user communication. In the AMPS system cells are spaced 15000 feet apart. Hence, the maximum distance from user-to-cell is 7500 feet. Assuming a hop rate Of FH - 2000 hops/s, the duration of a hop is 0.5ms, a time much larger than the time for a signal transmitted by a handiest to reach a cell (7500ns). In the PCS systems cells are spaced 1200 feet apart. Hence, the maximum distance from user-to-cell is 600 feet and the propagation time is 600ns.

As a result of the use of micro cells, the synchronization problem is greatly reduced. Indeed a hopping rate of 2 khops/s in a cellular system virtually eliminates all synchronization problems include those from users in adjacent cells.

To do this, each user would synchronize its transmission to the start of a received frequency hop. The transmissions received at the cell from each user would then be delayed by no more than  $2(d_{\max})$  measured in nanoseconds. Thus, for users no further than 15000 feet from a cell, the maximum delay between users is 30000ns round trip. and by adding in between the hops 50 microsecond dead time (no transmission ) we are going to eliminate any collision, In another word we guarantied synchronization FH.

The hopping sequences are designed to be orthogonal within a sector/ring, i.e., no two such sequences will have the same frequency The hopping sequences are designed for a less then one collision between two rings/sectors that are using the same set subset of frequencies. This was achieved by using a Reed Solomon code Figure 4.3.12a show for example a generator matrix with primitive element  $\alpha=5$  in  $GF(q)$  were  $q=23$ , the generator matrix is

$$G = \begin{bmatrix} 1 & 1 & 1 & \cdot & \cdot & \cdot & \cdot & \cdot & \cdot & 1 \\ 1 & \alpha & \alpha^2 & & & & & & & \alpha^{q-1} \end{bmatrix} \quad (4.3.12)$$

The code has length  $q-1$  and minimum distance  $q-2$  the code word generated by  $C=(n,r)*G$  Figure 4.3.12b show  $(n,r)$ for  $r=1$ ,  $r$  can go  $1.....q-1$  for  $q-1$  sets.

Figure 4.3.12c shows one set of 22 ( $q=23$ ) sequences. Figure 4.3.12d show table of Crosscorrelation of sequence # 1 with all the other sequences one can see that there is just one collision between two sequences.

#### **4.3.13 Synchronization**

Synchronization is always a major consideration in any spread spectrum system, but in a commercial, CDMA system it is even more critical. The reasons for this are (1) there are many users in the system, and hence the probability of a false synchronization is high, and (2) the synchronization system must be inexpensive. Synchronization consists of two parts: acquisition and tracking. This second task is extremely important in determining the needed processing gain and the code duration used.

The synchronization system proposed here is to have each cell transmit a "pilot" synchronization hopping sequence in addition to the  $K$  hopping sequences containing data.

Each user synchronizes to the pilot sequence. In a 7-cell code reuse system there will be 7 pilot sequences, one for each cell. The user searches all possible sequences and locks to the largest signal which then dictates the users operational cell.

A typical acquisition and tracking circuit showing is shown in Figure. 4.3.13. In this Figure, the center frequency of the incoming signal is  $w_i$ . Each  $T_H$  seconds (the hop duration) this frequency changes. The modulation (digital voice or data) is shown as  $\phi(t)$ . The bandpass filter has a bandwidth capable of passing the modulation. The local output of the frequency synthesizer "camps" and waits, at frequency  $w_0 + w_j$ , where  $w_0$  is the IF frequency and  $w_j$  is any one of the  $L$  hopping frequencies selected. When energy is detected at the frequency  $w_j$ , the synthesizer is hopped to the next frequency  $w_{j+1}$ , etc. The number of frequencies that must be considered to "assure" synchronization is a function of the number of interferes,  $K$ .

#### 4.3.14 Coding

Sec. 4.3.2-4.3.6 shows the effect of several  $(N,K)$  RS codes (15,5),(15,7) and (15,9). In the final system with 6 sectors and 6 rings it is shown in Figure 4.3.6.7c,f that in CCI from a near sector we can get  $10^{-5}$  to  $10^{-6}$  Block error rate. The CCI that need to be considered is all the CCI users that are covered by the base sector antenna, By simulation we found that the other five users that are using the same frequency are contribute on the average the same amount of spillover like the nearest sector., According to the SNR is degraded by 3 dB. According to that the (15,5) RS code will be safer. By deploying the voice activity algorithm the outage probability of the system is dropped by a factor of two and according to that the RS

(15,7) is good. One may consider, concatenated code like soft decision convolutional code with a RS code.

## 5. CONCLUSION

It has been shown that Spread Spectrum modulation is an excellent choice for implementing cellular systems. It can provide very high capacities and excellent quality service compared to the performance of existing modulation techniques. SS CDMA can be particularly attractive for an Overlay application.

### OVERLAY B-CDMA

Figure 6.1 is a complete simulation performed by InterDigital Corp. A plot of B-CDMA users vs. AMPS users is shown where both use a 1, 3 or 6 sector antenna. Both transmit and receive notches are utilized in the base. The B-CDMA data rate is 32 Kbps, the bandwidth is 10MHz, and voice activity detection is not employed. Tables 3.3.6.1 & 2 presents simulation data of the overlay system with emphasis on the APC levels. These results compare favorably with the 64 and 32 Kbps data rate 8 MHz B-CDMA experimental results obtained in the Clive and Ankeny B-CDMA overlay experiments.

We note that as the AMPS traffic decreases, the B-CDMA capacity for traffic can be increased dramatically. Furthermore, the rule-of-thumb, which states that the B-CDMA capacity in a clean channel should be:

$$N_B = W / 4f_b \quad (6.1)$$

is verified in Figure 6.1.

If wired-line voice quality is required, a data rate of 32kbps is needed.

**Speech Quality** - for Broadband-CDMA you can operate at 16 and 32 kbps. A narrower band CDMA requires the use of synthetic vocoders. This imposes minimum end-to-end delays of mobile to mobile communications of over 200 ms. In other words, B-CDMA has the quality of a satellite link.

Broadband-CDMA can support data rates up to ISDN rates, i.e., data rate on demand. Narrowband-CDMA never claims to be able to go beyond a limit of 9.6 Kbps.

Broadband-CDMA performs better indoors as well as outdoors than a narrower band CDMA. The reason for this is the significantly increased multipath rejection that you get from the wider bandwidth.

**Frequency management** - there is no frequency management necessary for Broadband-CDMA, it occupies the full 10MHz. Therefore it simplifies operations and deployment.

**Transition procedure** - at the very beginning there will be many AMPS users in the band. The number of cellular users are expected to grow over the next decade. However, as the number of AMPS users decrease, more and more CDMA users

can be deployed. Even, initially, while the AMPS users are plentiful no channels have to be removed. While AMPS operation continues, Broadband-CDMA is operating, overlaying on the same band, sharing the band, with the AMPS users.

Finally, Figure 6.2 shows the Efficiency, in terms of simultaneous Users/MHz, of FDMA, TDMA and CDMA. Note that B-CDMA has the highest capacity, since it minimizes the effect of multipath.

#### ***FH-CDMA***

It has been shown that FH like DS has very good potential, especially when the sectors and the rings approach is deployed. Overlay capability is a natural characteristic of Frequency Hopping. Simply avoid using (hopping into) frequency channels that are in use by others! It has been shown that with 6 sectors and 6 rings and with FEC of rate 1/2 to 1/3 we can gain a capacity of 4800 to 3200 users running at an 8 KHz rate. Voice activity detection is used as a last resort for reduce the CCI interference between sectors and bases. In another words FH-CDMA can have 320 to 480 users per MHz. This is a big number that will not have use in the immediate next five years so, initially, one can take some of features out and begin with a smaller capacity system with perhaps 100 users per base.

## Figures

PCSI

# Tentative Frequency Plan

No PCS

M = Major Trading Area License  
B = Basic Trading Area License

U-V = Unlicensed Voice  
U-D = Unlicensed Data

CC = Common Carrier  
MDS = Multipoint Distribution Systems

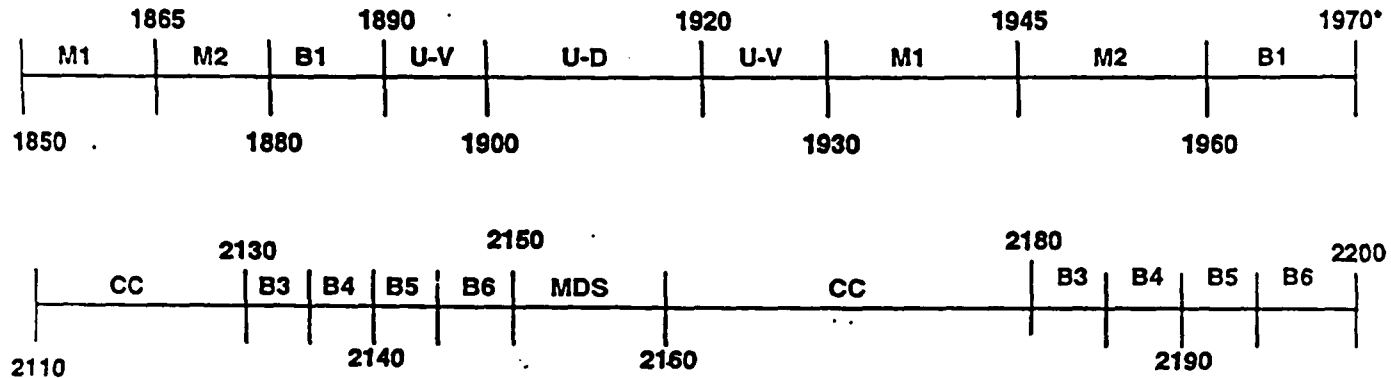


FIGURE 1: Tentative Frequency Plan.

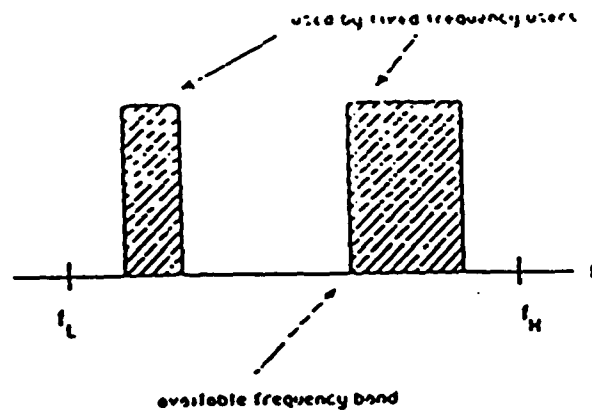
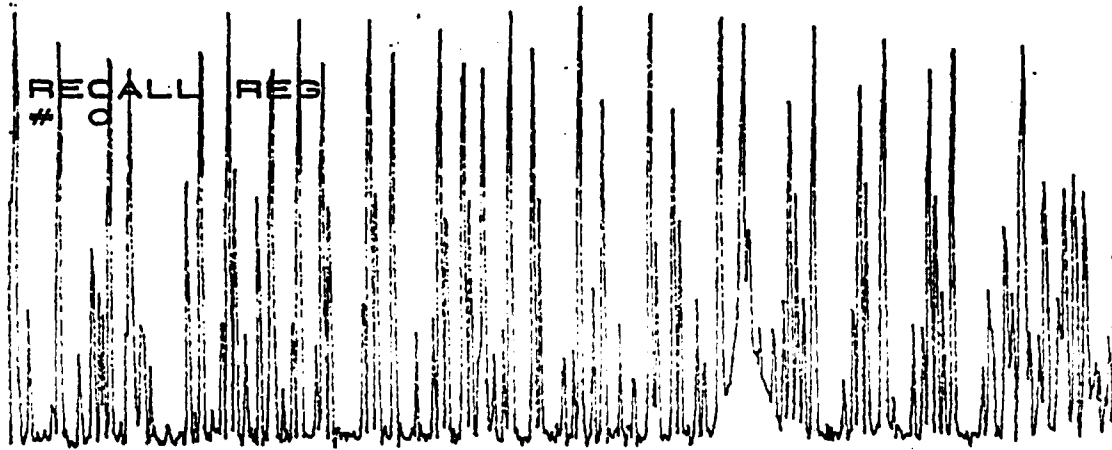


FIGURE 1.1a: SHOWING THE CONGESTION  
IN A SHARED FREQUENCY BAND

ATTEN 10dB  
RL -30.0dBm 10dB/



CENTER 875.70MHZ SPAN 10.00MHZ  
\*RBW 1.0KHZ \*VBW 300HZ SWP 90sec

Figure 1.1b: Showing the congestion in a AMPS cell.

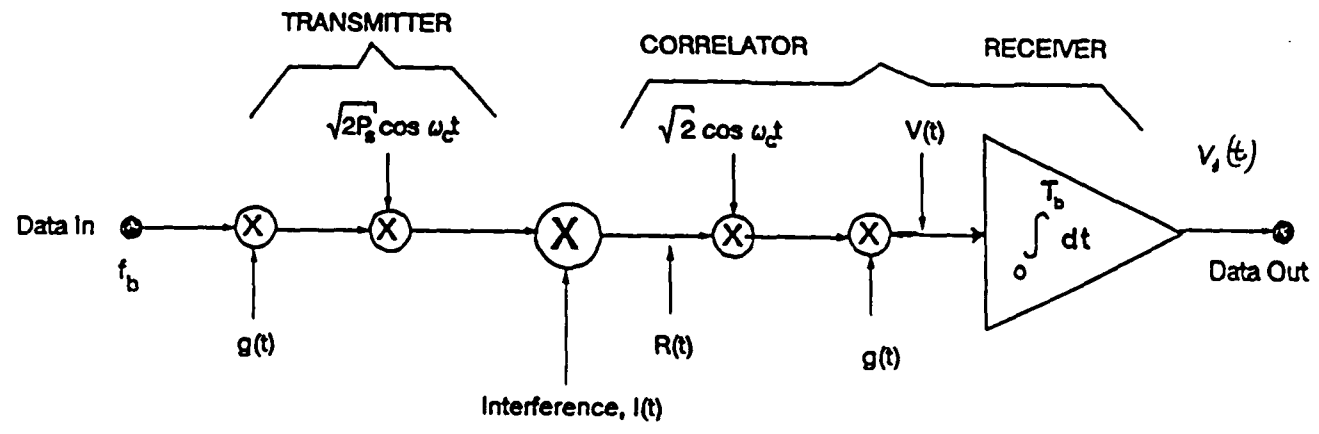


Figure 2.3a: Simplified Spread Spectrum Direct-Sequence System

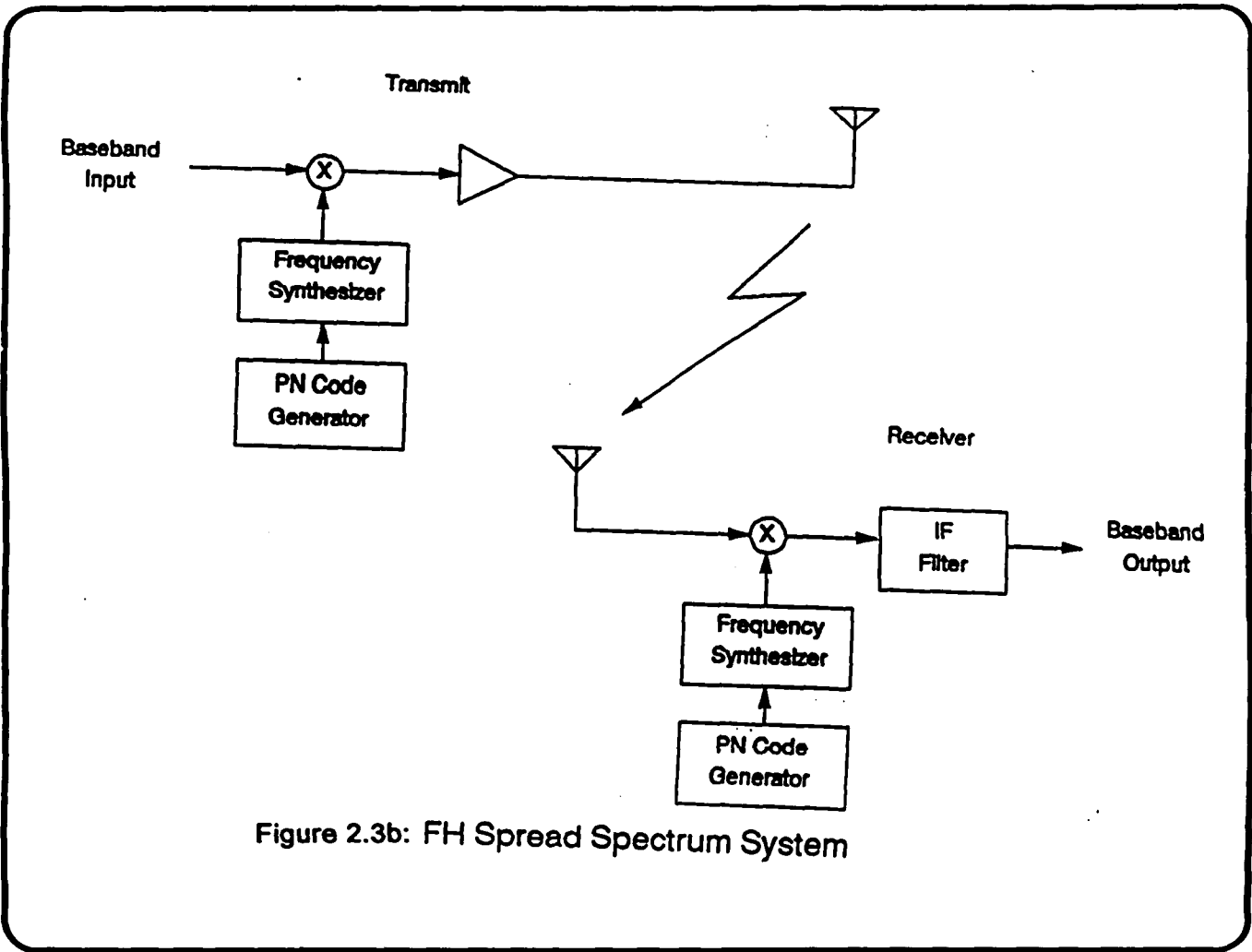
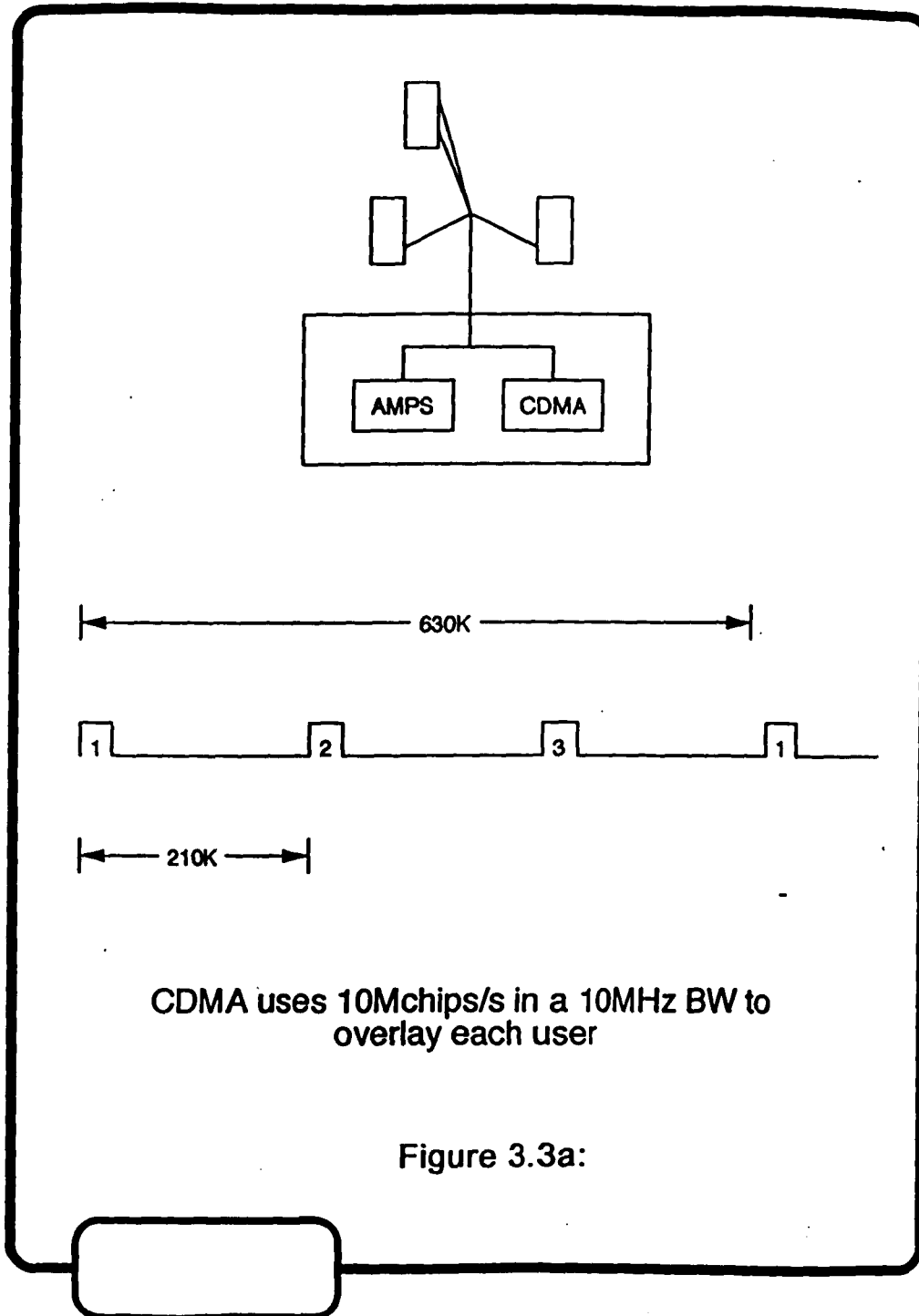
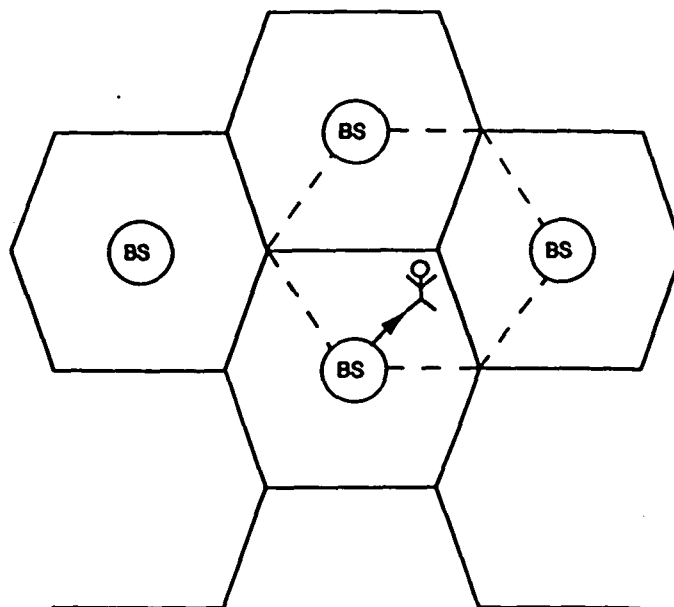


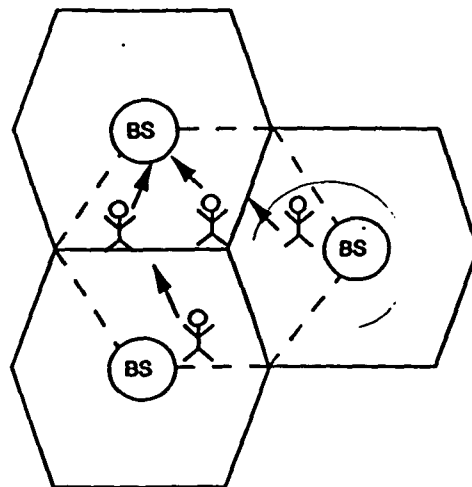
Figure 2.3b: FH Spread Spectrum System





- (1) CDMA BS Does Not Jam The AMPS Mobile
- (2) AMPS BS Does Not Jam The CDMA Mobile

**FIGURE 3.3b:**



(3) CDMA Mobiles Do Not Jam The AMPS BS

(4) AMPS Mobiles Do Not Jam The CDMA BS

Figure 3.3c:

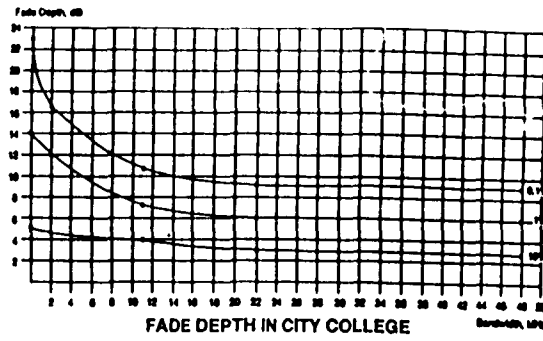


Figure 3.3.2.1:

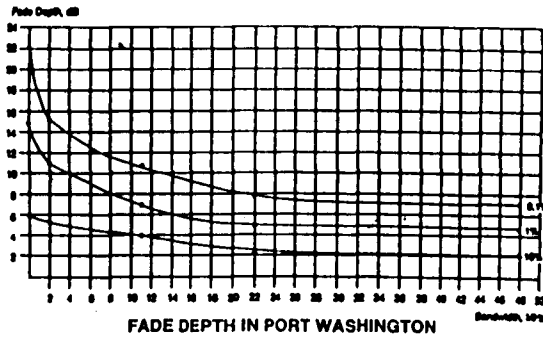


Figure 3.3.2.2:

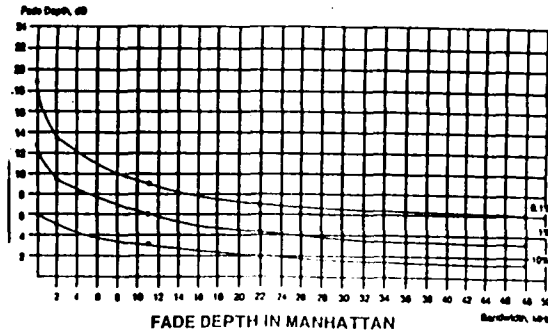
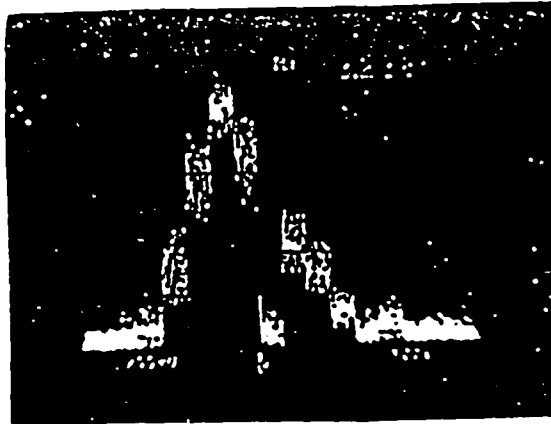


Figure 3.3.2.3



**Figure 3.3.2.4:**

Transmitter And Receiver Are  
Out-of-Sight Of One Another

500 ns Full Scale  
40 ns Each Dwell

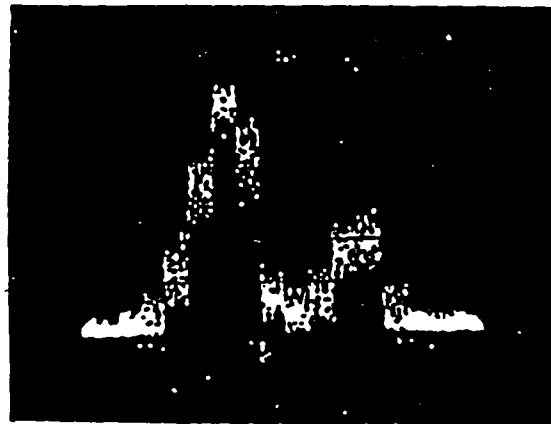


**Figure 3.3.2.5:**

**Delay Spread in Port Washington.**

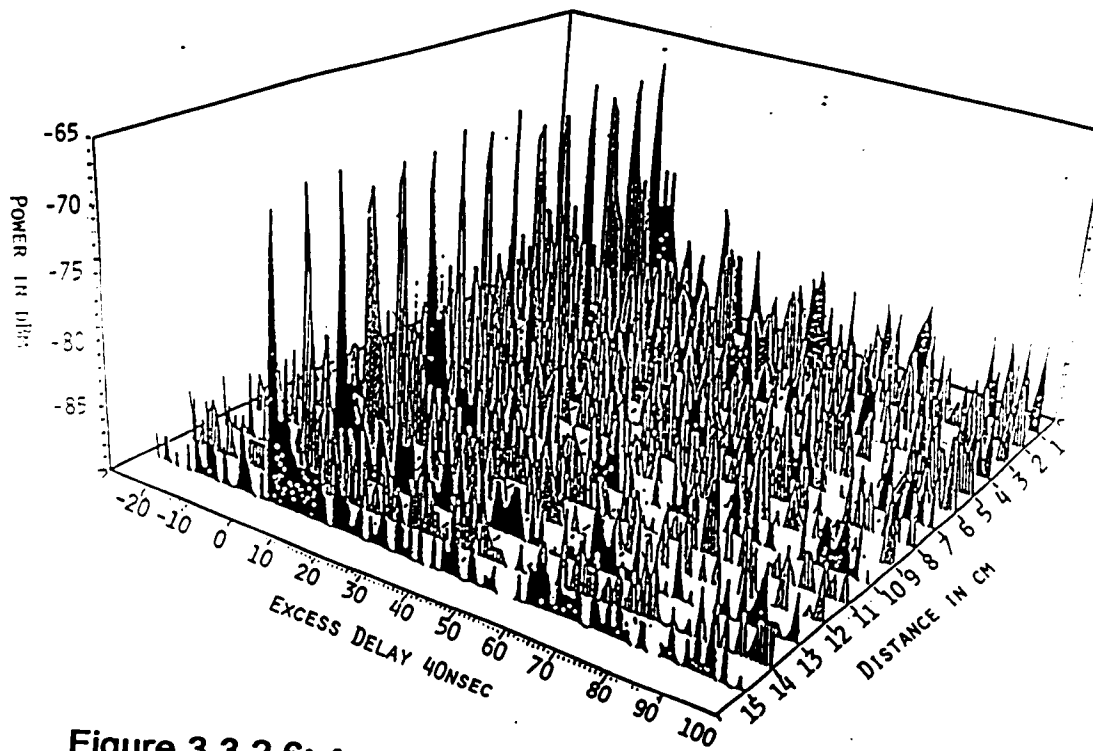


Figure 3.3.2.6: 6TH AVE. BETWEEN 27 AND 28 STREETS

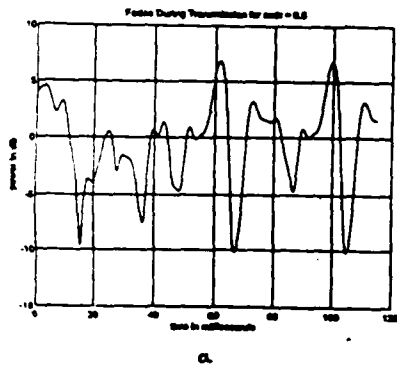


Figure 3.3.2.7a:  
Faded signal.

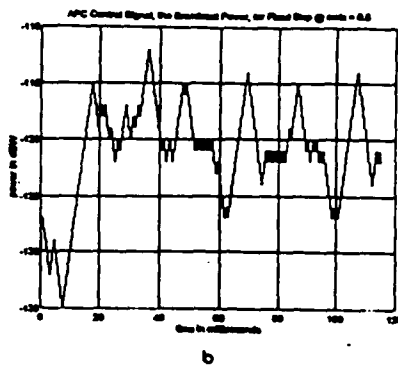


Figure 3.3.2.7b:  
APC control Signal.

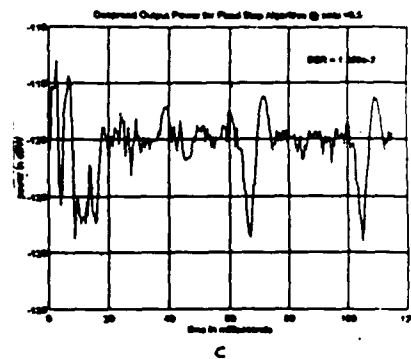


Figure 3.3.2.7c:  
Despread Output power for fixed step algorithm.

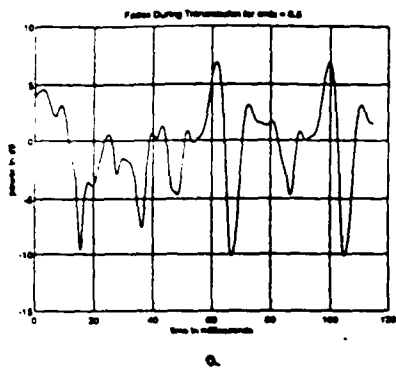


Figure 3.3.2.8a: Faded signal

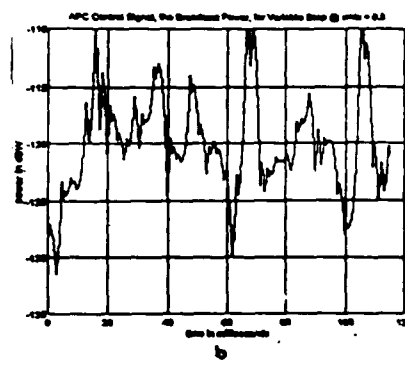


Figure 3.3.2.8b: APC control Signal.

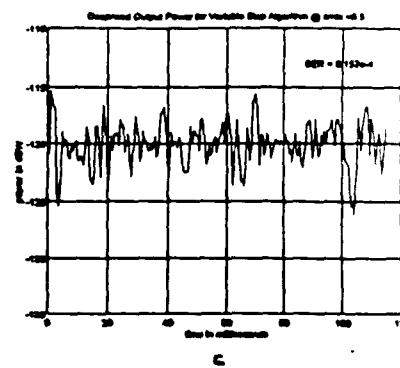


Figure 3.3.2.8 c:  
Despred Output power for adaptive step algorithm.

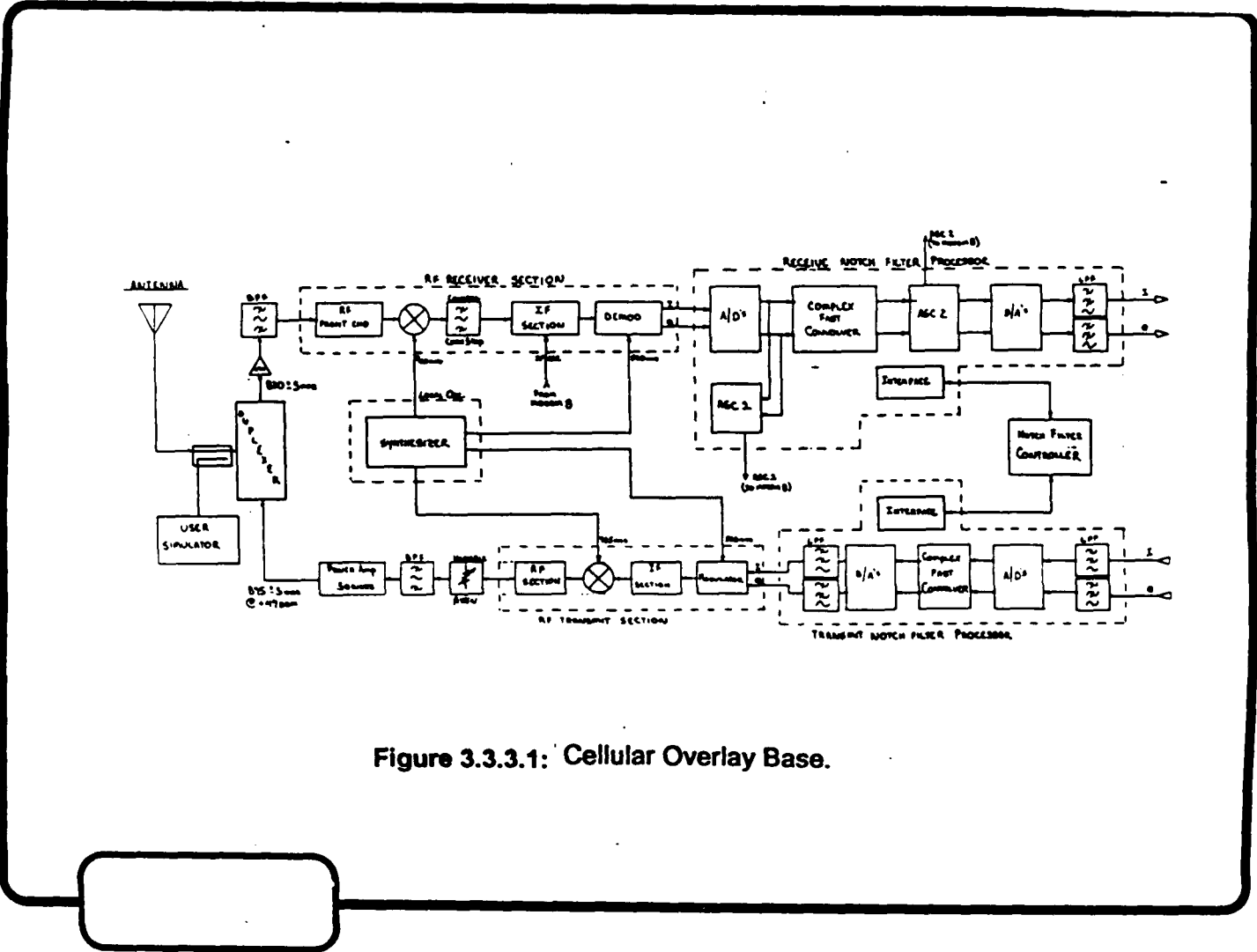


Figure 3.3.3.1: Cellular Overlay Base.

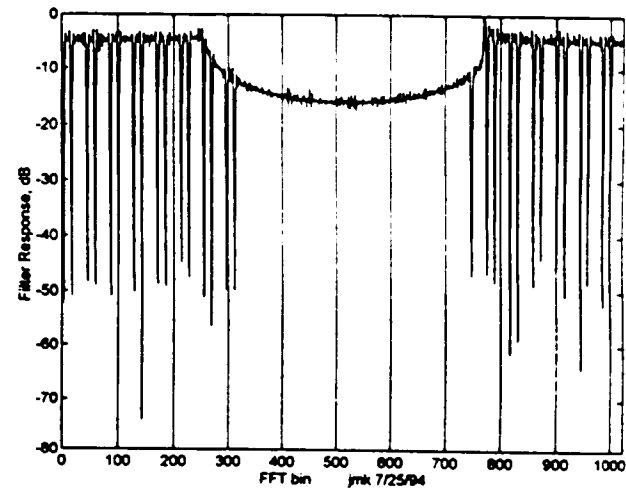
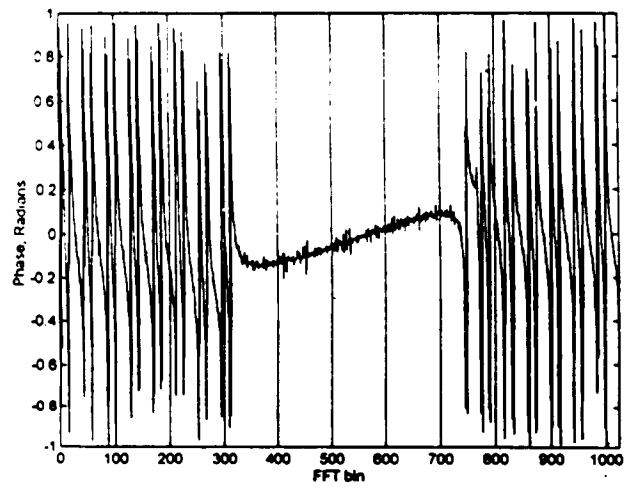
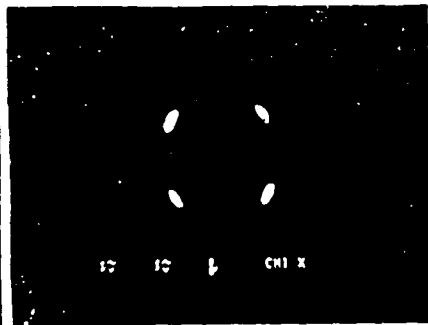


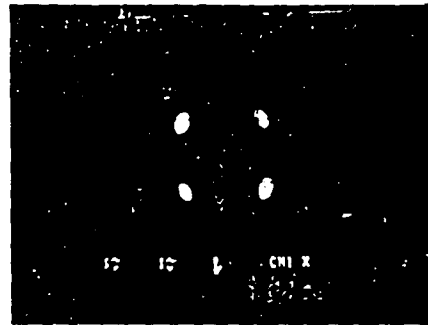
Figure 3.3.3.2a: Complex notch filter Phase response.

Figure 3.3.3.2b: Complex notch filter amplitude response.

Figure 3.3.3.2c:



**Figure 3.3.3.3c:**  
Output QPSK Constellation of Magnitude  
Notch Filter-No Notches.



**Figure 3.3.3.3b:**  
Output QPSK Constellation of Magnitude  
Notch Filter-50 Notches.

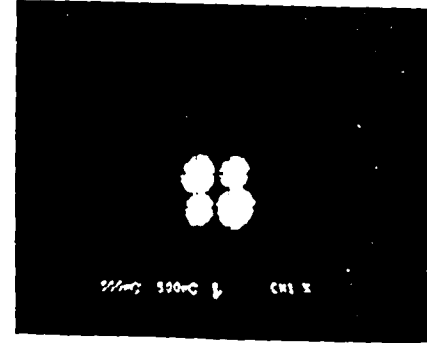
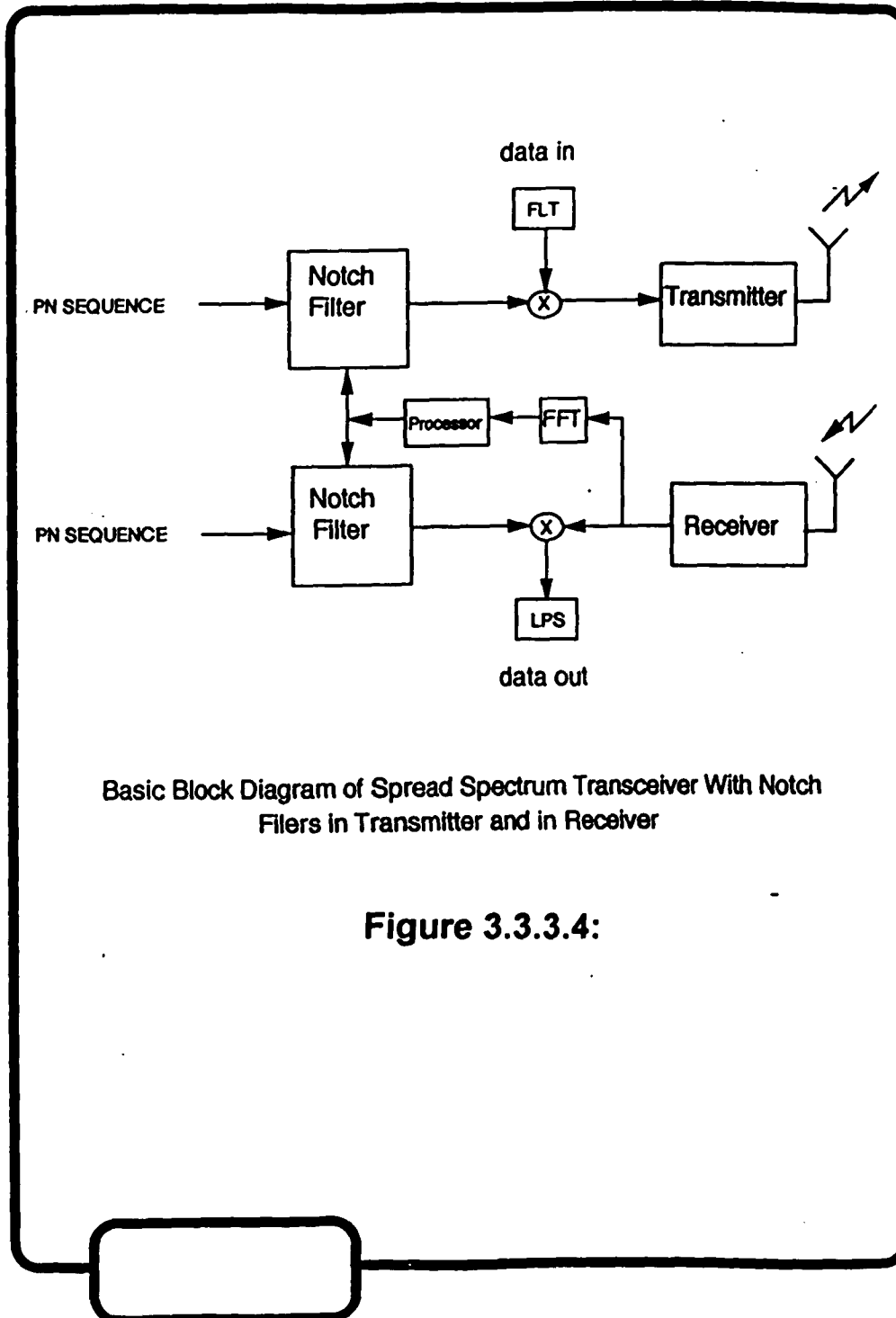


**Figure 3.3.3.3a:**  
Output QPSK Constellation of Complex Notch Filter.

**Figure 3.3.3.3**



Basic Block Diagram of Spread Spectrum Transceiver With Notch Filters in Transmitter and in Receiver

Figure 3.3.3.4:

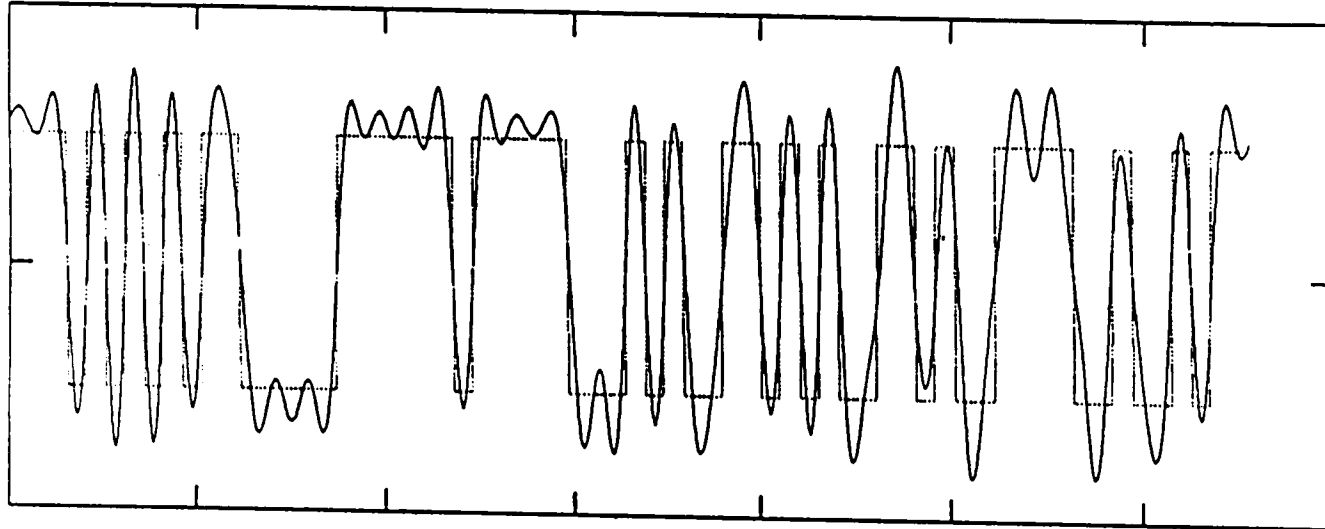
1 CDMA User

0 AMPS Jammers

0 Notches

0 CDMA Jammers

VOLTAGE



TIME

TRANSMIT 32kb/s DATA, LPF AT 20KHz

Figure 3.3.3.5:

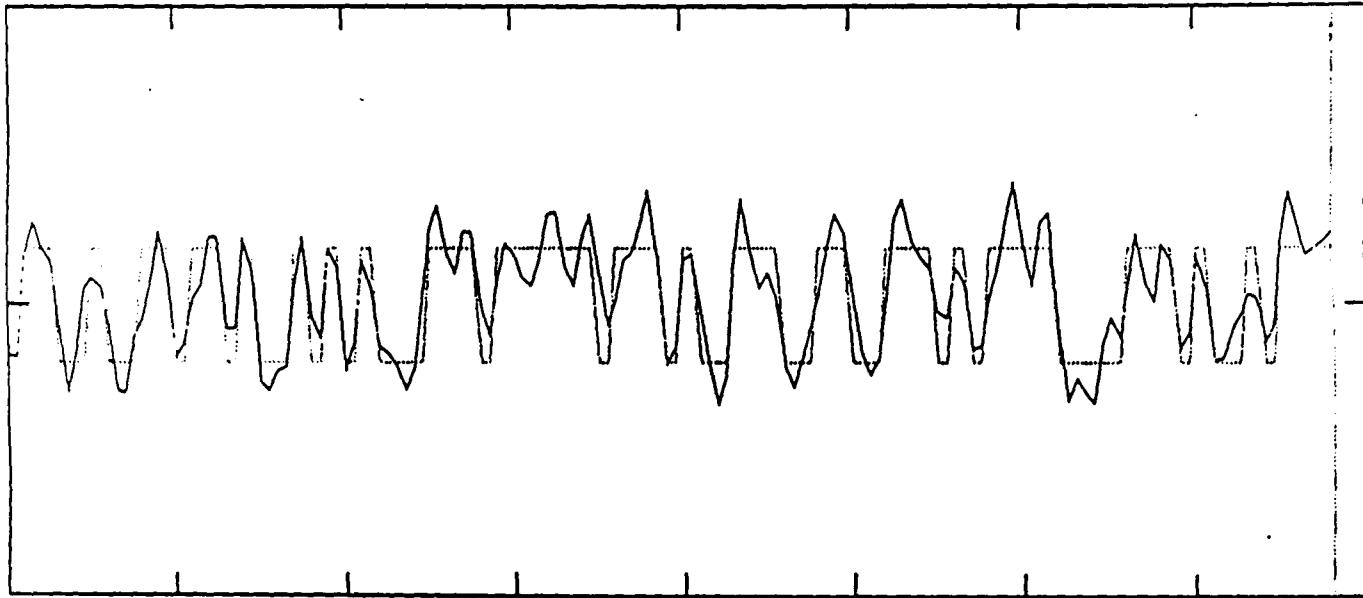
1 CDMA User

40 AMPS Jammers

40 Notches

100 CDMA Jammers

VOLTAGE



TIME

**8MCHIPS PN SEQUENCE**

**Figure 3.3.3.6:**



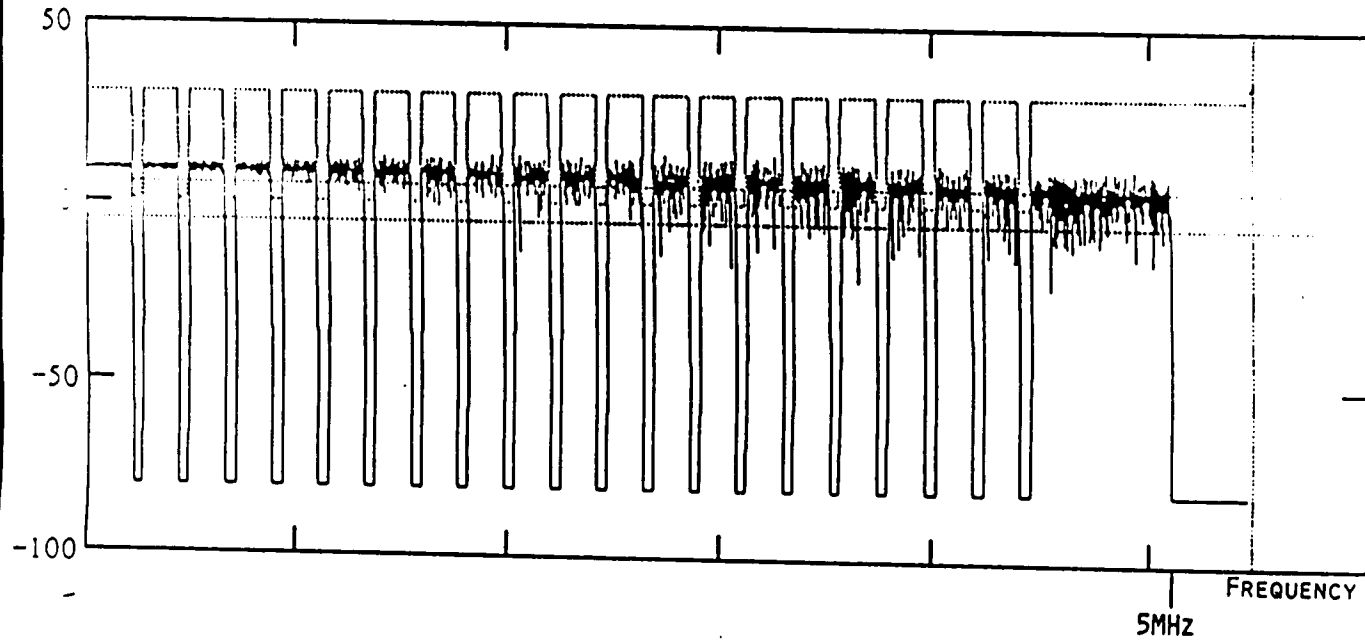
1 CDMA User

40 AMPS Jammers

40 Notches

100 CDMA Jammers

SPECTRUM, dB



SPECTRUM OF A NOTCHED FILTERED PN SEQUENCE

Figure 3.3.3.7:

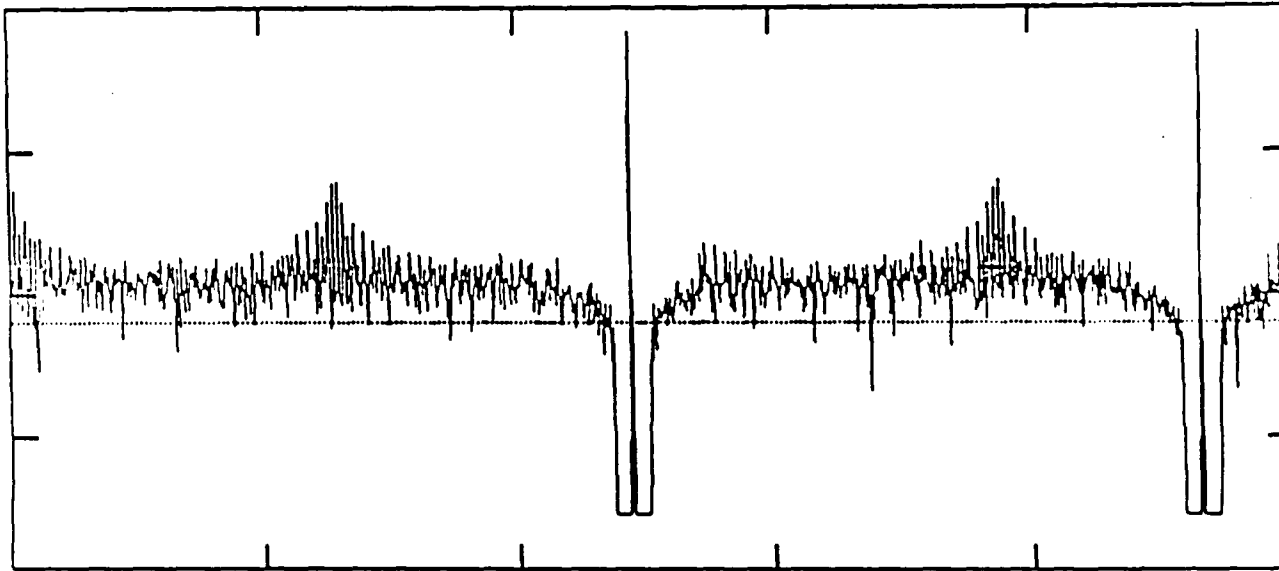
1 CDMA User

40 AMPS Jammers

40 Notches

100 CDMA Jammers

VOLTAGE



TIME

**ZOOMED RECEIVED SPECTRUM**

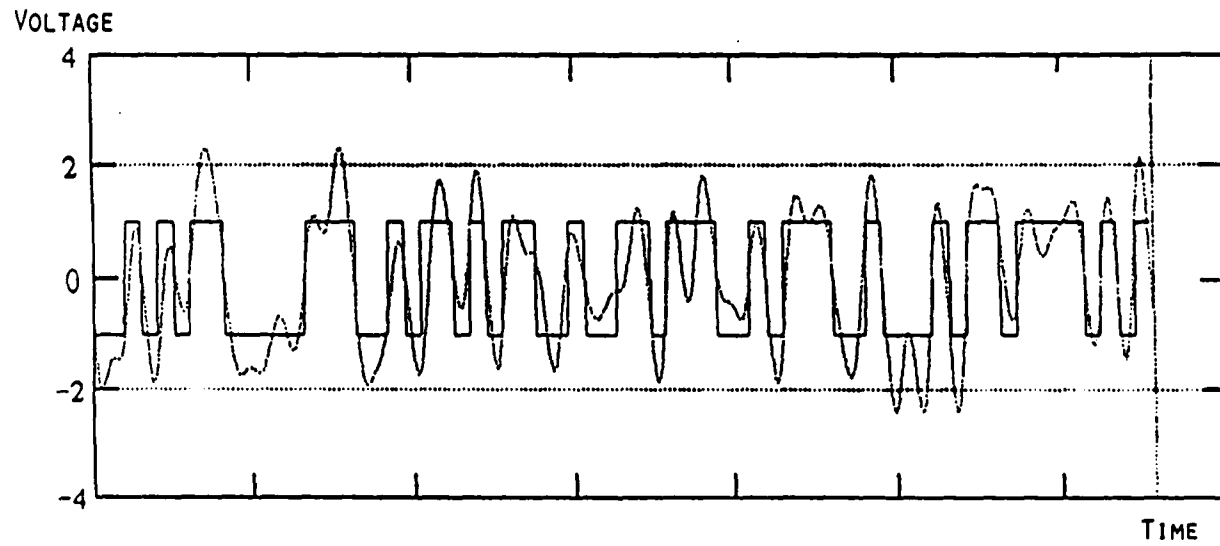
**Figure 3.3.3.8:**

1 CDMA User

40 AMPS Jammers

40 Notches

100 CDMA Jammers

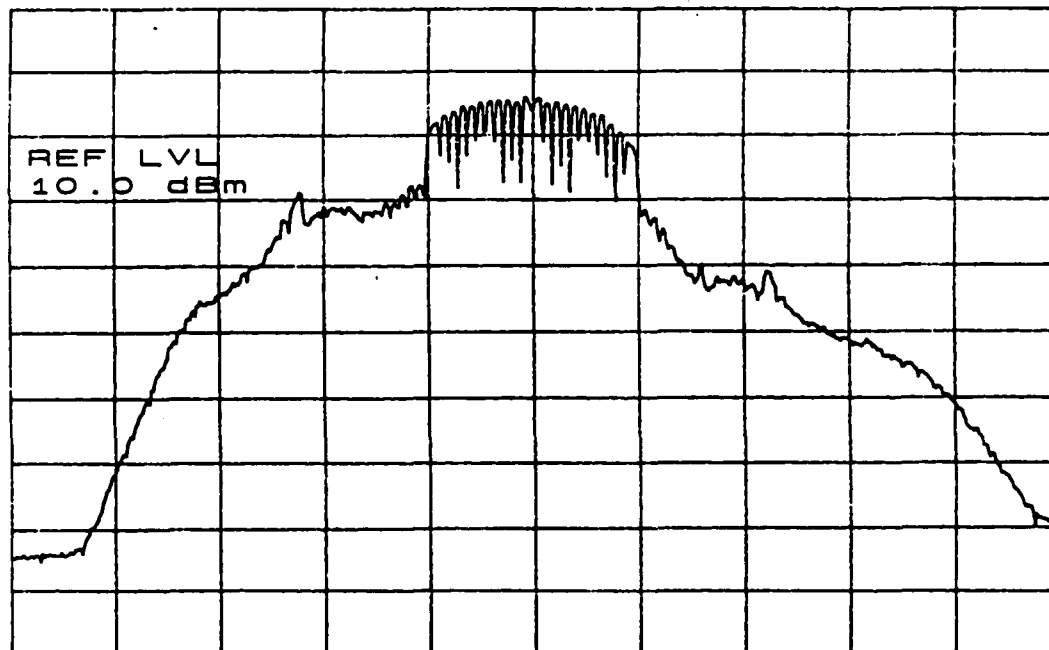


RECEIVED OUTPUT 32kb/s DATA AFTER DESPREADING AND LPF

Figure 3.3.3.9:

\*ATTEN 20dB

RL 10.0dBm 10dB/



CENTER 875.00MHz

SPAN 50.00MHz

\*RBW 100kHz \*VBW 300Hz

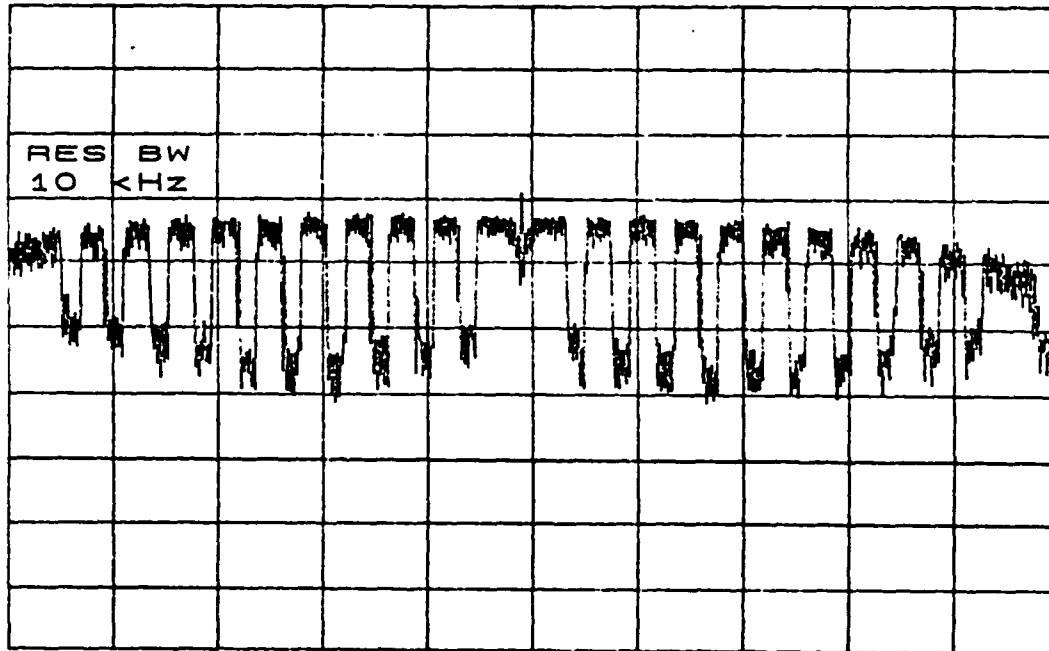
SWP 5.0sec

Figure 3.3.3.10a: Transmit notched O-B-CDMA signal at the output of PA 200 Watts (one dB compression).

\*ATTEN 30dB

RL 20.0dBm

10dB/



CENTER 875.00MHz

SPAN 10.00MHz

\*RBW 10KHZ

\*VBW 300HZ

SWP 9.0sec

Figure 3.3.3.10b: Zoomed Transmit notched O-B-CDMA signal  
at the output of PA 200 Watts (one dB compression).



**Figure 3.3.4.0: Base stations Coverage of US-CELLULAR at Des Moines IOWA.**



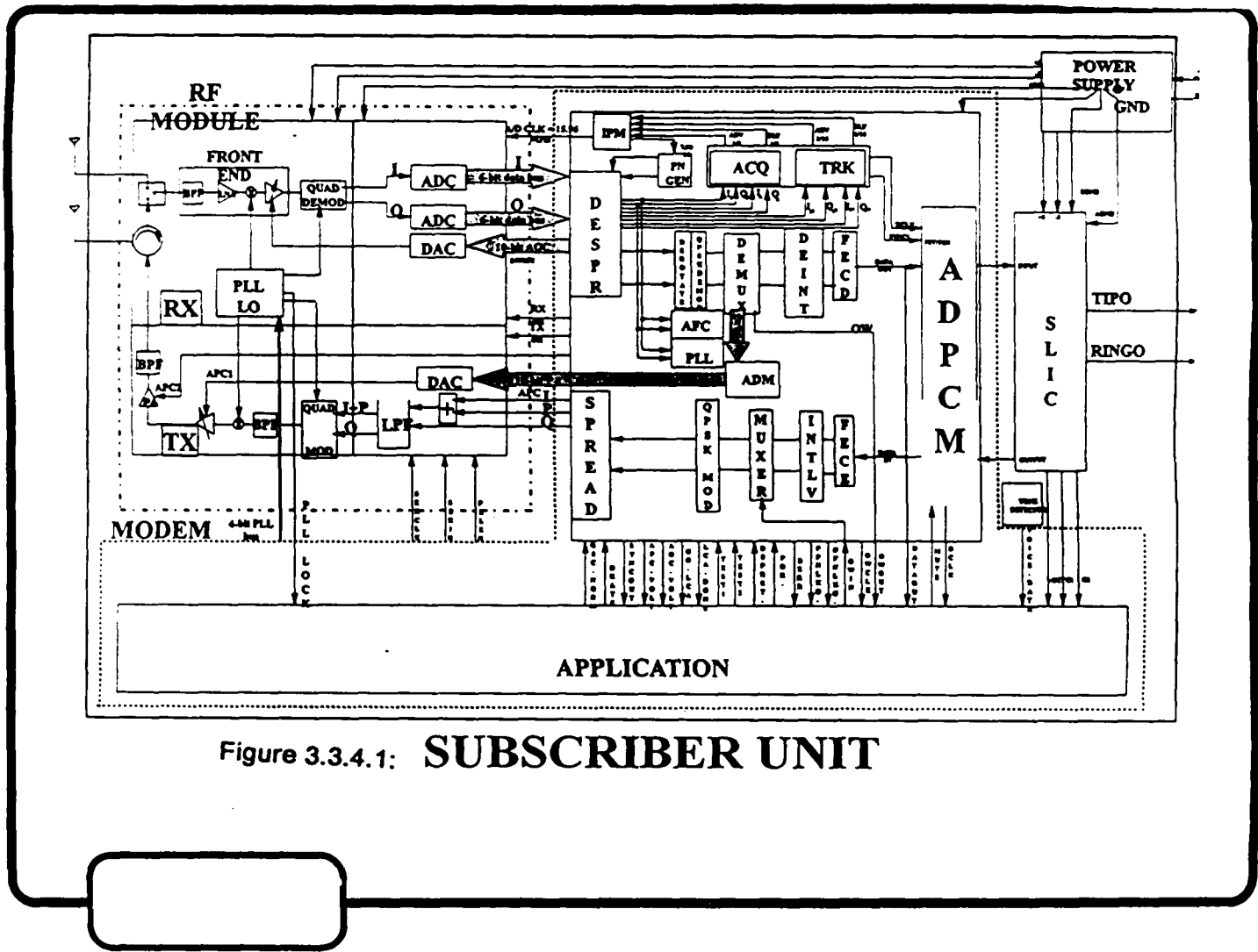
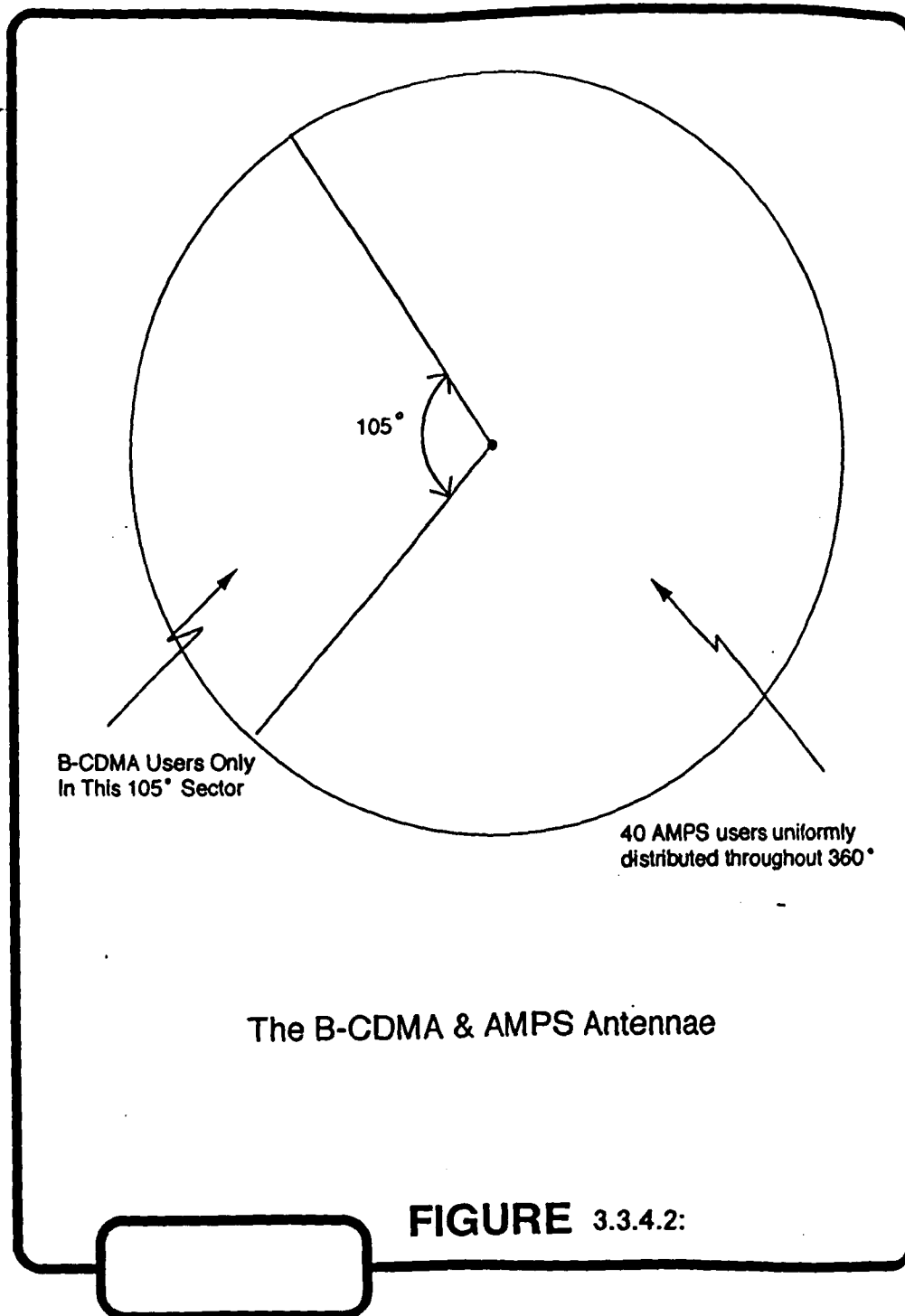
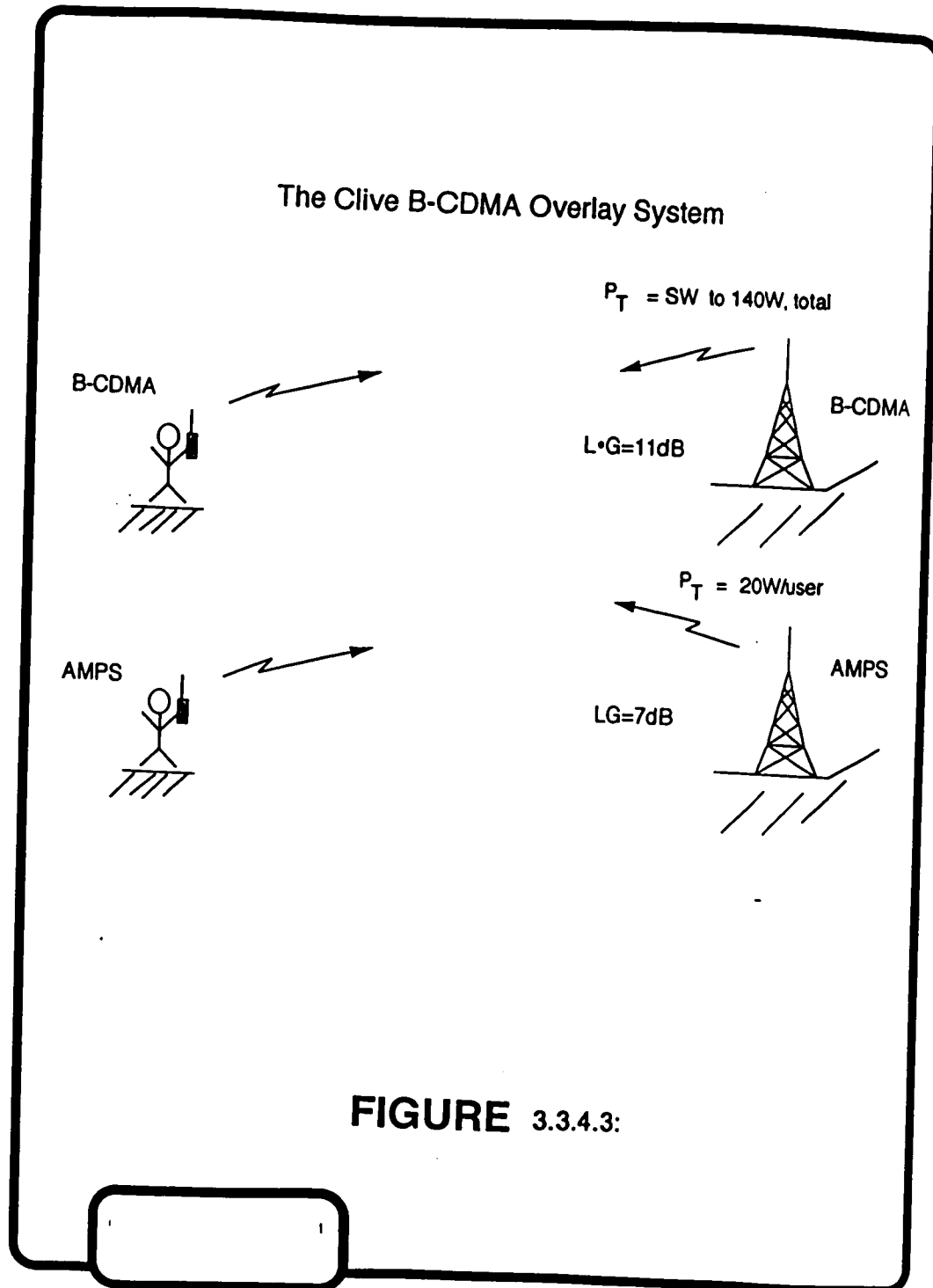


Figure 3.3.4.1: SUBSCRIBER UNIT





**FIGURE 3.3.4.3:**

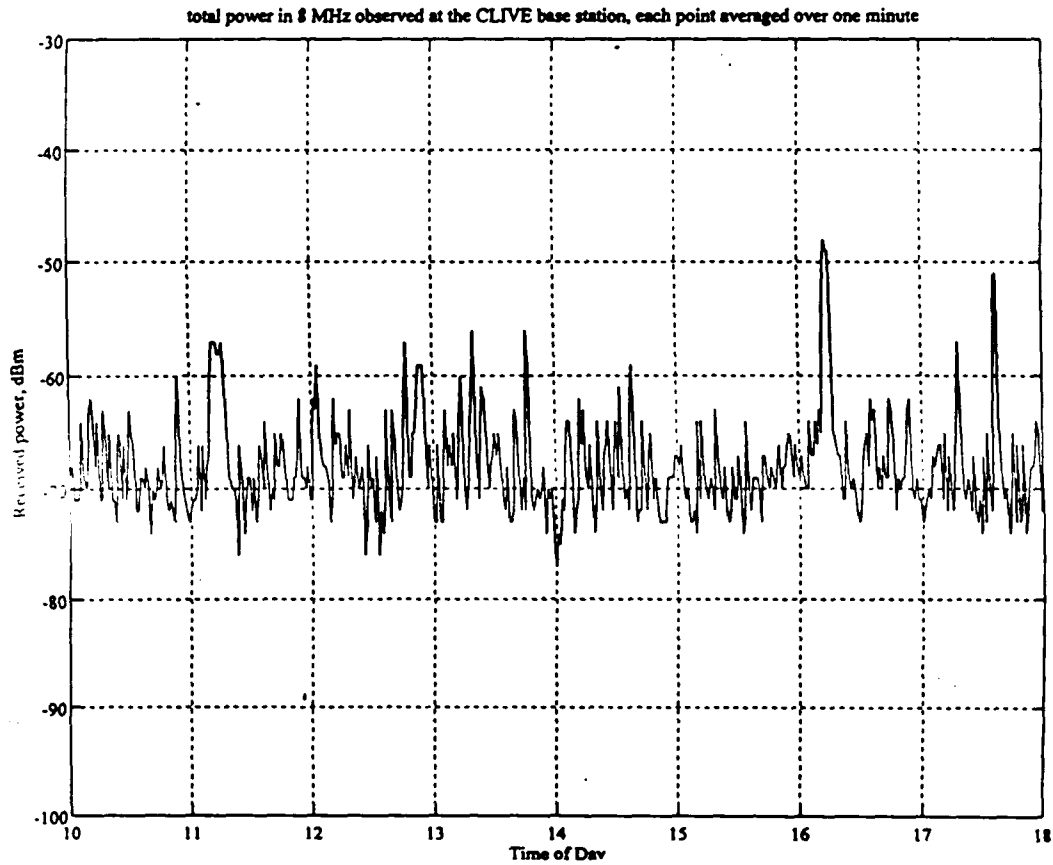
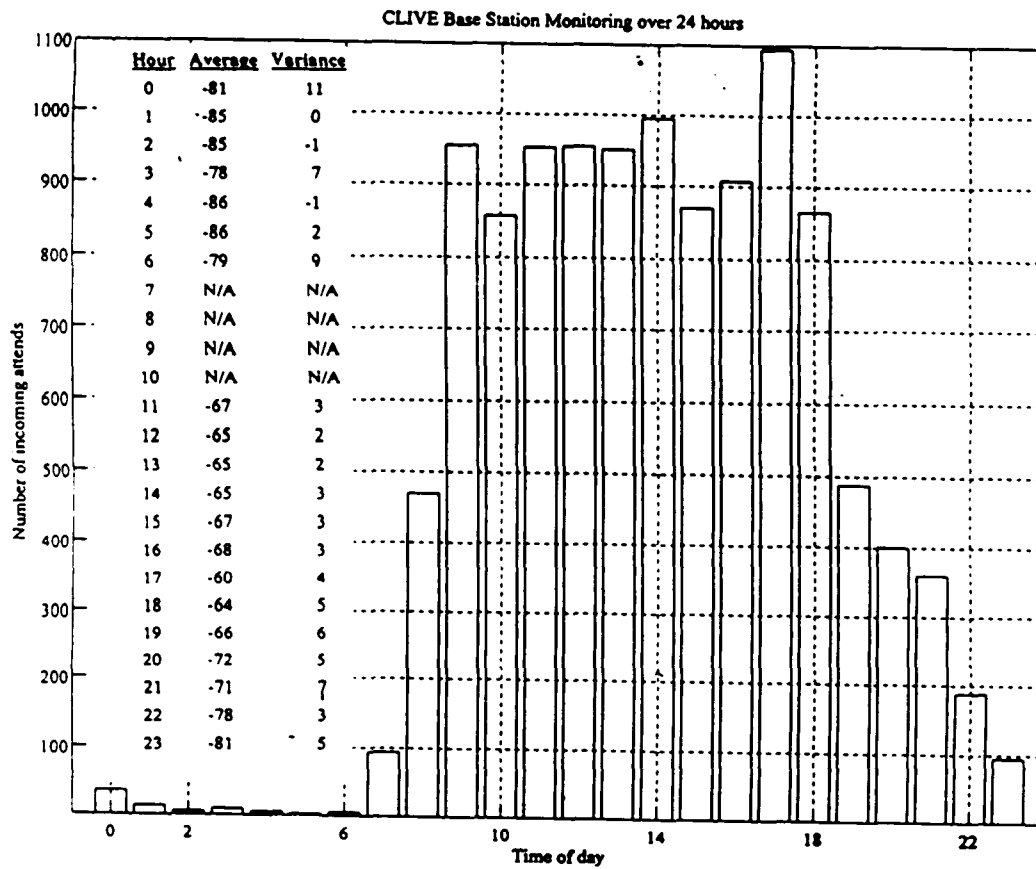


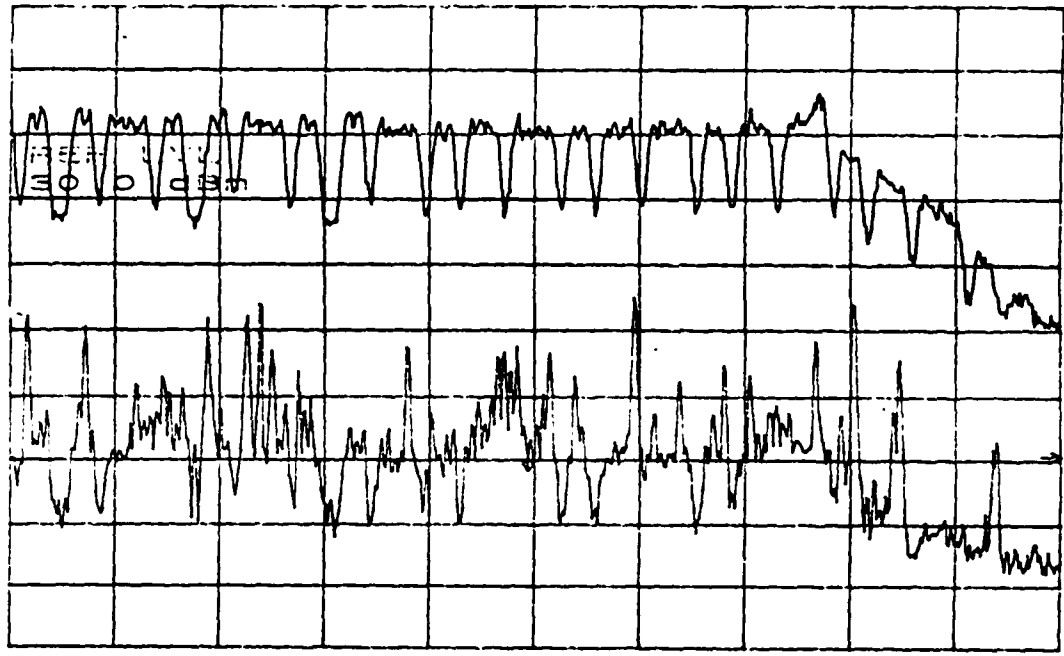
Figure 3.3.4.4: AMPS POWER Load at Clive base station  
at day time.



**Figure 3.3.4.5: AMPS POWER Load at Clive base station.**

START 500MHz  
STOP 3.000MHz

START 500MHz  
STOP 3.000MHz



START 500MHz  
STOP 3.000MHz

START 500MHz  
STOP 3.000MHz

SWP 5.0500

Figure 3.3.5.1a: 1 channel output from notch filter with AMPS  
(lower curve).

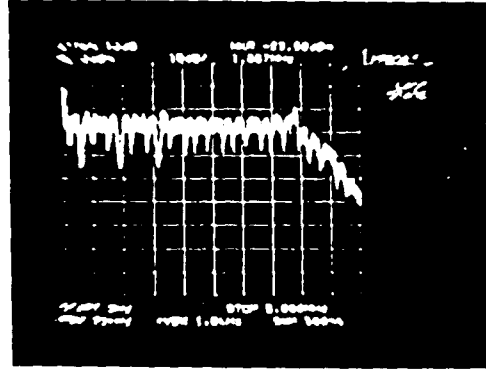
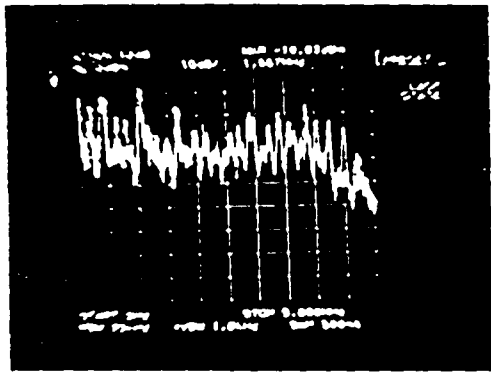


Figure 3.3.5.1b I channel output from notch filter with AMPS and CDMA (left curve ), No signal (right)

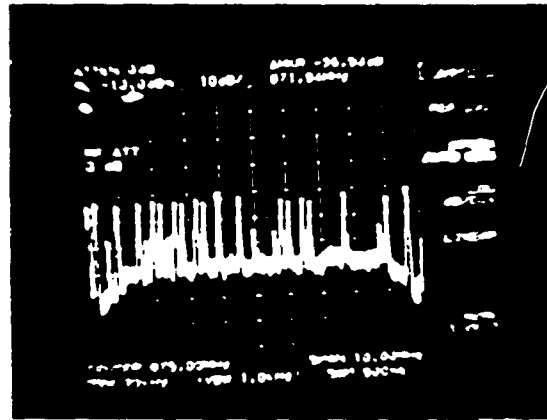


Figure 3.3.5.2a One CDMA with AMPS received at the Remote unit.

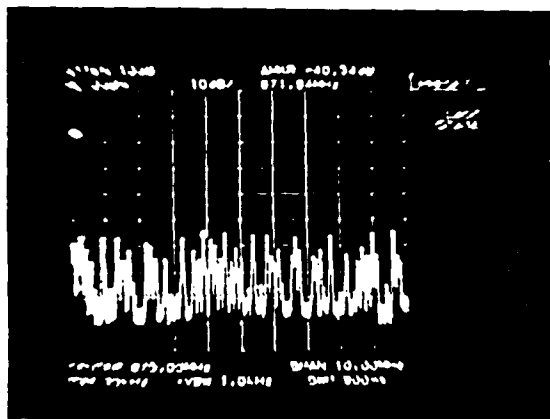


Figure 3.3.5.2b Spillover from Ankeny Base Station and down town Des Moines received at the remote unit.

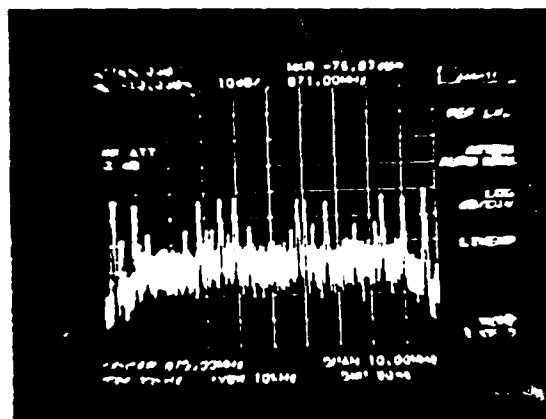


Figure 3.3.5.2c Received signal 5 miles from the BS.

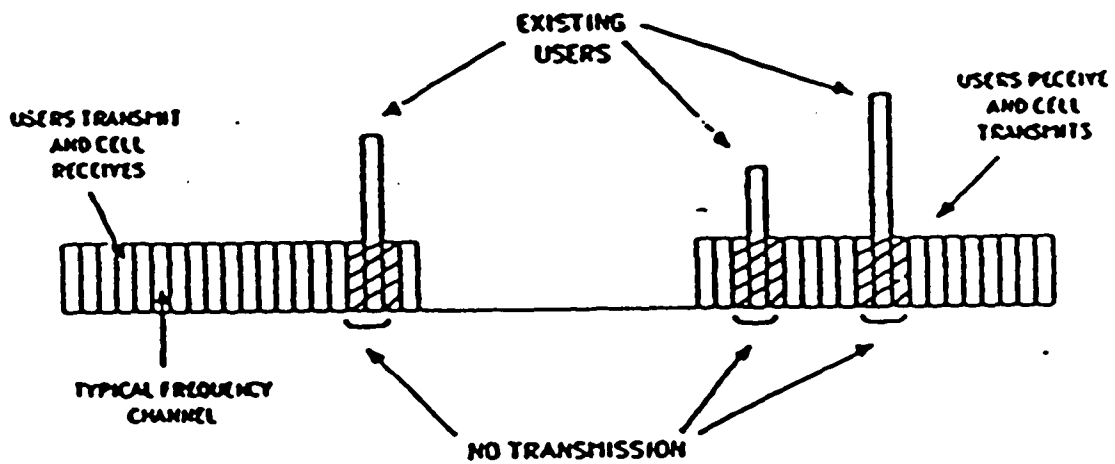


Figure 4.1 SHOWING THAT EXISTING USERS WILL NOT BE INTERFERED WITH

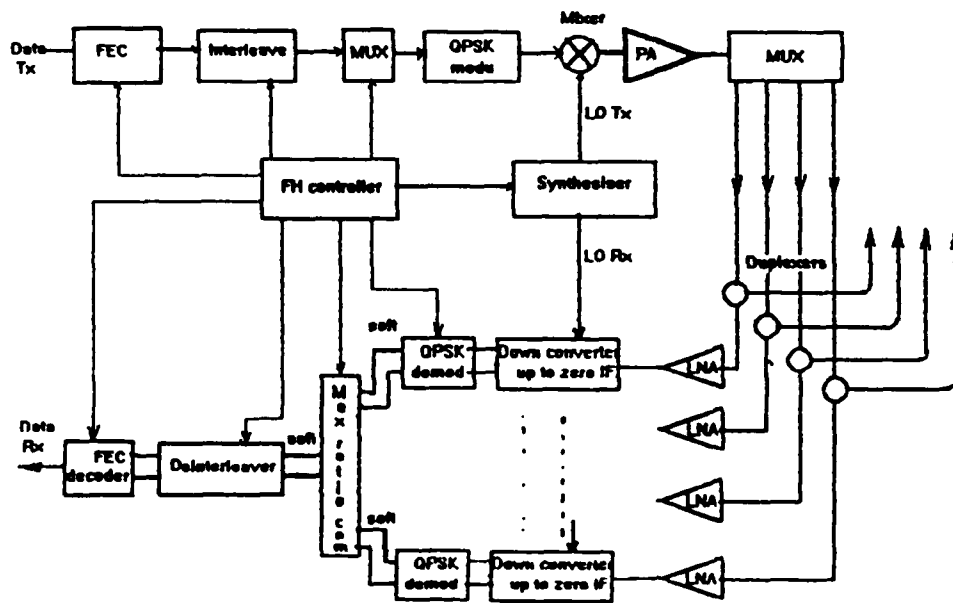
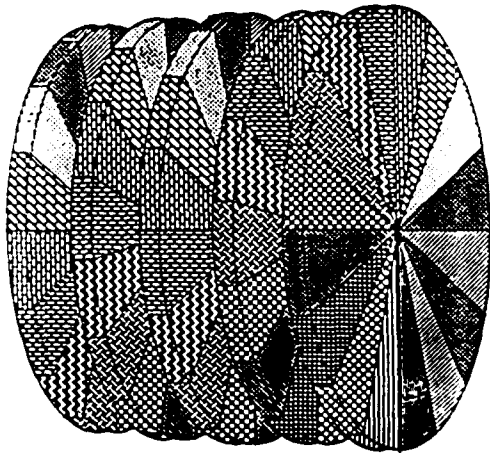
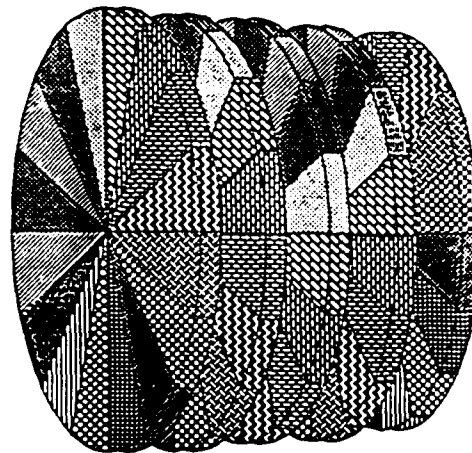


Figure 4.3.a FH-CDMA block diagram.

## Orthogonal & Non-Orthogonal Hopping



Non-Orthogonal



Orthogonal

Figure 4.3.b Orthogonal & Non-Orthogonal Frequency Hopping

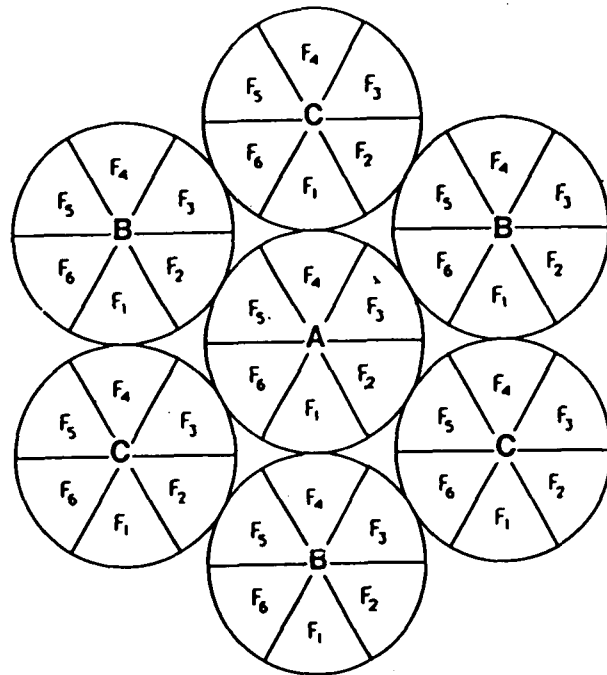


Figure 4.3.c FH-CDMA using concentric Frequency Bands.

Cell	A	B	C
$R_1$	1	2	3
$R_2$	4	5	6
$R_3$	6	1	5
$R_4$	5	6	4
$R_5$	2	3	1
$R_6$	3	1	2

**COLLISION RINGS**

- $R_{1,A}$   $R_{2,B}$   $R_{3,C}$
- $R_{2,A}$   $R_{3,B}$   $R_{4,C}$
- $R_{3,A}$   $R_{4,B}$   $R_{5,C}$
- $R_{4,A}$   $R_{5,B}$   $R_{6,C}$
- $R_{5,A}$   $R_{6,B}$   $R_{1,C}$
- $R_{6,A}$   $R_{1,B}$   $R_{2,C}$

Obtaining Capacity In a  
FH/CDMA System Using  
Concentric Frequency Bands

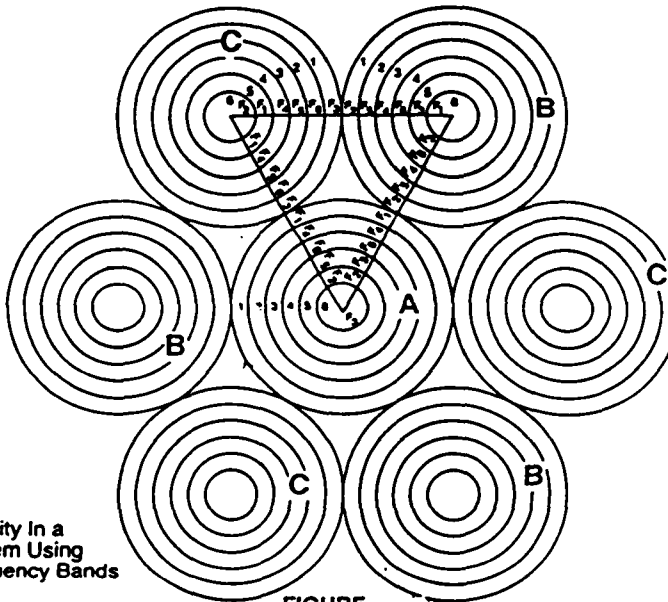
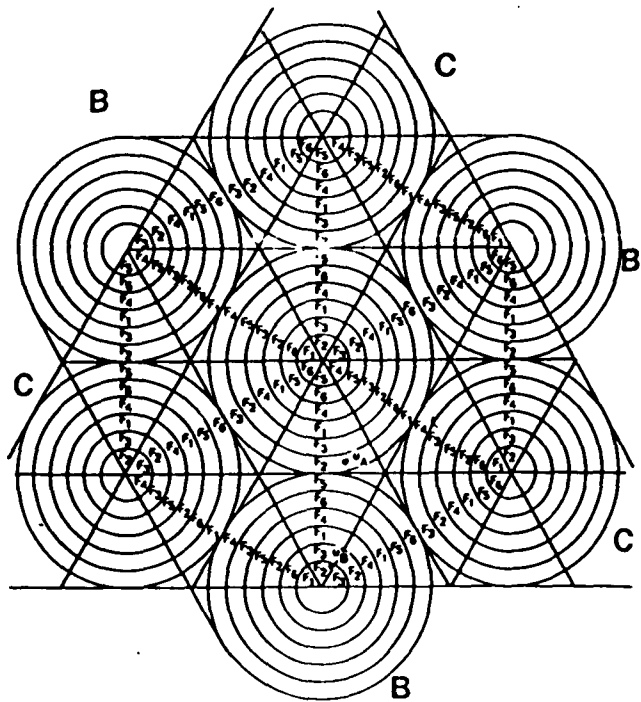


FIGURE .

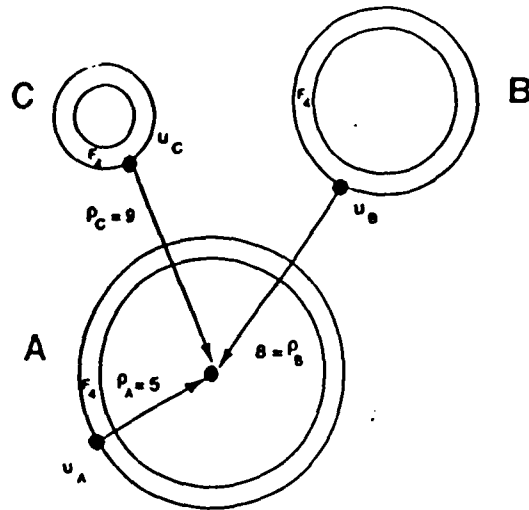
Figure 4.3.d

FH-CDMA using sectors Frequency Bands.



Obtaining Capacity In A FH/CDMA System Using Concentric Frequency Bands And A 6-Sector Antenna At Each Base

**Figure 4.3.e**      **FH-CDMA using concentric and sectors**  
**Frequency Bands.**



Calculation of Worst-Case S/I

Figure 4.3.1.1 SNR calculation for rings.

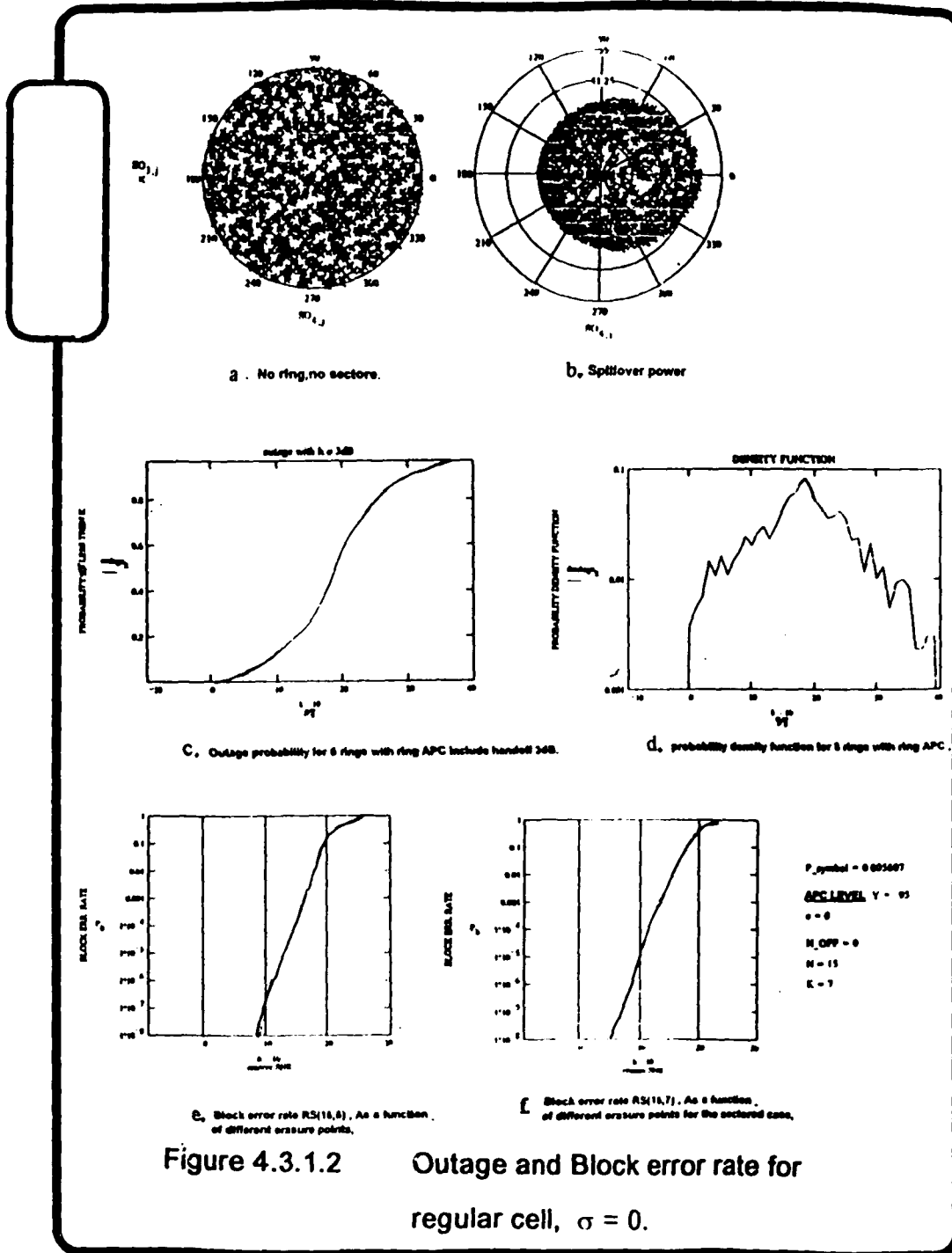


Figure 4.3.1.2 Outage and Block error rate for regular cell,  $\sigma = 0$ .

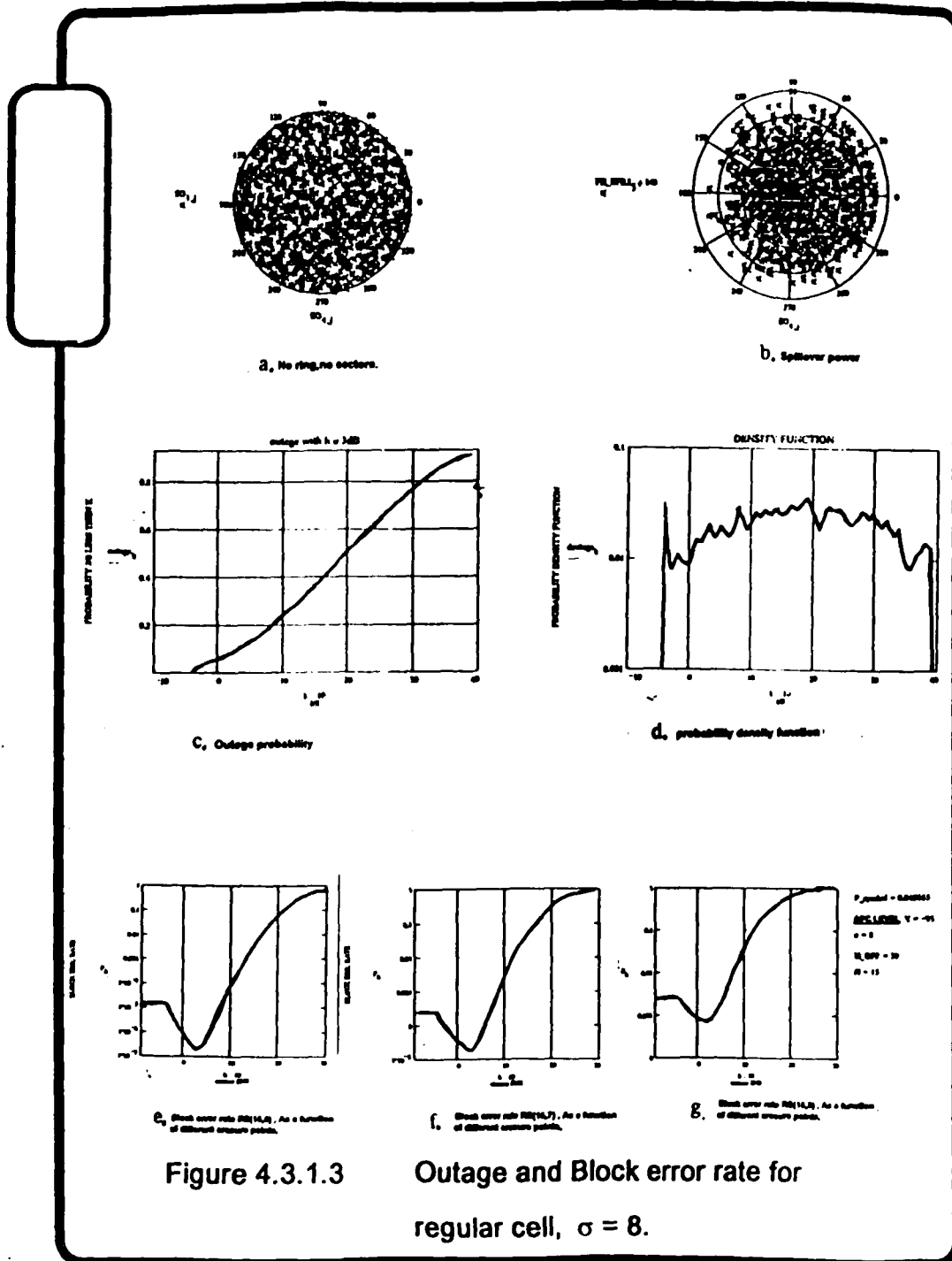


Figure 4.3.1.3 Outage and Block error rate for regular cell,  $\sigma = 8$ .

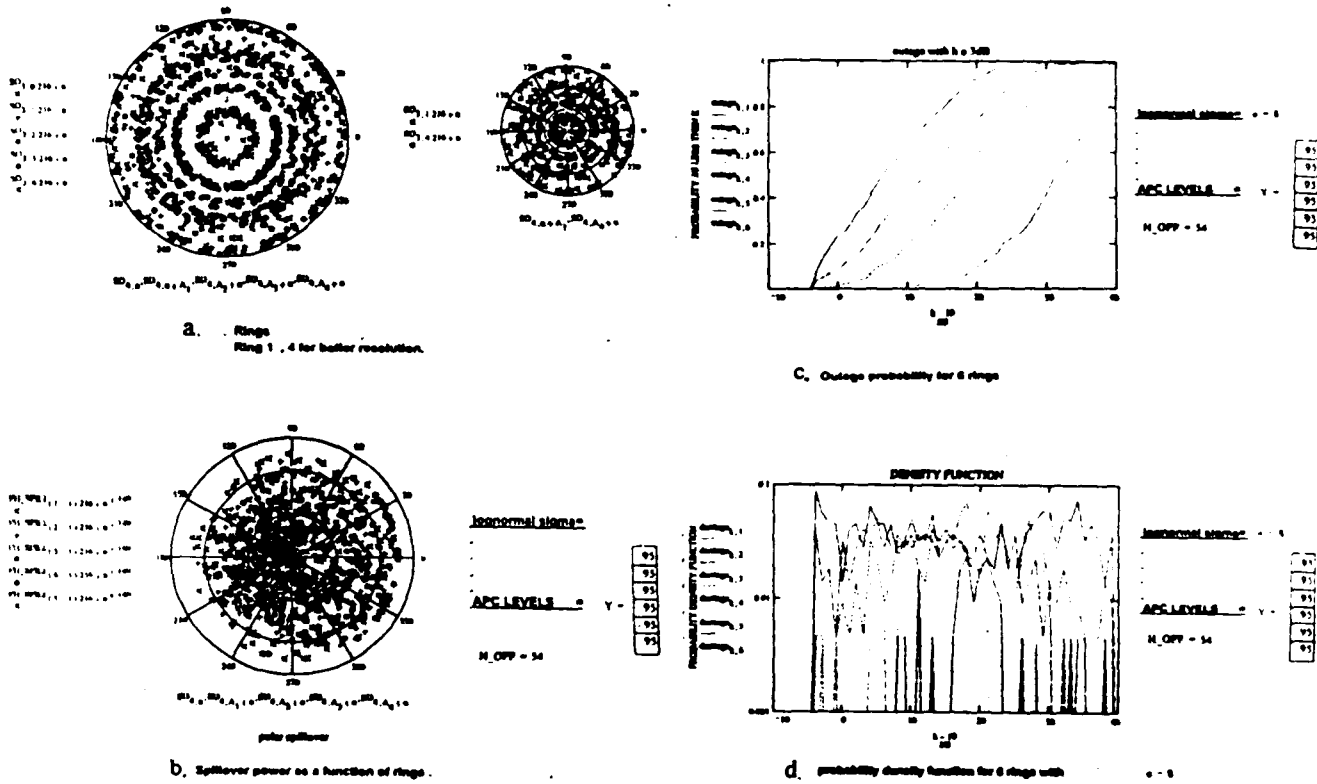
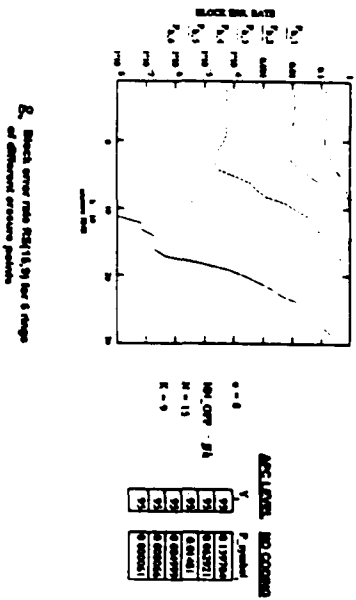
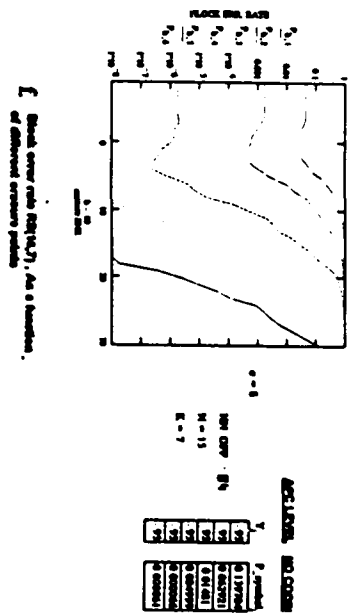


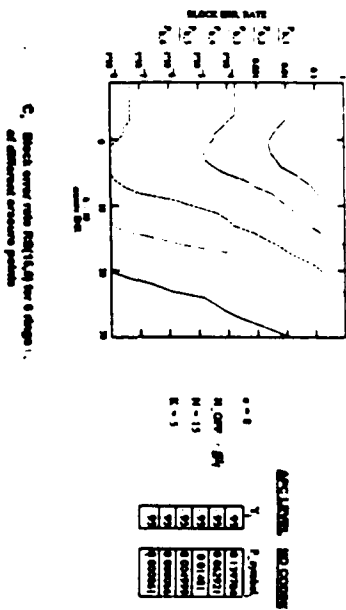
Figure 4.3.1.4 Outage and Block error rate for rings cell without APC correction,  $\sigma = 8$ .



G. Block error rate (BER) for 8 rings of different error rates.

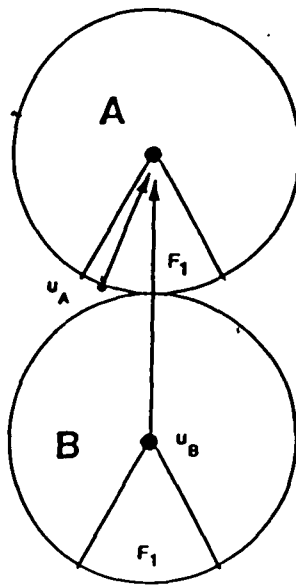


H. Block error rate (BER) for 8 rings of different error rates.



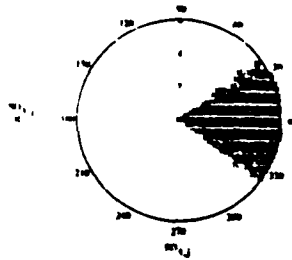
I. Block error rate (BER) for 8 rings of different error rates.

Figure 4.3.1.4 Outage and Block error rate for rings cell without APC correction,  $\sigma = 8$ .

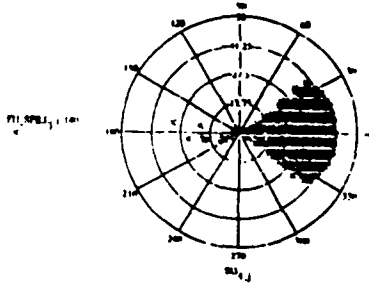


To Show That Interference Is Reduced By  $2^4 = 16$

Figure 4.3.2.1 SNR calculation for sectored cell.



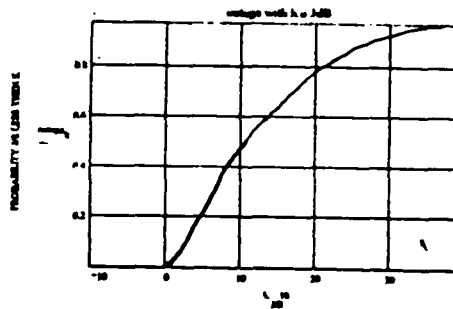
a No ring.



b polar plot

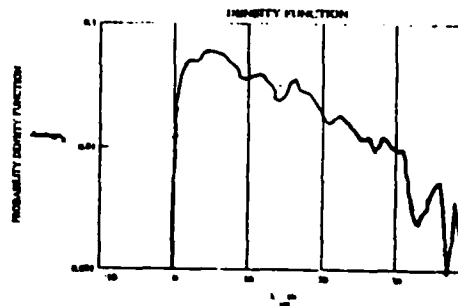
b Sufficient power for sectored case

Intersected plane:  $\sigma = 0$   
 $\Delta H_{OFF} = 0$   $\gamma = 95$



c Outage probability for 6 sectors include handoff call.

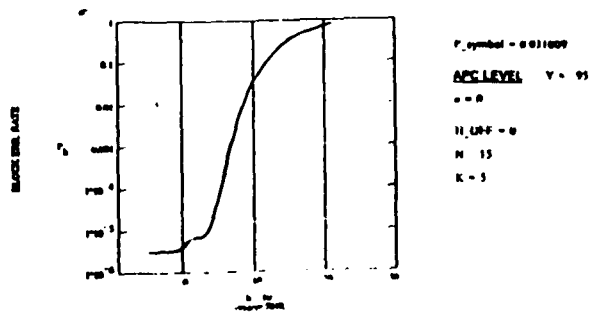
ACC LEVEL  $\gamma = 95$   
 $\sigma = 0$   
 $H_{OFF} = 0$



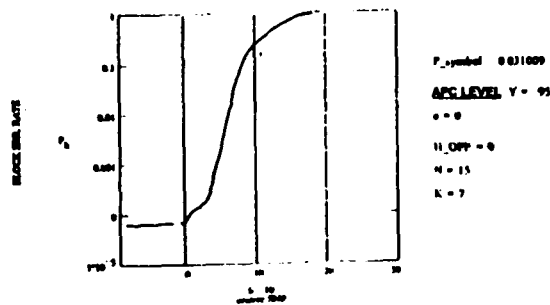
d probability density function for 6 sectors  $\sigma = 0$

ACC LEVEL  $\gamma = 95$   
 $\sigma = 0$   
 $H_{OFF} = 0$

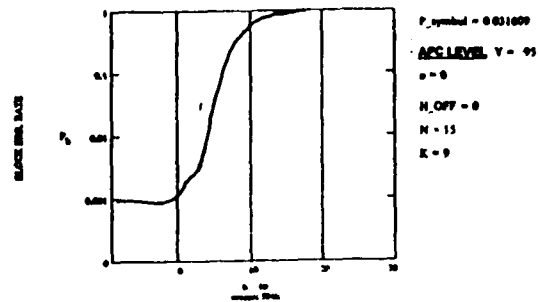
Figure 4.3.2.2 Outage and Block error rate for regular sectored cell,  $\sigma = 0$ .



e. Block error rate  $R_B(16,4)$ , As a function, of different outage points for the sectored case.



f. Block error rate  $R_B(16,7)$ , As a function, of different outage points for the sectored case.



g. Block error rate  $R_B(16,9)$ , As a function, of different outage points for the sectored case.

Figure 4.3.2.2 Outage and Block error rate for

regular sectored cell,  $\sigma = 0$ .

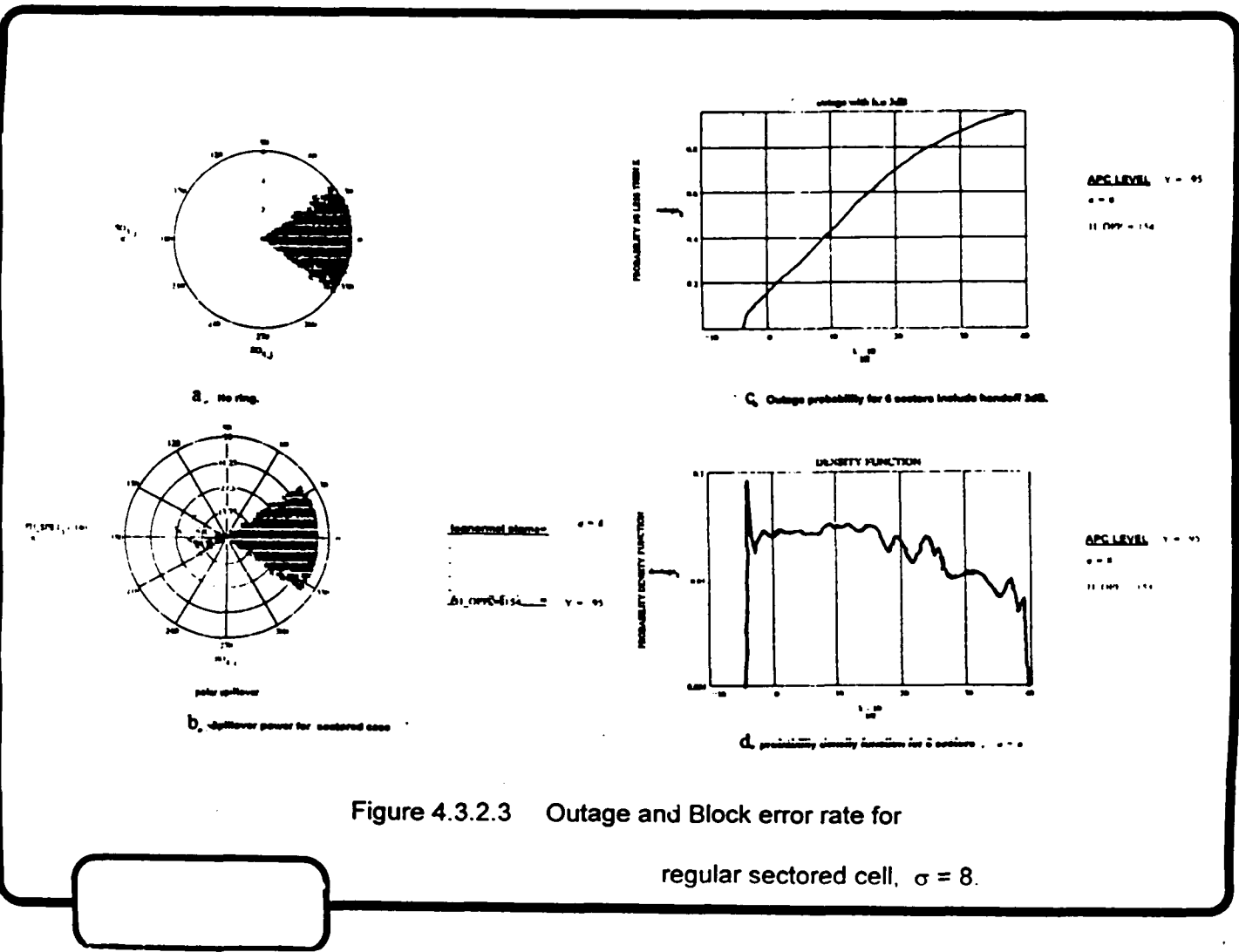
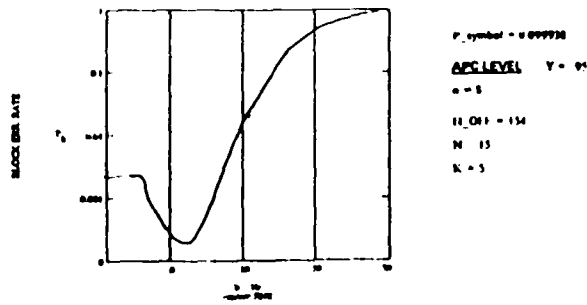
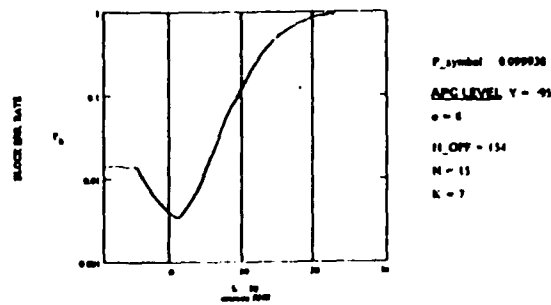


Figure 4.3.2.3 Outage and Block error rate for

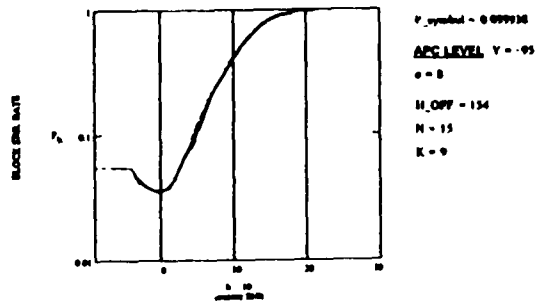
regular sectored cell,  $\sigma = 8$ .



e. Block error rate  $RB(16,6)$ . As a function of different outage points for the sectorized case.



f. Block error rate  $RB(16,7)$ . As a function of different outage points for the sectorized case.



g. Block error rate  $RB(16,9)$ . As a function of different outage points for the sectorized case.

Figure 4.3.2.3 Outage and Block error rate for regular sectorized cell,  $\sigma = 8$ .

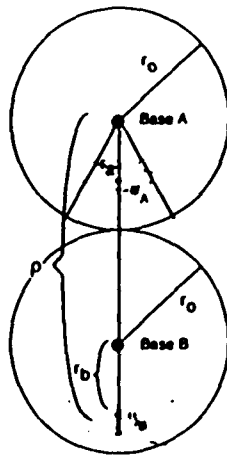


Figure 4.3.4

Calculation of the S/I Produced at Mobile  
Due to an Interfering Base.

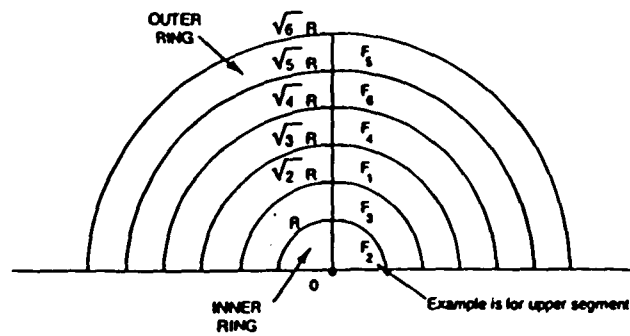


Figure 4.3.6.1 Showing The Radios of a Rings  
to achieve a constant user density.

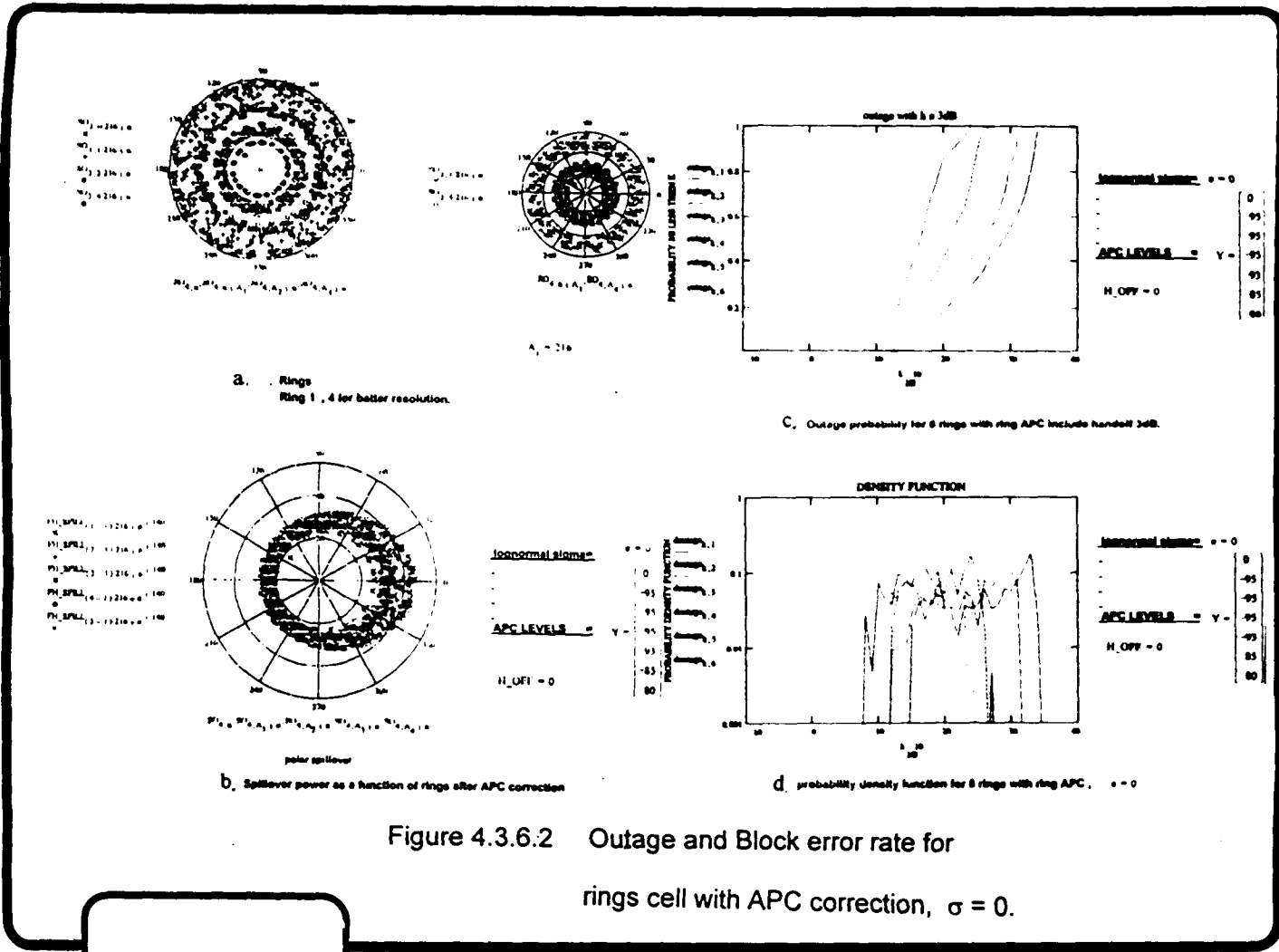
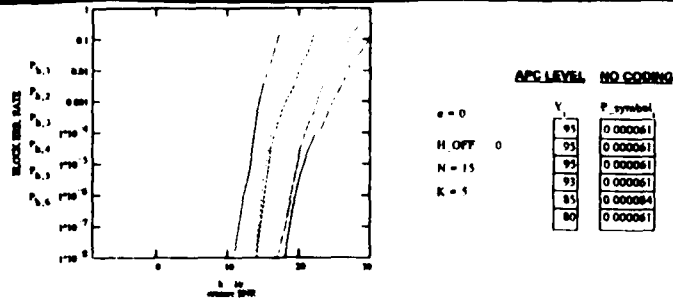
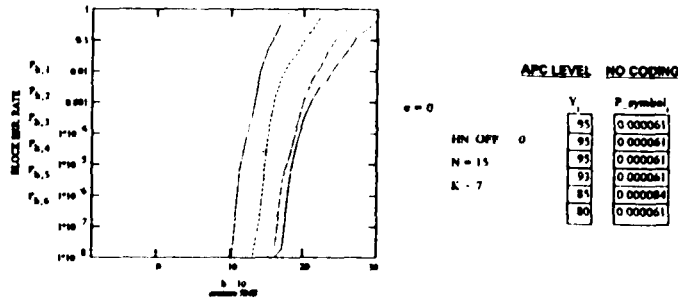


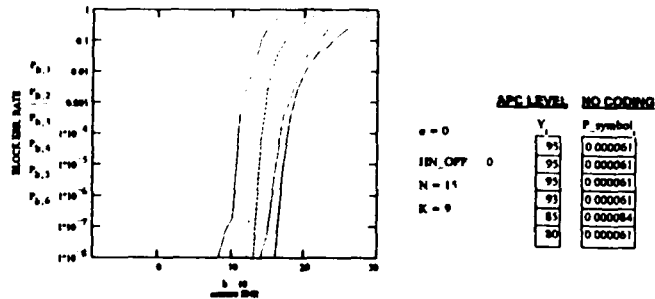
Figure 4.3.6.2 Outage and Block error rate for rings cell with APC correction,  $\sigma = 0$ .



C. Block error rate  $RB(15,6)$  for 6 rings with ring APC. As a function of different erasure points.



D. Block error rate  $RB(15,7)$  for 6 rings with ring APC. As a function of different erasure points.



E. Block error rate  $RB(15,9)$  for 6 rings with ring APC. As a function of different erasure points, No handoff.

Figure 4.3:6.2 Outage and Block error rate for rings cell with APC correction,  $\sigma = 0$ .

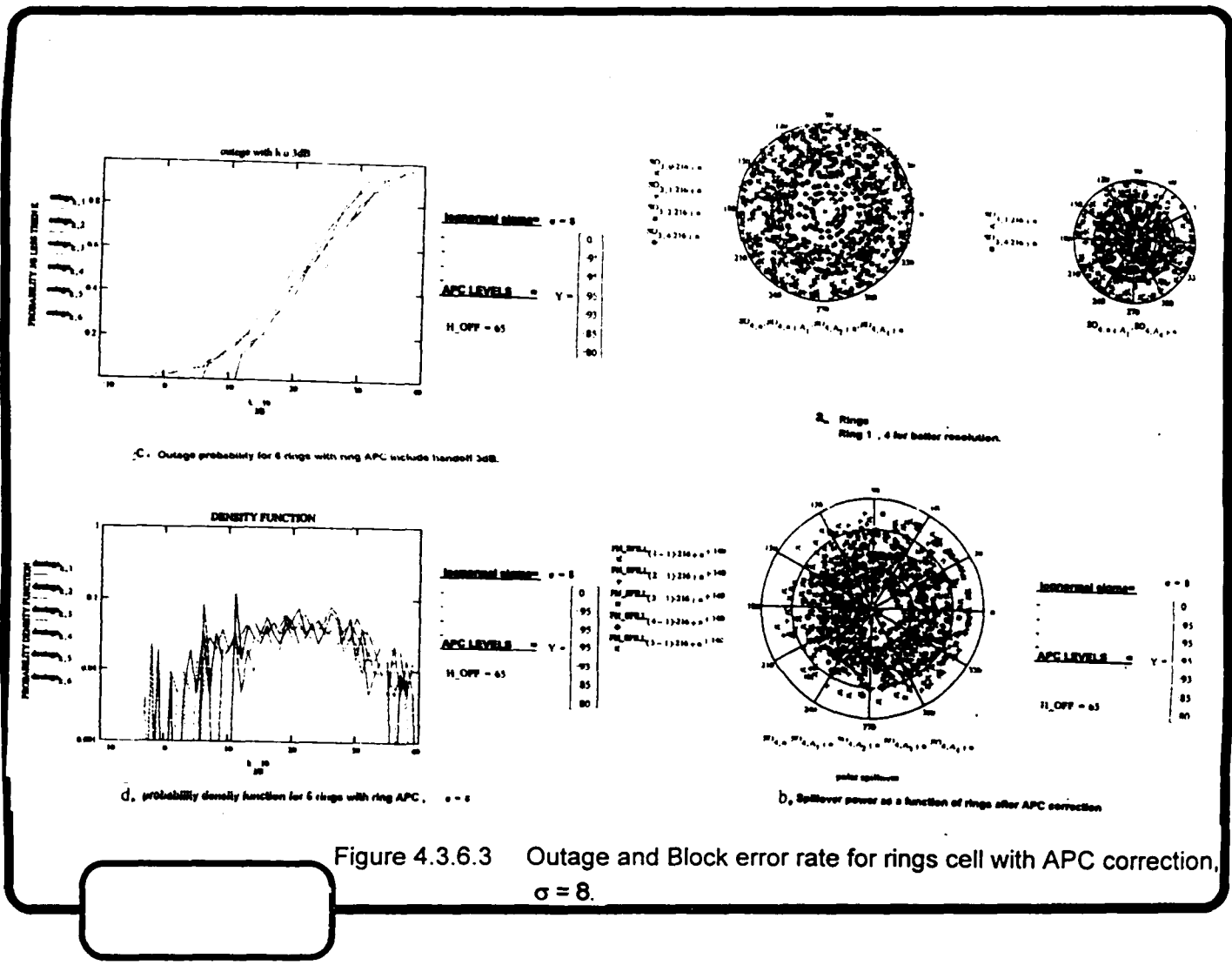
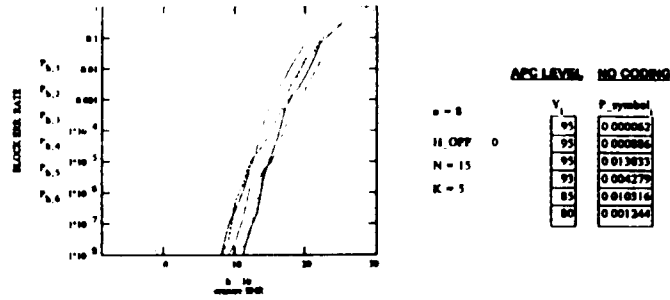
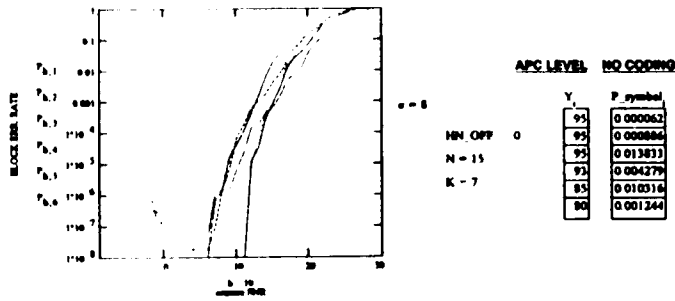


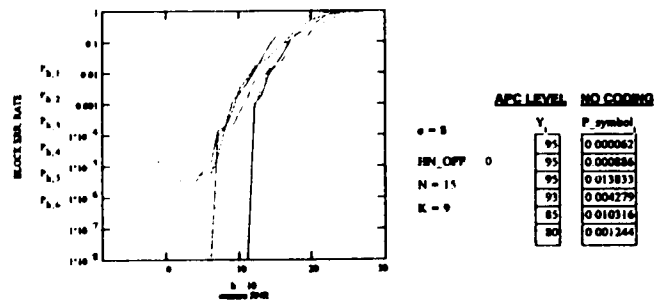
Figure 4.3.6.3 Outage and Block error rate for rings cell with APC correction,  $\sigma = 8$ .



c. Block error rate RS(16,6) for 6 rings with ring APC , As a function of different erasure points.

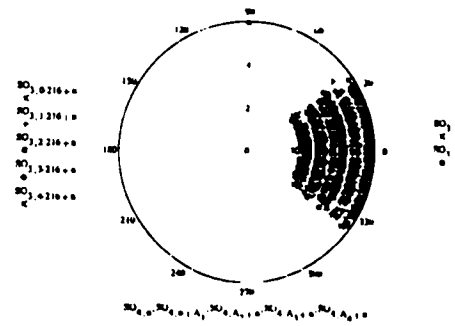


f. Block error rate RS(16,7) for 6 rings with ring APC , As a function of different erasure points

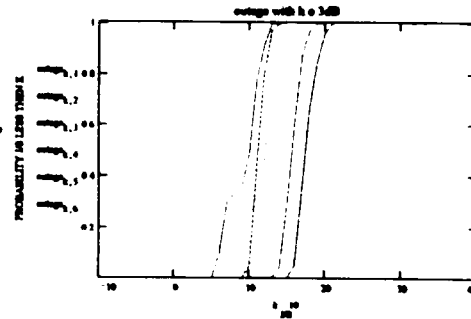
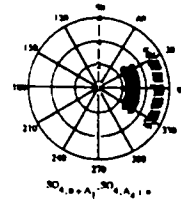


g. Block error rate RS(16,9) for 6 rings with ring APC , As a function of different erasure points, No handoff

Figure 4.3.6.3 Outage and Block error rate for rings cell with APC correction,  $\sigma = 8$ .



3. Rings and sector map.  
 Ring 1, 4 for better resolution

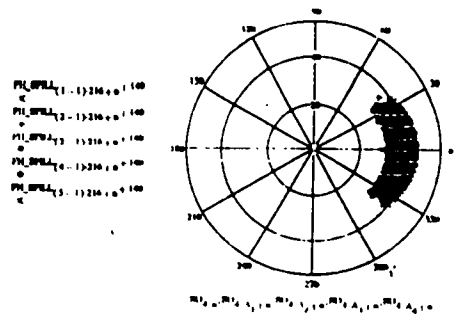


Intersect plane:  $\sigma = 0$

APC LEVELS = Y - 95

H\_OFF = 0

C. Outage probability for 6 rings with ring APC include handoff 3dB.

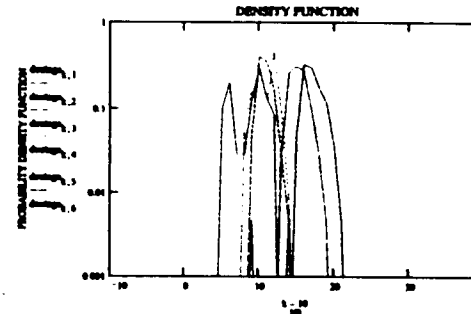


b. Spillover power as a function of rings after APC correction

Intersect plane:  $\sigma = 0$

APC LEVELS = Y - 95

SIRMI = 0



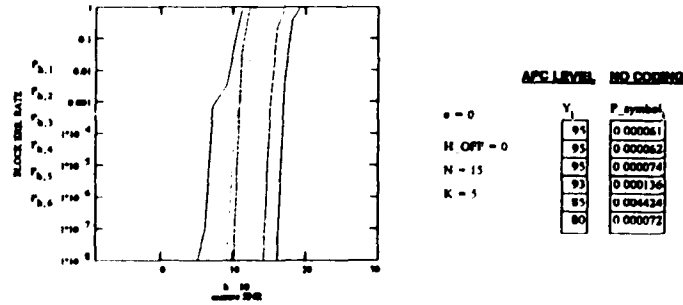
Intersect plane:  $\sigma = 0$

APC LEVELS = Y - 95

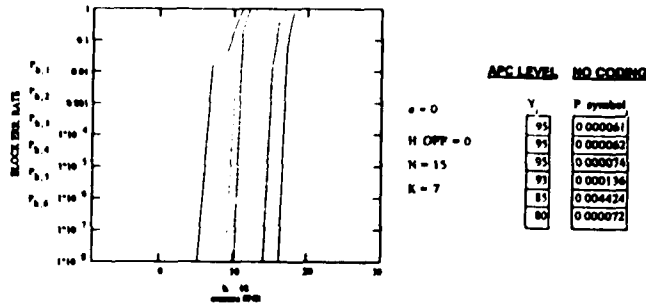
H\_OFF = 0

d. probability density function for 6 rings with ring APC.

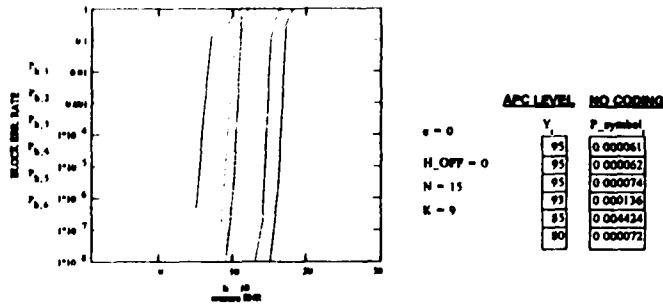
Figure 4.3.6.4 Outage and Block error rate for rings & sector cell with APC correction,  $\sigma = 0$ .



C. Block error rate RS(15,8) for 8 rings with ring APC . As a function of different erasure points



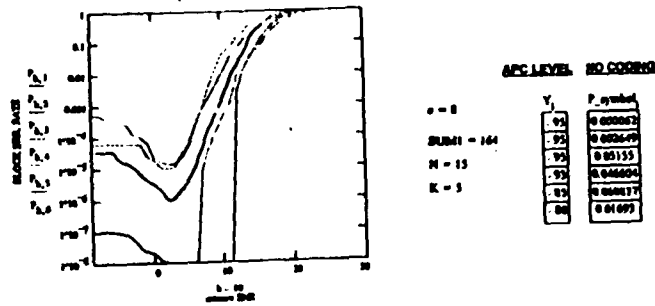
F. Block error rate RS(14,9) for 8 rings with ring APC . As a function of different erasure points



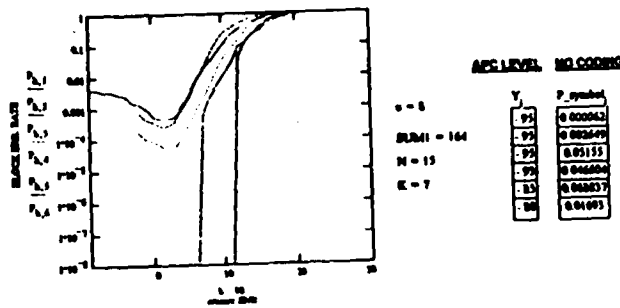
G. Block error rate RS(16,9) for 8 rings with ring APC . As a function of different erasure points

Figure 4.3.6.4 Outage and Block error rate for rings & sector cell with APC correction,  $\sigma = 0$ .

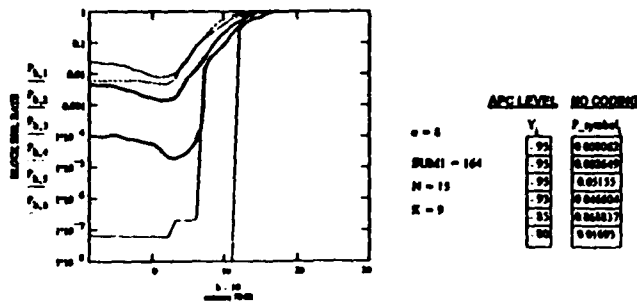




C. Block error rate  $R_B(14,8)$  for 6 rings with ring APC. As a function of different erasure points

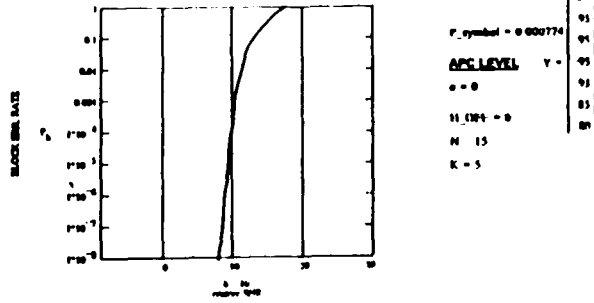


E. Block error rate  $R_B(14,8)$  for 6 rings with ring APC. As a function of different erasure points

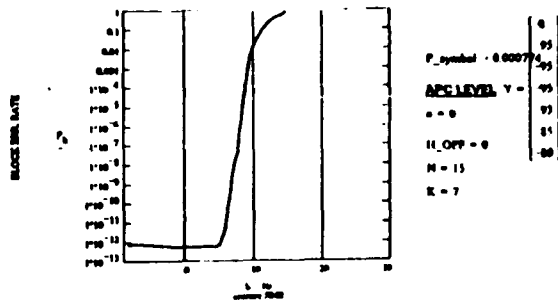


G. Block error rate  $R_B(14,8)$  for 6 rings with ring APC. As a function of different erasure points

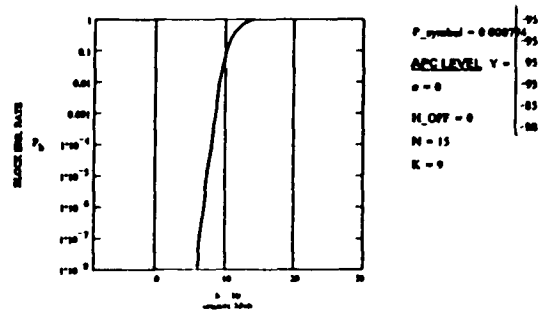
Figure 4.3.6.5 Outage and Block error rate for rings & sector cell with APC correction,  $\sigma = 8$ .



C. Block error rate  $RB(14,6)$ . As a function of different outage points for the sectorized case,  $P_{avg}$ .



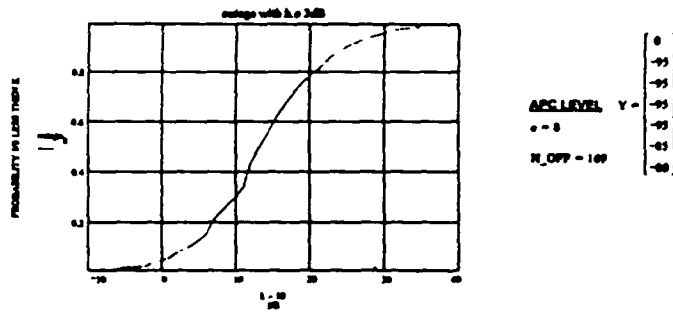
E. Block error rate  $RB(14,7)$ . As a function of different outage points for the sectorized case,  $P_{avg}$ .



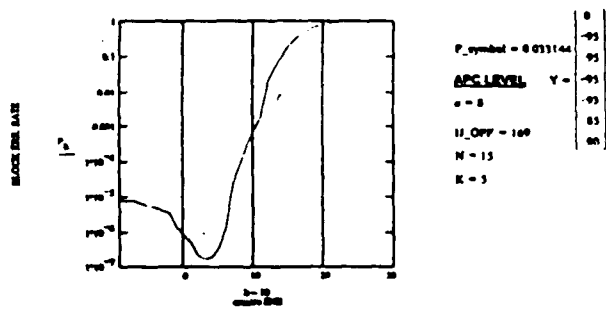
G. Block error rate  $RB(15,9)$ . As a function of different outage points for the sectorized case.

Figure 4.3.6.6 Average outage and Block error rate for

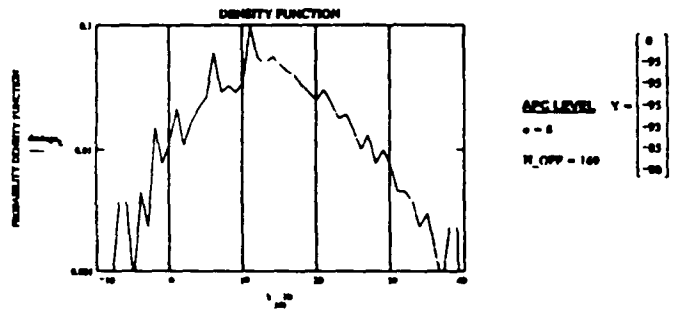
rings & sector cell with APC correction,  $\sigma = 0$ .



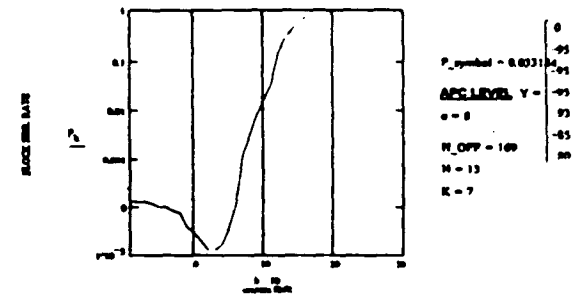
C. Outage probability for 6 sectors include handoff 3dB.



E. Block error rate  $RB(16,8)$ , As a function, of different error rate for the sectored case.



D. probability density function for 6 sectors,  $\sigma = 8$



F. Block error rate  $RB(16,7)$ , As a function, of different error rate for the sectored case.

Figure 4.3.6.7 Average outage and Block error rate for

rings & sector cell with APC correction,  $\sigma = 8$ .

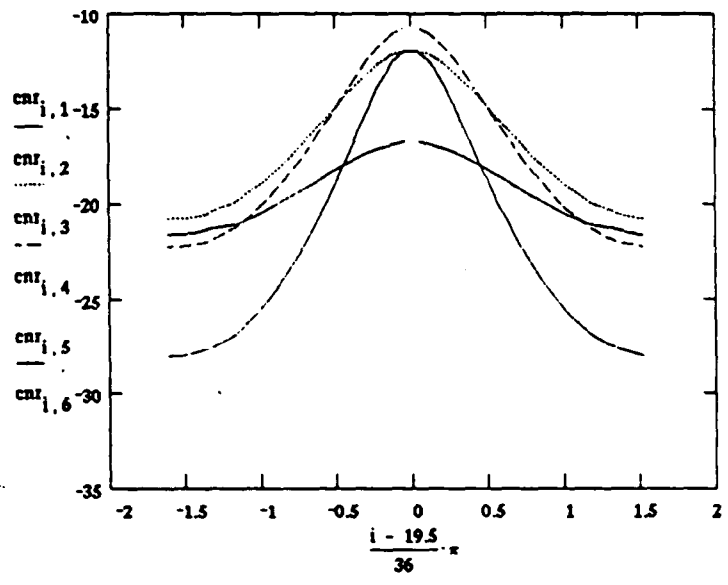


Figure 4.3.6.8a The SNR at the remote at different locations in the cell, with one cell interfere.

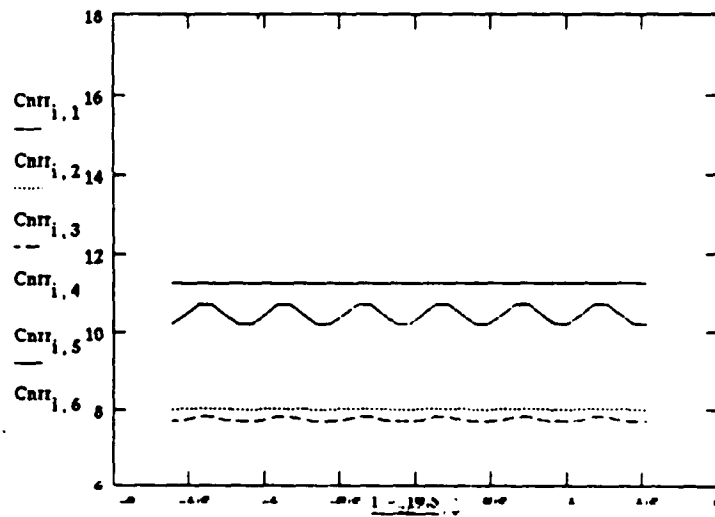


Figure 4.3.6.8b The SNR at the remote at different locations  
in the cell, with six cell interfere.

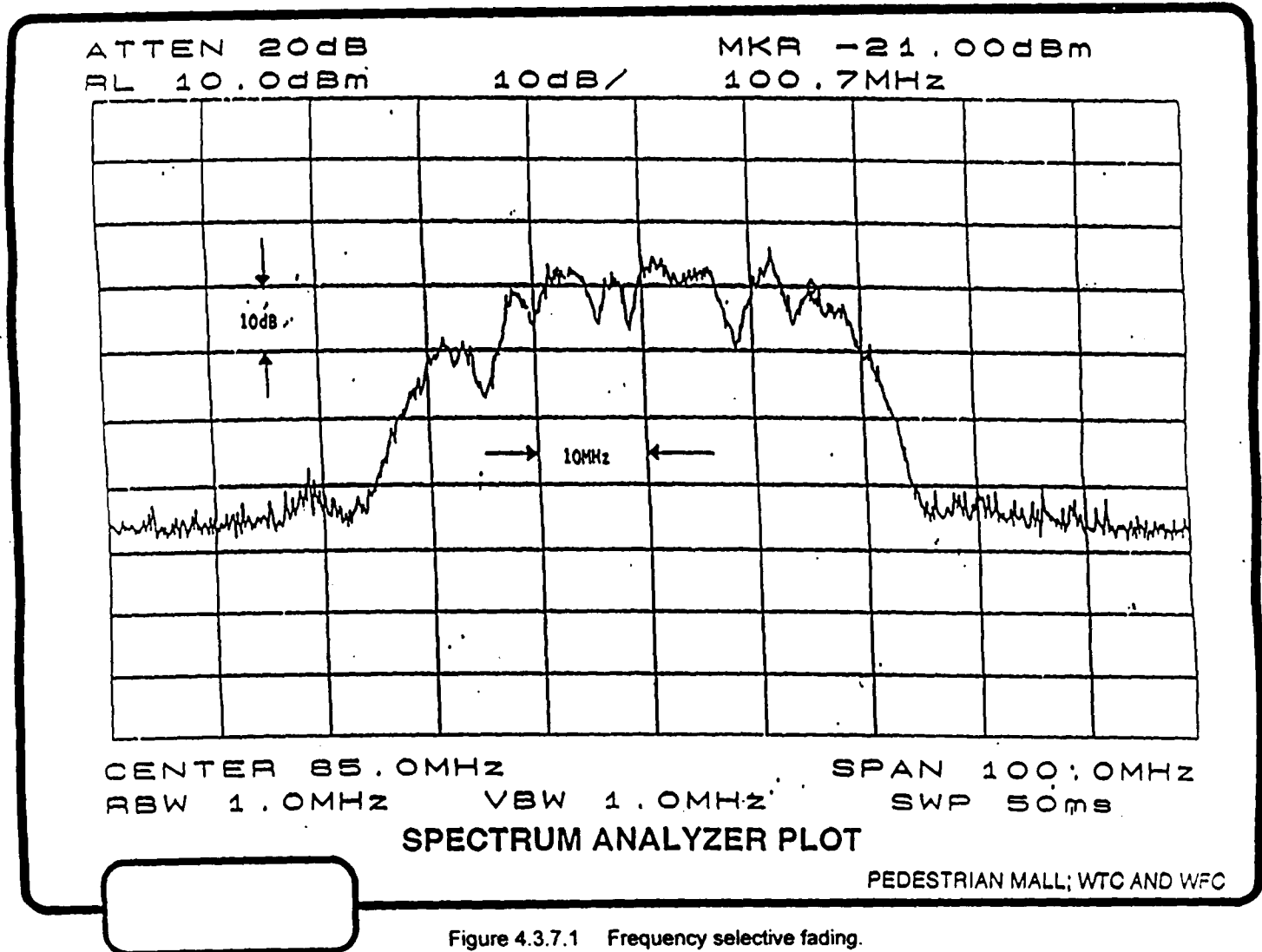


Figure 4.3.7.1 Frequency selective fading.

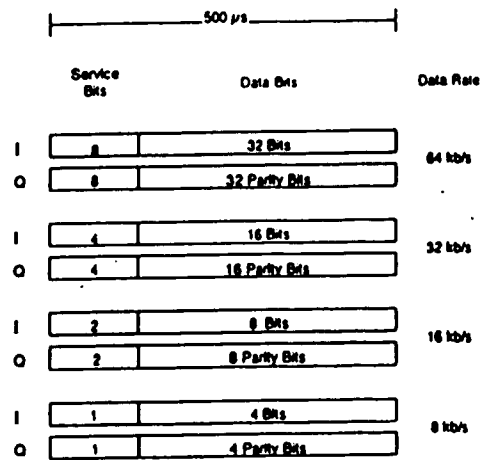


Figure 4.3.7.2 Proposed FH-CDMA Frame Structure.

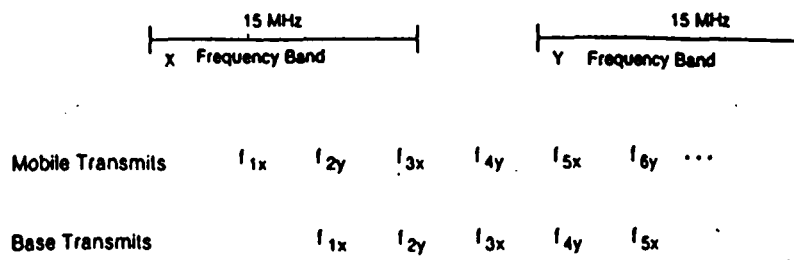


Figure 4.3.8 Showing How Frequencies Are Selected  
In FH-CDMA To Achieve Space Diversity.

TABLE 1. ACIPR CAPABILITIES FOR GTFM AND DCQPSK-SRC.

System Description	Channel Spacing	ACIPR (at $P_b=10^{-2}$ )	Required $E_b/N_0$ at $P_b=10^{-2}$ in AWGN (without ACT)
1. GTFM (8 kb/s) Linear Amplification TX/RCV Filters: 5.5 kHz 3 dB BW 80 dB stopband attenuation	6.25 kHz	13.22 dB	11.9 dB
2. GTFM (8 kb/s) Hardlimiter (Class C Approximation) No TX Filter RCV Filter: 5.5 kHz 3 dB BW 80 dB stopband attenuation	12.5 kHz	59.07 dB	10.5 dB
3. DCQPSK-SRC, $r = 0.3$ (8 kb/s) Linear Amplification TX/RCV Filters: 4 kHz 3 dB BW 80 dB stopband attenuation	6.25 kHz	77.57 dB	9 dB
4. DCQPSK-SRC, $r = 0.3$ (8 kb/s) Linear Amplification TX/RCV Filters: 4.5 kHz 3 dB BW 80 dB stopband attenuation	6.25 kHz	62.93 dB	7.25 dB
5. DCQPSK-SRC, $r = 0.3$ (8 kb/s) Linear Amplification TX/RCV Filters: 4 kHz 3 dB BW 80 dB stopband attenuation	12.5 kHz	100.6 dB	9 dB
6. DCQPSK-SRC, $r = 0.3$ (8 kb/s) Linear Amplification TX/RCV Filters: 4.5 kHz 3 dB BW 80 dB stopband attenuation	12.5 kHz	89.55 dB	7.25 dB

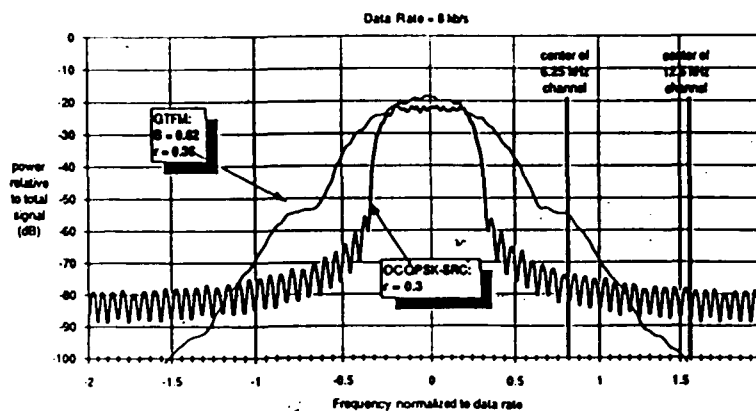
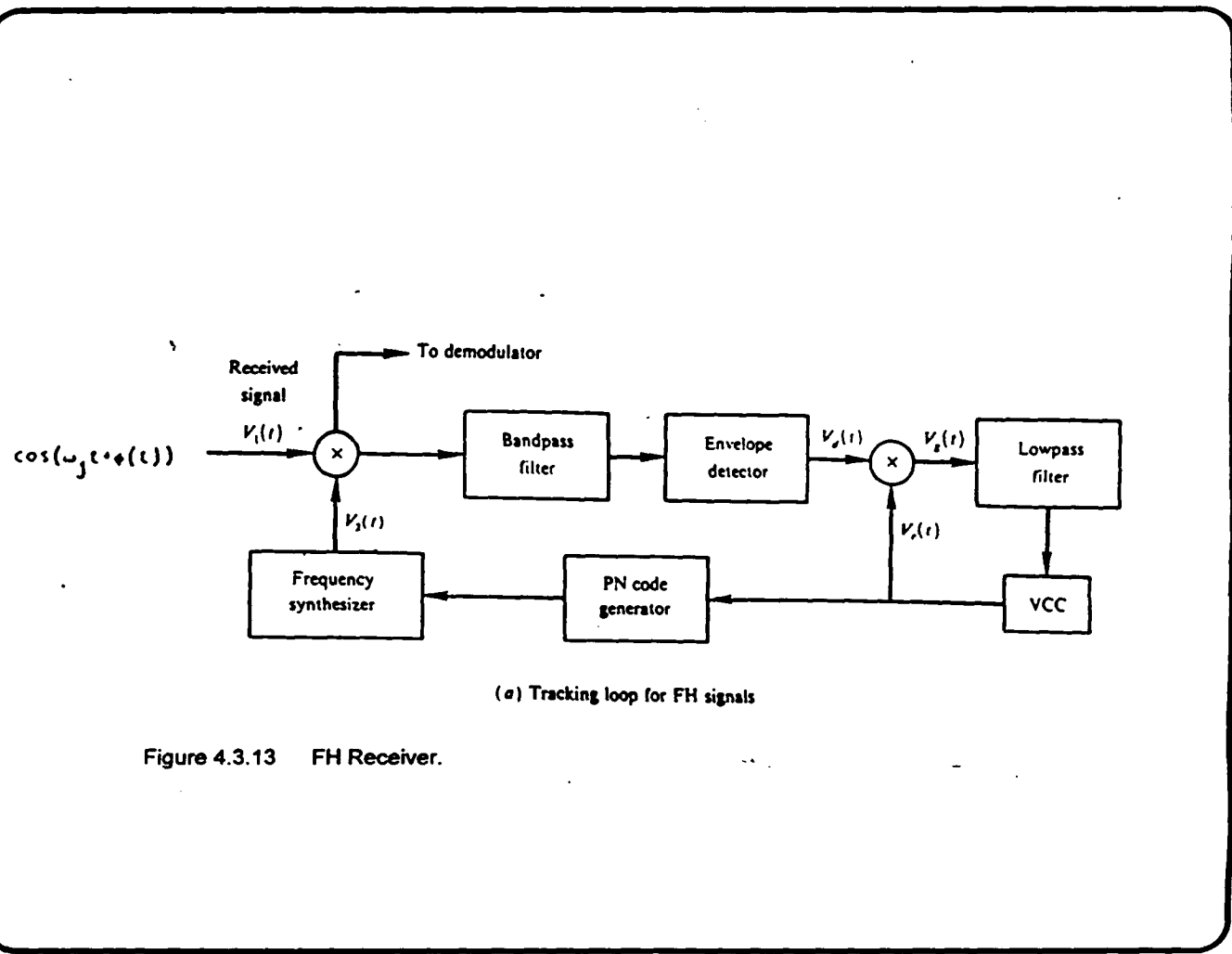


Figure 4.3.11 Power Spectral Densities of the Modulation.

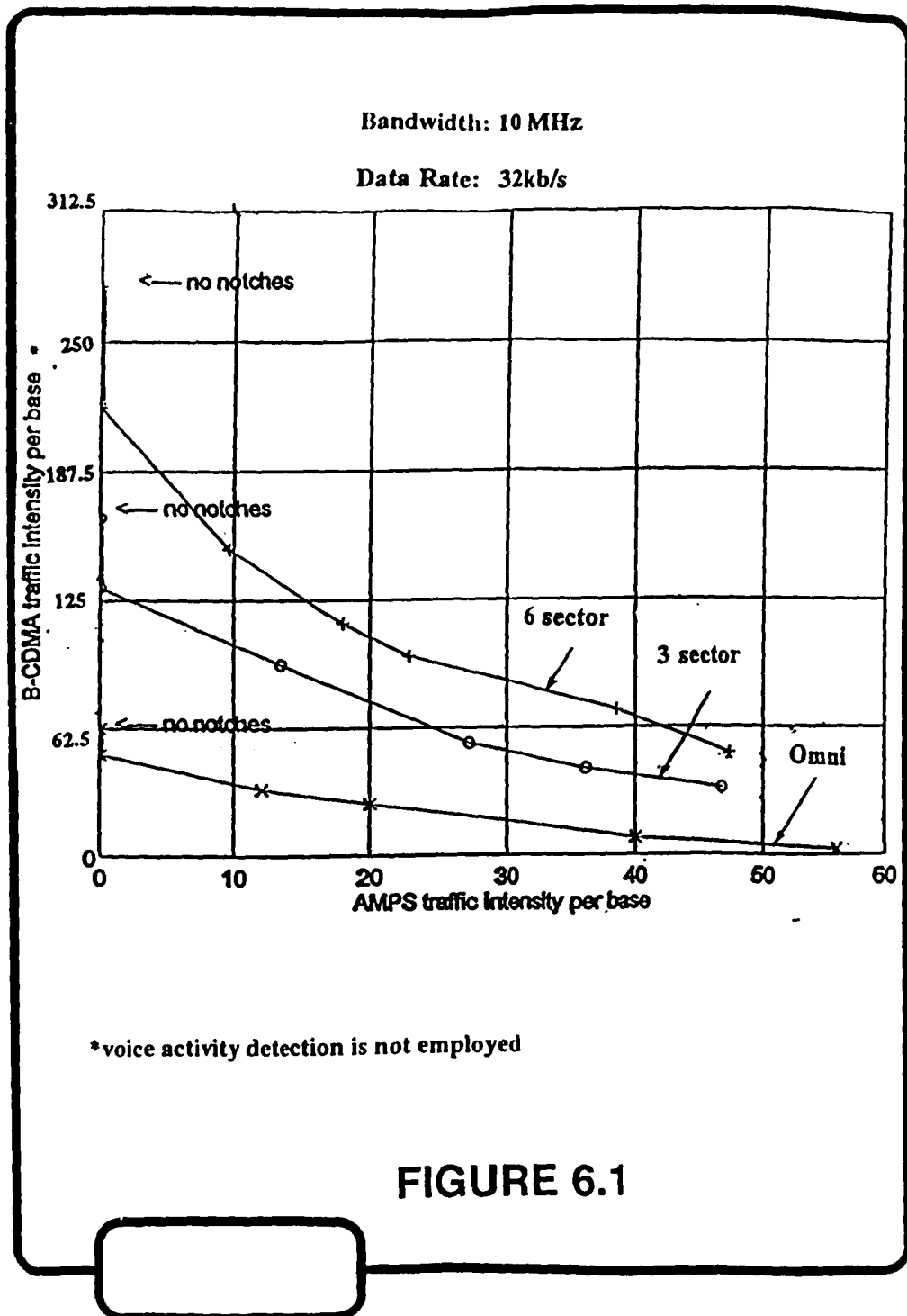






(a) Tracking loop for FH signals

Figure 4.3.13 FH Receiver.



MOBILE TECHNOLOGIES EFFICIENCY COMPARISON

Technology	Efficiency (Users/MHz)	Voice Data Rate (kb/s)	Frequency Reuse	Comments
AMPS	2.24	Analog	7	BASELINE
NAMPS	6.72	Analog	7	x 3 AMPS
IS54	6.72	8	7	x 3 AMPS
ETDMA	18.0	4	7	x 8 AMPS; Includes VAD
GSM	5	13	4	Includes Fec, Rate 1/2
NCDMA	22.4	8	1	x 10 AMPS; Includes VAD and Variable Rate Coder
BCDMA	32 8	8 32	1 1	For a 3-Sector antenna

**FIGURE 6.2**

**TABLES**

# Digital Telephony - Common Air Interfaces

(excluding Spread Spectrum / CDMA)

Wireless Communications Products

	Cellular			Prototype PCN			Cordless CPE			
	IS-54	GSM	JDCRS	Bellcore	PHP	DCS 1800	DECT	CT-2	CT-2a	CT-3
Frequency Band (MHz)	824-849 869-894	890-915 935-960	810-830 840-860	various 2 GHz range	1.9 GHz	1710-1785 1805-1860	1800-1900	864-868	930-931 940-941	various 1 GHz range
Available Bandwidth	50 MHz	50 MHz	40 MHz	90 MHz	90 MHz	150 MHz	20 MHz	4 MHz	4 MHz	8 MHz
Multiple Access Technique	TDMA/FDMA	TDMA/FDMA	TDMA/FDMA	TDMA/FDMA	TDMA/FDMA	TDMA/FDMA	TDMA/FDMA	FDMA	FDMA	TDMA/FDMA
Freq Channel Spacing	30 kHz	200kHz	25 kHz	300 kHz	300 kHz	200 kHz	1.728 MHz	100 kHz	100 kHz	1000 kHz
# Freq Channels	1666	250	1500	300	300	750	11	40	40	8
TDM Channel per Freq Channel	3	8	3	10	4	16	12	1	1	8
Duplex Method	FDD	FDD	FDD	FDD	TDD	FDD	TDD	TDD	TDD	TDD
Total Duplex Channels	2496	1000	2400	1500	1200	6000	132	40	40	64
Eqvlr BW per Duplex Channel	20 kHz	80 kHz	17kHz	80 kHz	75 kHz	25 kHz	144 kHz	100 kHz	100 kHz	125 kHz
Channel Bit Rate	48.6 kbps	270 kbps	42 kbps	450 kbps	384 kbps	270 kbps	1152 kbps	72 kbps	72kbps	640 kbps
Data Service	8 kbps	16 kbps	6.7 kbps	32-320 kbps	32 kbps	8 kbps	32-736 kbps	32 kbps	32 kbps	32 kbps
Voice Digitization Algorithm	VSELP	RPE-LTP	VSELP	ADPCM	ADPCM	RPE-LTP	ADPCM	ADPCM	ADPCM	ADPCM
Voice Bit Rate	8 kbps	13 kbps	6.7 kbps	32 kbps	32 kbps	6.7 kbps	32 kbps	32 kbps	32 kbps	32 kbps
Forward Error Corr.	5 kbps	9.8 kbps	4.5 kbps	none	none	4.5 kbps	none	none	none	none
Frame Length	40 msec	4.6 msec	20 msec	2 msec	20msec	4.6 msec	10 msec	2 msec	2 msec	16 msec
Baseband Modulation	PV4 DQPSK	GMSK	PV4 DQPSK	PV4 DQPSK	PV4 DQPSK	GMSK	GMSK	FFSK	FFSK	FFSK
Handset Xmt Pwr	.6-1.2 W	variable	variable	100 mW max	100 mW max	variable	10 mW	5-10 mW	5-10 mW	5-10 mW
Cell Size	.5-30 miles	1-5 miles	.5-20 miles	2000 ft. max	150 m max	4-5 miles	40-140 m	41-140 m	40-140 m	150 m max
Handoff	Yes	Yes	Yes	Yes	Yes	Yes	Yes	no	Yes	Yes
Delay Spread Equal	41.2 usec	16 usec	10 usec	none	none	16 usec	none	none	none	none
Availability	1991-2	1991	1991-2	1994	1992-3	1993	1992	1989	1991	1991
Adherents	CTIA	ETSI	Japan	Bellcore	Japan	ETSI	EC-ETSI	U. Britain Muterole Sony	N. Telecom	Ericsson NovAtel
Norm. DELAY (yr)	1.0012	4.32	0.21							



Rockwell International Digital Communications Division

July 1991 (18)

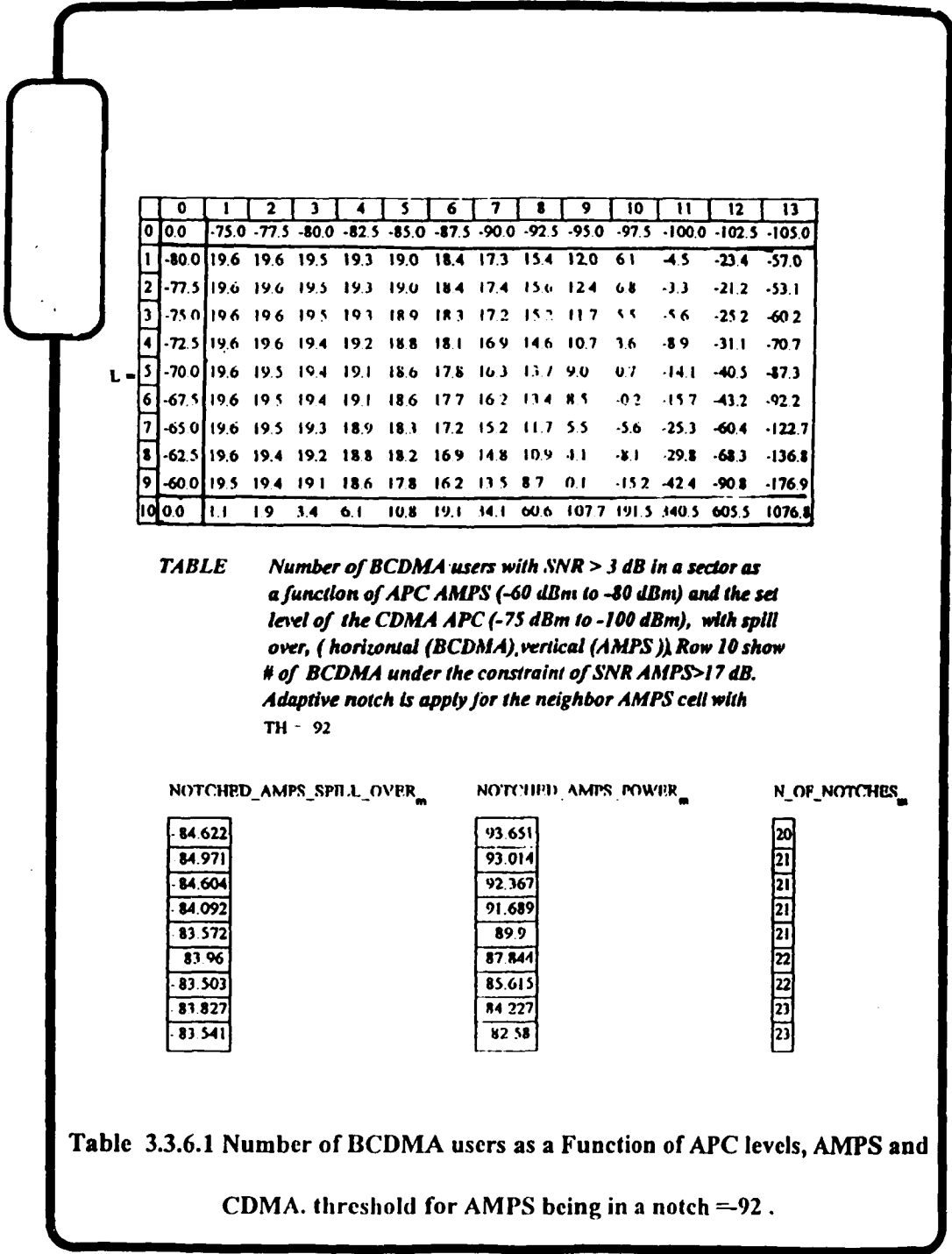
Table 2.2.1 Digital Telephony - Common Air Interfaces

**Spillover Results for  
B-CDMA Adjacent Cell Interference**

<b>h (dB)</b>	<b>S = 1</b>	<b>S = 3</b>	<b>S = 6</b>
<b>0</b>	<b>k = 0.22</b>	<b>k = 0.25</b>	<b>k = 0.48</b>
<b>3</b>	<b>k = 0.31</b>	<b>k = 0.41</b>	<b>k = 0.66</b>
<b>6</b>	<b>k = 0.48</b>	<b>k = 0.66</b>	<b>k = 0.96</b>

**S** = Number of Sectors  
**h** = Handover Threshold  
**k** = Spillover Factor  
**FTB** = 10 dB

Table 3.3.1:



	0	1	2	3	4	5	6	7	8	9	10	11	12	13
0	0.0	-75.0	-77.5	-80.0	-82.5	-85.0	-87.5	-90.0	-92.5	-95.0	-97.5	-100.0	-102.5	-105.0
1	-80.0	19.6	19.6	19.5	19.3	19.0	18.4	17.3	15.4	12.0	6.1	-4.5	-23.4	-57.0
2	-77.5	19.6	19.6	19.5	19.3	19.0	18.4	17.4	15.6	12.4	6.8	-3.3	-21.2	-53.1
3	-75.0	19.6	19.6	19.5	19.3	18.9	18.3	17.2	15.3	11.7	5.5	-5.6	-25.2	-60.2
4	-72.5	19.6	19.6	19.4	19.2	18.8	18.1	16.9	14.6	10.7	3.6	-8.9	-31.1	-70.7
5	-70.0	19.6	19.5	19.4	19.1	18.6	17.8	16.3	13.7	9.0	0.7	-14.1	-40.5	-87.3
6	-67.5	19.6	19.5	19.4	19.1	18.6	17.7	16.2	13.4	8.5	-0.2	-15.7	-43.2	-92.2
7	-65.0	19.6	19.5	19.3	18.9	18.3	17.2	15.2	11.7	5.5	-5.6	-25.3	-60.4	-122.7
8	-62.5	19.6	19.4	19.2	18.8	18.2	16.9	14.8	10.9	-1.1	-8.1	-29.8	-68.3	-136.8
9	-60.0	19.5	19.4	19.1	18.6	17.8	16.2	13.5	8.7	0.1	-15.2	-42.4	-90.8	-176.9
10	0.0	1.1	1.9	3.4	6.1	10.8	19.1	34.1	60.6	107.7	191.5	340.5	605.5	1076.8

**TABLE** Number of BCDMA users with SNR > 3 dB in a sector as a function of APC AMPS (-60 dBm to -80 dBm) and the set level of the CDMA APC (-75 dBm to -100 dBm), with spill over, ( horizontal (BCDMA), vertical (AMPS )). Row 10 show # of BCDMA under the constraint of SNR AMPS>17 dB. Adaptive notch is apply for the neighbor AMPS cell with TH = 92

NOTCHED_AMPS_SPILL_OVER <sub>m</sub>	NOTCHED_AMPS_POWER <sub>m</sub>	N_OF_NOTCHES <sub>m</sub>
-84.622	93.651	20
-84.971	93.014	21
-84.604	92.367	21
-84.092	91.689	21
-83.572	89.9	21
-83.96	87.844	22
-83.503	85.615	22
-81.827	84.227	23
-83.541	82.58	23

**Table 3.3.6.1** Number of BCDMA users as a Function of APC levels, AMPS and CDMA. threshold for AMPS being in a notch =92 .

	0	1	2	3	4	5	6	7	8	9	10	11	12	13
0	0.0	-75.0	-77.5	-80.0	-82.5	-85.0	-87.5	-90.0	-92.5	-95.0	-97.5	-100.0	-102.5	-105.0
1	-80.0	19.7	19.7	19.6	19.5	19.4	19.1	18.6	17.8	16.2	13.5	8.7	0.1	-15.1
2	-77.5	19.7	19.6	19.6	19.5	19.3	19.0	18.4	17.5	15.7	12.6	7.0	-2.9	-20.5
3	-75.0	19.7	19.6	19.6	19.5	19.2	18.9	18.2	17.1	15.0	11.3	4.7	-6.9	-27.6
4	-72.5	19.7	19.6	19.6	19.5	19.3	18.9	18.2	17.1	15.1	11.4	5.0	-6.5	-26.9
5	-70.0	19.7	19.6	19.5	19.4	19.1	18.7	17.9	16.5	13.9	9.4	1.4	-12.8	-38.1
6	-67.5	19.6	19.6	19.5	19.3	19.0	18.5	17.6	15.9	12.9	7.6	-1.9	-18.7	-48.6
7	-65.0	19.6	19.6	19.4	19.2	18.8	18.1	16.8	14.5	10.4	3.1	-9.9	-32.9	-73.9
8	-62.5	19.6	19.5	19.4	19.1	18.6	17.7	16.1	13.3	8.3	0.6	-16.3	-44.4	-94.3
9	-60.0	19.6	19.5	19.3	18.9	18.3	17.2	15.2	11.7	5.5	-5.5	-25.1	-60.0	-122.0
10	0.0	11	19	34	61	108	191	341	606	1077	1915	3405	6055	10768

L =

**TABLE** Number of BCDMA users with SNR > 3 dB in a sector as a function of APC AMPS (-60 dBm to -80 dBm) and the set level of the CDMA APC (-75 dBm to -100 dBm), with spill over, ( horizontal (BCDMA) vertical (AMPS )) Row 10 show # of BCDMA under the constraint of SNR AMPS>17 dB. Adaptive notch is apply for the neighbor AMPS cell with T11 = 97

NOTCHED_AMPS_SPILL_OVER_m	NOTCHED_AMPS_POWER_m	N_OF_NOTCHES_m
88.763	93.651	25
88.14	93.014	25
-87.411	92.367	25
-87.746	91.689	27
-87.207	89.9	27
-87.42	87.844	28
-87.01	85.615	28
-87.013	84.227	29
-87.823	82.58	31

**Table 3.3.6.2** Number of BCDMA users as a Function of APC levels, AMPS and CDMA. threshold for AMPS being in a notch=-97.

	0	1	2	3	4	5	6	7	8	9	10	11	12	13
0	0.0	-75.0	-77.5	-80.0	-82.5	-85.0	-87.5	-90.0	-92.5	-95.0	-97.5	-100.0	-102.5	-105.0
1	-80.0	19.7	19.7	19.6	19.6	19.5	19.3	19.0	18.5	17.6	15.9	12.9	7.6	-1.8
2	-77.5	19.7	19.7	19.7	19.6	19.5	19.3	19.0	18.5	17.6	15.9	13.0	7.8	-1.5
3	-75.0	19.7	19.7	19.6	19.6	19.5	19.3	19.0	18.4	17.4	15.6	12.4	6.7	-3.5
4	-72.5	19.7	19.7	19.6	19.6	19.5	19.3	19.0	18.4	17.4	15.5	12.3	6.5	-3.9
5	-70.0	19.7	19.7	19.6	19.5	19.4	19.2	18.7	17.9	16.6	14.1	9.7	2.0	-11.8
6	-67.5	19.7	19.6	19.6	19.5	19.3	18.9	18.3	17.3	15.3	11.9	5.9	-4.9	-24.1
7	-65.0	19.7	19.6	19.5	19.4	19.1	18.6	17.7	16.1	13.1	8.4	-0.4	-16.1	-44.0
8	-62.5	19.6	19.6	19.4	19.2	18.9	18.2	17.0	15.0	11.3	-1.7	-7.0	-27.9	-64.9
9	-60.0	19.6	19.5	19.3	19.0	18.5	17.6	15.9	13.0	7.8	-1.5	-18.0	-47.3	-99.5
10	0.0	1.1	1.9	3.4	6.1	10.8	19.1	34.1	60.6	107.7	191.5	340.5	605.5	1076.8

**TABLE** Number of BCDMA users with SNR > 3 dB in a sector as a function of APC AMPS (-60 dBm to -80 dBm) and the set level of the CDMA APC (-75 dBm to -100 dBm), with spill over, ( horizontal (BCDMA) vertical (AMPS )) Row 10 show # of BCDMA under the constraint of SNR AMPS > 17 dB. Adaptive notch is apply for the neighbor AMPS cell with TTI - 102

NOTCH'D AMPS SPILL OVER	NOTCH'D AMPS POWER	N. OF NOTCHES
91.825	93.631	30
92.404	93.014	33
92.265	92.367	34
92.878	91.689	36
92.422	89.9	36
92.411	87.844	37
93.195	85.615	39
92.991	84.227	39
92.9	82.58	39

**Table 3.3.6.3** Number of BCDMA users as a Function of APC levels, AMPS and CDMA. threshold for AMPS being in a notch.- 102

**References**

- [1] W.Y.C. Lee, *Mobile Cellular Telecommunications Systems*. New York: McGraw-Hill, 1989.
  
- [2] S.S. Ghassemzadeh dissertation. *Effects of channel fading on Direct Sequence-Spread Spectrum Signal at 2 GHz*. The City University of New York 1994.
  
- [3] John W. Ketchum and John G. Proakis. "Adaptive Algorithm for Estimating and Suppressing Narrow-Band Interference in PN Spread-Spectrum Systems." *IEEE Trans. Commun.*, vol. COM-30, pp 913-924, May 1982.
  
- [4] R.S. Gilhausen, I.M. Jacobs, R. Padovani, A.J. Viterbi, L.A. Weaver Jr., C.E. Weatley III, "On the Capacity of a Cellular CDMA system," *IEEE Veh. Technology*, pp. 303-312, May 1991.

- [5] K. Parsa. "B-CDMA Overlay Forward Link and Reverse Link Capacity Based on Random Traffic and a New CDMA Call Blocking Model" Submitted to ICC '1995.
  
- [6] L.B. Milstein, D.L. Schilling, R.L. Pickholtz, V. Erceg, M. Kullback, E. Kanterakis, D. Fishman, W.H. Biederman, and D. Salreno, "On the Feasibility of a CDMA Overlay for Personal Communication Networks," IEEE J. Select. Area in Commun., vol. SAC-10, No. 4, pp. 655-668, May 1992.
  
- [7] D.L. Schilling, K. Parsa, Z. Hadad, J. Garodnick, G. Lomp, D. Greico, "Broadband CDMA Overlay" ICCT Conference, Shanghai, China, June 1994.
  
- [8] H. Taub and D.L. Schilling, " Principles of Communication Systems," 2nd ed., New York: McGraw-Hill, 1986.
  
- [9] R.L. Pickholtz, D. L. Schilling, L. B. Milstein, "Theory of Spread Spectrum Commercial Communications", IEEE Trans. Commun. COM-30, pp 855-884, May 1982.
  
- [10] R.W. Lucky, J. Salz, and E.J. Weldon Jr., "Principles of Data Communication," New York: McGraw-Hill, 1968.

- [11] J.G. Proakis, Digital Communications. New York: MacGraw-Hill, 3rd ed., 1989.
- [12] Donald M. Grieco "The Capacity Achievable with a Broadband CDMA Microcell Underlay to an Existing Cellular Macro system," in IEEE J. Select. Areas Commun. ,pp.744-750 , May 1994.
- [13] W .Lee, "Overview of Cellular CDMA " , IEEE Transaction on Vehicular Technology, Vol. 40, No 2, pp 291-302, May 1991.
- [14] J.G. Proakis and D.G. Manolakis, Introduction to Digital Signal Processing, New York: MacMillan Publishing co., 1988.
- [15] S.S. Ghassemzadeh, V. Erceg, M. Taylor, D.L. Schilling, H. Arshad, "Indoor Propagation and Fading Characteristics of Spread Spectrum Signals at 2 GHz", Globecom 92, Tutorial Conference.

- [16] I Kalet, S. Shitz, Z. Hadad, Trachtman, and Y. Baruch, "Examples of continuous phase modulation using discriminator detection," *IEEE Trans. Commun.*, vol. COM-34, PP. 1148-1150, Nov. 1986.
  
- [17] Phillip D. at all Slow Frequency-Hop TDMA/CDMA for Macrocellular Personal Communications *IEEE Personal Communications Second Quarter*, vol. 1 No. 2 pp. 26-35, 1994.